D 2017

U.PORTO

FMUP FACULDADE DE MEDICINA
UNIVERSIDADE DO PORTO

Strontium rich hybrid injectable system for bone regeneration

NUNO NEVES

TESE DE DOUTORAMENTO APRESENTADA

À FACULDADE DE MEDICINA DA UNIVERSIDADE DO PORTO EM

MEDICINA

D 2017

U.PORTO

FMUP FACULDADE DE MEDICINA
UNIVERSIDADE DO PORTO

Strontium rich hybrid injectable system for bone regeneration

NUNO NEVES

TESE DE DOUTORAMENTO APRESENTADA

À FACULDADE DE MEDICINA DA UNIVERSIDADE DO PORTO EM

MEDICINA

Nuno Silva Morais Neves

Strontium rich hybrid injectable system for bone regeneration

Tese de Candidatura ao grau de Doutor em Medicina, submetida à Faculdade de Medicina da Universidade do Porto.

Orientador – Professor Doutor Gilberto Costa

Categoria – Professor Associado

Afiliação – Centro Hospitalar São João (CHSJ) e Faculdade de Medicina da Universidade do Porto (FMUP)

Coorientador – Professor Doutor Mário A. Barbosa

Categoria – Professor Catedrático

Afiliação – Instituto de Ciências Biomédicas Abel Salazar (ICBAS), Instituto de Investigação e Inovação em Saúde (i3S) e Instituto de Engenharia Biomédica (INEB), Universidade do Porto

U.PORTO

FMUP FACULDADE DE MEDICINA
UNIVERSIDADE DO PORTO

Nomeação do Júri da Prova de Doutoramento de

- NUNO SILVA DE MORAIS NEVES -

Programa Doutoral em *Medicina*

Nos termos do disposto do n.º 2 do art.º 18.º do Regulamento dos Terceiros Ciclos de Estudos da Universidade do Porto, a seguir se publicita o júri de doutoramento em Medicina, do licenciado Nuno Silva de Morais Neves, nomeado por despacho vice-reitoral de 27 de setembro de 2017, com a tese "Strontium rich hybrid injectable system for bone regeneration":

Presidente: Doutor José Agostinho Marques Lopes, professor catedrático da Faculdade de Medicina da Universidade do Porto.

VOGAIS: Doutor Jacinto Manuel de Melo Oliveira Monteiro, professor catedrático da Faculdade de Medicina da Universidade de Lisboa;

Doutor José Manuel Lopes Teixeira Amarante, professor catedrático da Faculdade de Medicina da Universidade do Porto;

Doutor António da Fonseca Oliveira, professor catedrático convidado do Instituto de Ciências Biomédicas Abel Salazar da Universidade do Porto.

Doutor José Guimarães Consciência, professor associado da Faculdade de Ciências Médicas da Universidade Nova de Lisboa;

Doutor Fernando Gilberto Melo Costa, professor associado da Faculdade de Medicina da Universidade do Porto e orientador da tese;

Doutor Manuel António Pereira Gutierres, professor auxiliar da Faculdade de Medicina da Universidade do Porto;

Serviço Académico, 17 de outubro de 2017.

A Diretora da Faculdade

(Doutora Maria Amélia Ferreira)

Al. Prof. Hernâni Monteiro, 4200-319 Porto telefone +351 22 551 36 04
internet http://www.med.up.pt e-mail servicoacademico@med.up.pt

Table of Contents

ACKNOWLEDGEMENTS

This thesis would not have been possible without the collaboration and involvement of several people to whom I am deeply grateful. I would particularly like to thank the following:

Professor Gilberto Costa, supervisor of this thesis in very special circumstances. I am grateful for your support and guidance. Already as your student and since my early years in residency, you have been an example of a dedicated doctor, surgeon, teacher, and friend;

Professor Mário Barbosa, co supervisor of this thesis, for setting up this challenge and introducing me to a new world of laboratorial and scientific research. In the difficult moments, your leadership, perseverance and ethics were inspiring;

Professor Cristina Ribeiro, my research companion. I am grateful for your interest, commitment, rigor, opinions and suggestions;

All my colleagues at INEB and i3S, especially Filipa Lourenço, Daniel Vasconcelos, Serafim Oliveira, Bruno Campos, Cláudia Carvalho, Susana Sousa, Meriem Lamghari, Cristina Barrias, Susana Santos, Raquel Gonçalves, Pedro Granja, for all the collaboration and support;

Dr. Rui Pinto, Chair of the Orthopedic Department of Centro Hospitalar de São João, for the continuing confidence, support, and incentive for excellence;

Professor Manuel Gutierres, with whom I shared my first steps in Orthopedics, for the true friendship that bonds us;

All my colleagues at the Orthopedic Department of Hospital de São João, especially Manuel Ribeiro da Silva, Pedro Negrão, Rui Matos, Pedro Cacho Rodrigues, Daniela Linhares and João Santos Carvalho, for all the cooperation, insight, collaboration and friendship;

Professor Manuel Barbosa and Professor Dulce Madeira, with whom I started my academic career, for the opportunity given, the example of leadership, mutual respect, and scientific and educational standards.

The Radiology Department of FMUP, and its Chair Professor Isabel Ramos, the Nefrology Department of FMUP, and its Chair Professor Manuel Pestana, the Instituto de Medicina Legal – Delegação Norte, especially Professor Agostinho Santos, the Department of Pharmaceutical Technology of FFUP, namely Professor Paulo Costa and Professor Isabel Almeida, and the Department of Mechanics of FEUP, particularly Professor Mário Vaz, for their contribution to the work developed;

My parents, José and Teresa, for all the love and unconditional support, and for having transmitted the values that guide my life;

My wife, Patrícia, and my children, João and Luísa, always supportive, loving, and caring, in spite of the professional and academic life that separates us so often. You are always on my thoughts;

Lastly, Professor Abel Trigo Cabral, the inspirer of this thesis and its first supervisor, unfortunately unable to see it come to an end. He was my mentor, my master and my friend, an example of rectitude, honesty and professionalism. To him I dedicate this work.

LIST OF PUBLICATIONS

The work performed in the frame of this thesis resulted in the following publications:

Neves N, Linhares D, Costa G, Ribeiro CC, Barbosa MA. In vivo and clinical application of strontium-enriched biomaterials for bone regeneration. Bone Joint Res. 2017 Jun;6(6):366-375. doi: 10.1302/2046-3758.66.BJR-2016-0311.R1.

Neves N, Campos BB, Almeida IF, Costa PC, Trigo Cabral A, Barbosa MA, Ribeiro CC. Strontium-rich injectable hybrid system for bone regeneration. Mater Sci Eng C Mater Biol Appl. 2016 Feb;59:818-827. doi: 10.1016/j.msec.2015.10.038.

Lourenço AH*, Neves N*, Ribeiro-Machado C, Sousa SR, Lamghari M, Barrias C, Trigo Cabral A, Barbosa MA, Ribeiro CC. Injectable hybrid system for strontium local delivery promotes bone regeneration in a rat critical-sized defect model. Sci Rep. 2017 Jul 11;7(1):5098. doi: 10.1038/s41598-017-04866-4

* equal contribution

ABSTRACT

Bone tissue can spontaneously heal through a characteristic, complex, and highly regulated process of consecutive and closely linked stages of inflammation, repair and remodelling. Trauma, extensive bone loss, systemic inflammation, and multiple diseases may disrupt this process, impair healing and result in non-union and bone defects. Osteoporosis is increasing in the progressively older population of western countries. As it results in loss of mineralization and subsequent changes in bone architecture, related fractures and bone loss can be anticipated. The management of fractures and bone defects, especially in osteoporotic conditions, remains a significant surgical challenge. Autologous grafts are still considered the current gold standard for bone tissue replacement but are also associated with significant problems and insufficiencies. Accordingly, tissue engineering has been focusing on developing bone substitutes that can withstand normal dynamic physiological mechanical stresses and provide a matrix capable of supporting cell migration and tissue ingrowth.

In this doctoral dissertation we aim to contribute to the development of alternative injectable biomaterials to be used in the management of bone defects, particularly adapted to the osteoporotic patient.

First we assessed the *in vivo* efficacy and safety of strontium (Sr) enriched biomaterials in bone formation and/or remodelling. There is considerable evidence that Sr has a beneficial influence in bone strength and architecture, and incorporating Sr in biomaterials is a strategy to locally improve osteogenesis without inducing detrimental side effects. With this purpose, we conducted a systematic review on the effect of Sr-enriched biomaterials on bone remodelling, when compared to Sr-free similar ones. 27 papers were included, and all showed similar or increased effect of Sr in bone formation and/or regeneration, in both healthy and osteoporotic models, an effect impacted by time and concentration. Only one article reported systemic

effects from Sr addition. This review, the first of its kind on this subject, confirmed the safety and effectiveness of Sr-enriched biomaterials for stimulating bone formation and remodelling in animal models. However, the wide range of study methods impaired an adequate quantitative synthesis of the results.

In the second part we describe the development and characterization of a hybrid polymer-ceramic injectable system that consists of an alginate matrix cross-linked *in situ* in the presence of Sr, and Sr-rich hydroxyapatite microspheres. Different formulations were tested for injectability and mechanical properties. A 3.5% (w/v) ultrapure sodium alginate solution was used as the vehicle and its *in situ* gelation was promoted by the addition of calcium or Sr carbonate, and Glucone-δ-lactone. Compositions with 35% w of 555 μm microspheres presented the best compromise between injectability and compression strength of the system. Micro-CT analysis revealed a homogeneous distribution of the microspheres inside the vehicle, and a mean inter-microspheres space of 220 μm, adequate for tissue and vascular ingrowth.

Finally we evaluated the *in vivo* response to this Sr-enriched system and its influence on new bone formation compared to a similar Sr-free material. Both systems were injected in a critical-size metaphyseal femoral bone defect rat model and results were assessed at 15 and 60 days post surgery. Micro-CT results show a trend towards higher new bone formed in Sr-hybrid group. Greater cell invasion was detected at the center of the defect of Sr-hybrid group after 15 days with earlier bone formation. Higher material degradation with increase of collagen fibers and bone formation in the center of the defect after 60 days was observed, as opposed to bone formation restricted to the periphery of the defect in the control. These imaging and histological findings support the evidence of an improved response with the Sr enriched material. Moreover, no alterations were observed in the Sr levels in systemic organs or serum.

In conclusion, this thesis: (I) confirms the effectiveness and safety of Sr-enriched biomaterials for bone regeneration; (II) develops an alternative viscoelastic biomaterial for the management of bone defects, which can be manually injected, sets *in situ,* and offers structural support and a temporary scaffold for bone growth; (III) provides additional evidence of enhanced bone formation with the incorporation of Sr on the biomaterial, without detrimental systemic effects.

RESUMO

O tecido ósseo tem a capacidade de regeneração através de um processo característico, complexo e altamente regulado, envolvendo fases consecutivas e intimamente ligadas de inflamação, reparação e remodelação. O trauma, perda óssea significativa, inflamação sistémica e múltiplas doenças podem alterar este processo, impedir a reparação, e resultar em não união e defeitos ósseos. A osteoporose está a aumentar na população cada vez mais envelhecida dos países ocidentais. Uma vez que desta doença resulta uma perda da mineralização e subsequentes alterações da arquitetura óssea, são de esperar fraturas e perdas ósseas. O tratamento das fraturas e defeitos ósseos, especialmente em condições osteoporóticas, permanece um desafio cirúrgico significativo. Os enxertos autólogos são ainda considerados o padrão para a substituição do tecido ósseo, mas estão associados a problemas e insuficiências relevantes. Consequentemente, a engenharia de tecidos tem-se focado no desenvolvimento de substitutos ósseos que possam suportar as forças mecânicas dinâmicas fisiológicas e fornecer uma matriz capaz de suportar a migração celular e a invasão tecidular.

Nesta dissertação doutoral procuramos contribuir para o desenvolvimento de biomateriais injetáveis alternativos para o tratamento de defeitos ósseos, particularmente adaptados ao doente osteoporótico.

Começámos por avaliar a eficácia e segurança *in vivo* de materiais enriquecidos em estrôncio (Sr) na formação e/ou remodelação ósseas. Há evidência considerável que o Sr tem uma influência benéfica na resistência e arquitetura ósseas, e a incorporação de Sr em biomateriais é uma estratégia para melhorar a osteogénese localmente sem induzir efeitos laterais deletérios. Neste sentido, realizámos uma revisão sistemática sobre a evidência que compara o efeito de um material enriquecido em Sr na regeneração óssea quando comparado com um material semelhante livre de Sr. Foram incluídas 27 publicações, e todos os estudos

mostraram um efeito similar ou acrescido do Sr na formação e/ou regeneração óssea, tanto em modelos saudáveis como osteoporóticos. Este efeito é positivamente influenciado pelo tempo e pela concentração. Apenas um artigo reportou um efeito sistémico resultante da adição de Sr. Esta revisão, a primeira do género, confirmou a segurança e eficácia de biomateriais enriquecidos em Sr na formação e remodelação ósseas em modelos animais. Contudo, a elevada variabilidade dos métodos de estudo impediu uma síntese quantitativa adequada dos resultados.

Na segunda parte descrevemos o desenvolvimento e caracterização de um sistema híbrido polímero-cerâmico injetável que é formado por uma matriz de alginato reticulada *in situ* na presença de Sr, e microesferas de hidroxiapatite ricas em Sr. Foram testadas diferentes formulações quanto à injectabilidade e propriedades mecânicas. Uma solução de alginato de sódio ultrapuro a 35% (w/v) foi usada como veículo e a gelação *in situ* foi promovida pela adição de carbonato de cálcio ou Sr, e glucono-δ-lactona. As composições com 35% de microesferas de 555 μm apresentaram o melhor compromisso entre injectabilidade e força de compressão do sistema. A análise por Micro-CT revelou uma distribuição homogénea das microesferas dentro do veículo, e um espaçamento médio entre as mesmas de 220 μm, adequado para invasão tecidular e vascular.

Por último, avaliámos a resposta *in vivo* a este sistema e a sua influência na formação de novo osso comparadas com um material similar livre de Sr. Ambos sistemas foram injetados num modelo de defeito ósseo metafisário femoral crítico de rato, e os resultados avaliados aos 15 e 60 dias após a cirurgia. Os resultados do Micro-CT mostraram uma tendência para formação acrescida de novo osso no grupo do híbrido de Sr. Foi detetada uma maior invasão celular no centro do defeito no grupo do híbrido de Sr aos 15 dias com formação óssea mais precoce. Foi observada uma maior degradação do material com aumento de fibras de colagénio e

formação óssea no centro do defeito aos 60 dias, enquanto que no controlo a formação óssea se limitou à periferia. Estes achados imagiológicos e histológicos confirmam a evidência de uma melhor resposta com material enriquecido em Sr. Adicionalmente, não foram observadas alterações nos níveis séricos de Sr ou em órgãos sistémicos.

Em conclusão, esta tese: (I) confirma a eficácia e segurança de biomateriais enriquecidos em Sr utilizados para regeneração óssea; (II) desenvolve um biomaterial viscoelástico alternativo para o tratamento de defeitos ósseos que pode ser injetado manualmente, reticula *in situ* e garante suporte estrutural e uma matriz temporária para crescimento ósseo; (III) fornece evidência adicional de melhoria da formação óssea com a incorporação de Sr no biomaterial, sem efeitos sistémicos deletérios.

CHAPTER I

GENERAL INTRODUCTION
AIMS OF THE THESIS

Bone tissue has the ability to spontaneously heal through a characteristic, complex, and highly regulated process with consecutive and closely linked stages of inflammation, repair and remodeling [1]. However, disruption of this process caused by trauma, extensive bone loss, systemic inflammation, such as in diabetes mellitus, sepsis and rheumatoid arthritis, and diseases like cancer and osteoporosis, can impair healing and result in non-union and bone defects [1]. As the expectancy of life rises in western countries, an increase in the prevalence of osteoporosis, related fractures and bone loss can be anticipated. The management of fractures and bone defects, especially in osteoporotic conditions, remains a significant surgical challenge and there is a need for improved tissue engineering strategies with either biological or synthetic bone substitutes [2, 3].

This introduction will focus the problems and drawbacks of currently used bone grafts and substitutes, the experience with ceramics and hydrogels, and the potential benefits of doping biomaterials with other elements, especially with strontium.

Bone grafts

Autologous grafts are considered the current gold standard for bone tissue replacement because of easy harvest, osteogenic potential and long record of successful use in clinical practice. Nevertheless, autografts are limited in supply, need an additional time-consuming harvest surgery, with associated morbidity, pain and poor cosmetic appearance at the donor site, and their properties, shape and size do not exactly match those of the bone to be replaced [4-6]. Allografts and xenografts have also been extensively studied but the risks of immune rejection and disease transfer have limited their use [4].

Bone substitutes

In order to overcome the problems with bone grafts, alternative bone substitutes, including hard and soft biomaterials, have been introduced for bone tissue engineering. Ideally, a bone substitute should conform to Giannoudis' ''Diamond theory'' where osteogenic cells and vascularization, mechanical stability, growth factors, and osteoconductive scaffolds, are a prerequisite for adequate bone healing [7]. It should also be sterilizable, easily handled and molded into the bone defect, radiolucent for prompt radiographic assessment, and readily available, with minimal morbidity, at a reasonable cost [3, 4]. None of the bone substitutes available fulfills yet all the necessary requirements for each clinical situation.

Ceramic bone substitutes

Ceramic substitutes have been used for decades and present several advantages, notably adequate biological response, osteoconductivity and mechanical properties [8-10]. Hydroxyapatite (HA), the primary mineral component of teeth and bone, can be used either alone or in combination with tricalcium phosphate (TCP) to produce blocks and granules [11, 12]. Combining the two allows an adequate balance between the rapid degradation of TCP and the high mechanical strength of HA, for optimal bone substitution [4].

Ceramic micro or nanoparticles can be suspended in appropriate vehicles to be used as injectable materials [13-15]. They can be applied by minimally invasive surgical procedures effectively filling irregularly shaped cavities, with reduced tissue damage and limited exposure to infectious agents. Spherical particles are more suitable for implantation than non-homogeneous granules, since they conform better to irregular implant sites and present more predictable flowing properties during injection [16-19]. Still, handling and brittleness of calcium phosphate cements are frequently cited limitations [20, 21].

Scaffold porosity is essential to support differentiation of cells into bone forming osteoblasts, migration of bone progenitor cells, and ingrowth of blood vessels and nerves, to repair the defect site [22, 23]. It has been suggested that a minimum pore size of ~100-150 microns is necessary for bone formation, and at least 300 microns for vascular ingrowth [23]. Although increased porosity improves biological response, at the same time mechanical properties may be compromised.

Another challenge for bone substitutes is the resorption rate, as they are expected to be progressively substituted by newly formed bone [24]. A very fast degradation rate will not allow sufficient support for adequate cell invasion, whereas if too slow, this invasion may actually be impaired, both resulting in failure.

Hydrogels in bone tissue engineering

Because of their biocompatibility both natural and synthetic polymers have also been used for bone tissue engineering, either as solid scaffolds or hydrogels. Hydrogels are water-swollen, networked, hydrophilic polymeric materials, typically formed via cross-linking or chain entanglement, that maintain a distinct three-dimensional structure [25, 26]. They have been shown to support cell culture within the gel and on its surface, and to increase angiogenesis and osteoconductivity in different bone repair models [27-30]. However, hydrogels, as soft materials, have an elastic modulus inferior to that of bone, significantly limiting their use in load bearing areas [31]. Nevertheless, the number of cross-links, type of monomer, and local environment can be adjusted to modify mechanical properties [32].

An emerging trend is combining hydrogels with other materials, resulting in hybrid composites that mimic both the organic and inorganic phases of natural bone. Combined with ceramic granulates they form moldable pastes and putties through improved cohesion, and can also be used as carriers for injectable composites [31, 33]. Hydrogels, can thus form a three dimensional environment with the suspended

ceramic particles, providing support and modulating cell invasion for bone tissue repair [31].

Alginate

Alginate is a natural polymer composed of guluronic and mannuronic acids, found in seaweeds and typically extracted from brown algae (*Phaeophyceae*). It is considered to be biocompatible, non-toxic, non-immunogenic and biodegradable, and is easily extracted at low price, making it adequate for biomedical applications [34, 35]**.** Alginate has the ability to form hydrogels under mild chemical conditions, in the presence of divalent cations, such as Ca^{2+}, Ba^{2+} and Sr^{2+}, through a cytocompatible physical gelation process. These cations bind homoguluronic blocks in adjacent alginate chains in a cooperative manner (egg-box model) producing a cross-linked hydrogel network [36].

Both biodegradability and mechanical properties can be tuned by using varied ratios of different molecular weights [34, 37]. Besides, alginate can be combined with inorganic materials like HA to improve mechanical strength and bone tissue formation, or be used as a carrier for ceramic components, as an injectable system, taking advantage of its *in situ* gel forming ability [38-40]. *In situ* gelation allows easy injection through minimally invasive procedures, while providing cohesion and resistance to washing-out at the implant site. Different particle size and shape, polymer concentration, and sterilization can influence both injectability and mechanical properties [31]. Low viscosity allows easier injectability, but induces greater particle sedimentation, and filtering, with phase separation upon injection. This can be minimized by smaller particle size, higher viscosity, high liquid to powder ratio, quicker extrusion, small syringe size, and use of short cannula [31, 41]. However, carriers featuring excessive rigidity and lack of degradation exhibit decreased bioactivity, delaying cellular colonization, impairing vascularization, and directing bone healing away from an endochondral pathway [31, 42].

A strategy to promote cellular infiltration within the hydrogel and to direct *de novo* bone formation at the local implant site is the incorporation of bio-adhesive motifs derived from extracellular matrices into alginate. Covalently binding of the RGD (arginine-glycine-aspartic acid) sequence onto alginate promotes osteogenic cell adhesion, focal adhesion formation, proliferation, and differentiation [43].

Other advantages of alginate are its potential use as a controlled release vehicle of enzymes, drugs and cytokines, and its ability to encapsulate and deliver cells that support natural tissue regeneration [44-48].

Strontium

Strontium (Sr) is a trace element that plays a dual role in bone metabolism, simultaneously stimulating bone formation and inhibiting bone resorption [49-54]. At least three mechanisms have been implicated in these opposite effects of Sr: activation of the calcium-sensing receptor (CaSR), nuclear factor of activated Tc (NFATc)/Wnt signaling, and modulation of osteoprotegerin (OPG) and receptor activator of nuclear factor κ-B ligand (RANKL) [49]. Several *in vitro* studies have shown that Sr decreases bone resorption, by reducing osteoclast activity [55-57], decreasing functional osteoclast markers expression [55], disrupting osteoclasts cytoskeleton [56], and increasing osteoclast apoptosis [58]. Simultaneously, it induces positive effects on osteoblastogenesis and osteoblast activity in different *in vitro* models [59], namely by enhancing replication of preosteoblastic cells [56, 60-63], increasing osteogenesis [56, 60, 64-66], decreasing osteoblast apoptosis [61, 67], and promoting terminal differentiation of osteoblasts into osteocytes [60].

Pre-clinical *in vivo* studies confirm *in vitro* data showing the beneficial effect of Sr on bone formation and remodeling in both normal and osteopenic/osteoporotic animal models [50, 68-73].

Sr, administered orally as Sr ranelate has been in clinical use as an effective anti-osteoporotic drug in the prevention of both vertebral and non-vertebral osteoporotic fractures [49, 74, 75].

However, cardiovascular safety of oral intake of Sr ranelate has been questioned due to a small but significant increase in non-fatal myocardial infarctions [76-78].

According to current strict guidelines [78], the drug is authorized for the treatment of severe osteoporosis, in postmenopausal women and in adult men, at high risk of fracture for whom treatment with other medicinal products approved for the treatment of osteoporosis is not possible. Additionally, its use should be restricted to patients with no past or current history of ischemic heart disease, peripheral arterial disease and/or cerebrovascular disease or uncontrolled hypertension.

Doping calcium phosphate cements and other ceramics with bioactive drugs is a recent trend to improve their regeneration potential. Incorporating Sr in biomaterials is a strategy to achieve high concentrations in a local environment, using the Sr osteoanabolic and anti-osteoclastic properties to enhance new bone formation, while avoiding its systemic effects [79-81]. These composite hybrid enriched biomaterials may lead to improved results in the management of bone defects in osteoporosis.

Aims of the Thesis

The main objective of this PhD thesis is the development of strontium enriched injectable materials to be used in the management of bone defects, particularly adapted to the osteoporotic patient.

Thereby, the following specific objectives were defined:

1) Assess the in vivo *efficacy and safety of Sr enriched biomaterials in bone formation and/or remodeling*

A systematic review on evidence that compares the effect of a Sr-enriched and a similar Sr-free biomaterial was conducted in PubMed and Scopus. Data showed increased bone formation and remodeling with the use of biomaterials enriched with Sr, an effect impacted by time and concentration, with adequate safety. These results are presented in Chapter II.

2) Development and characterization of a new injectable biomaterial to be used for bone regeneration

Following previous works carried out by our group, an injectable hybrid system that consists of an alginate matrix cross-linked in situ with Sr, reinforced with Sr-rich hydroxyapatite microspheres, was developed. Different formulations were tested for injectability and mechanical properties. These results are described in Chapter III.

3) Evaluate the in vivo *response to the Sr enriched hybrid system and its influence on new bone formation compared to a similar Sr-free material*

Both systems were injected in a critical-size metaphyseal femoral bone defect rat model and results were assessed at 15 and 60 days post surgery. Micro CT and histological findings support the evidence of an improved response with the Sr enriched material. Moreover, no changes were observed in Sr levels in systemic organs or serum. These findings are presented in Chapter IV

References

[1] Claes L, Recknagel S, Ignatius A. Fracture healing under healthy and inflammatory conditions. Nat Rev Rheumatol. 2012;8:133-43.

[2] Goldhahn J, Scheele WH, Mitlak BH, Abadie E, Aspenberg P, Augat P, et al. Clinical evaluation of medicinal products for acceleration of fracture healing in patients with osteoporosis. Bone. 2008;43:343-7.

[3] Marmor M, Alt V, Latta L, Lane J, Rebolledo B, Egol KA, et al. Osteoporotic Fracture Care: Are We Closer to Gold Standards? J Orthop Trauma. 2015;29 Suppl 12:S53-6.

[4] Campana V, Milano G, Pagano E, Barba M, Cicione C, Salonna G, et al. Bone substitutes in orthopaedic surgery: from basic science to clinical practice. J Mater Sci Mater Med. 2014;25:2445-61.

[5] Nandi S, Roy S, Mukherjee P, Kundu B, De D, Basu D. Orthopaedic applications of bone graft & graft substitutes : a review. Indian Journal of Medical Research. 2010;132:15-30.

[6] Arner JW, Santrock RD. A historical review of common bone graft materials in foot and ankle surgery. Foot Ankle Spec. 2014;7:143-51.

[7] Giannoudis PV, Einhorn TA, Marsh D. Fracture healing: the diamond concept. Injury. 2007;38 Suppl 4:S3-6.

[8] Chai YC, Carlier A, Bolander J, Roberts SJ, Geris L, Schrooten J, et al. Current views on calcium phosphate osteogenicity and the translation into effective bone regeneration strategies. Acta Biomater. 2012;8:3876-87.

[9] Dorozhkin SV. Bioceramics of calcium orthophosphates. Biomaterials. 2010;31:1465-85.

[10] Larsson S. Calcium phosphates: what is the evidence? J Orthop Trauma. 2010;24 Suppl 1:S41-5.

[11] Damien E, Hing K, Saeed S, Revell PA. A preliminary study on the enhancement of the osteointegration of a novel synthetic hydroxyapatite scaffold in vivo. J Biomed Mater Res A. 2003;66:241-6.

[12] Burg KJ, Porter S, Kellam JF. Biomaterial developments for bone tissue engineering. Biomaterials. 2000;21:2347-59.

[13] Dupraz A, Nguyen TP, Richard M, Daculsi G, Passuti N. Influence of a cellulosic ether carrier on the structure of biphasic calcium phosphate ceramic particles in an injectable composite material. Biomaterials. 1999;20:663-73.

[14] Maruyama M, Ito M. In vitro properties of a chitosan-bonded self-hardening paste with hydroxyapatite granules. J Biomed Mater Res. 1996;32:527-32.

[15] Low KL, Tan SH, Zein SH, Roether JA, Mourino V, Boccaccini AR. Calcium phosphate-based composites as injectable bone substitute materials. J Biomed Mater Res B Appl Biomater. 2010;94:273-86.

[16] Qiu QQ, Ducheyne P, Ayyaswamy PS. New bioactive, degradable composite microspheres as tissue engineering substrates. J Biomed Mater Res. 2000;52:66-76.

[17] Hsu FY, Chueh SC, Wang YJ. Microspheres of hydroxyapatite/reconstituted collagen as supports for osteoblast cell growth. Biomaterials. 1999;20:1931-6.

[18] Sunny MC, Ramesh P, Varma HK. Microstructured microspheres of hydroxyapatite bioceramic. J Mater Sci Mater Med. 2002;13:623-32.

[19] Sivakumar M, Rao KP. Preparation, characterization, and in vitro release of gentamicin from coralline hydroxyapatite-alginate composite microspheres. J Biomed Mater Res A. 2003;65:222-8.

[20] Xu HH, Quinn JB. Calcium phosphate cement containing resorbable fibers for short-term reinforcement and macroporosity. Biomaterials. 2002;23:193-202.

[21] Friedman CD, Costantino PD, Takagi S, Chow LC. BoneSource hydroxyapatite cement: a novel biomaterial for craniofacial skeletal tissue engineering and reconstruction. J Biomed Mater Res. 1998;43:428-32.

[22] Guldberg RE, Duvall CL, Peister A, Oest ME, Lin AS, Palmer AW, et al. 3D imaging of tissue integration with porous biomaterials. Biomaterials. 2008;29:3757-61.

[23] Karageorgiou V, Kaplan D. Porosity of 3D biomaterial scaffolds and osteogenesis. Biomaterials. 2005;26:5474-91.

[24] Koerten HK, van der Meulen J. Degradation of calcium phosphate ceramics. J Biomed Mater Res. 1999;44:78-86.

[25] Kopecek J. Hydrogel biomaterials: a smart future? Biomaterials. 2007;28:5185-92.

[26] Peppas NA, Bures P, Leobandung W, Ichikawa H. Hydrogels in pharmaceutical formulations. Eur J Pharm Biopharm. 2000;50:27-46.

[27] Kim J, Kim IS, Cho TH, Lee KB, Hwang SJ, Tae G, et al. Bone regeneration using hyaluronic acid-based hydrogel with bone morphogenic protein-2 and human mesenchymal stem cells. Biomaterials. 2007;28:1830-7.

[28] Fellah BH, Weiss P, Gauthier O, Rouillon T, Pilet P, Daculsi G, et al. Bone repair using a new injectable self-crosslinkable bone substitute. J Orthop Res. 2006;24:628-35.

[29] Short AR, Koralla D, Deshmukh A, Wissel B, Stocker B, Calhoun M, et al. Hydrogels That Allow and Facilitate Bone Repair, Remodeling, and Regeneration. J Mater Chem B Mater Biol Med. 2015;3:7818-30.

[30] Elisseeff J, McIntosh W, Anseth K, Riley S, Ragan P, Langer R. Photoencapsulation of chondrocytes in poly(ethylene oxide)-based semi-interpenetrating networks. J Biomed Mater Res. 2000;51:164-71.

[31] D'Este M, Eglin D. Hydrogels in calcium phosphate moldable and injectable bone substitutes: Sticky excipients or advanced 3-D carriers? Acta Biomater. 2013;9:5421-30.

[32] Anseth KS, Bowman CN, Brannon-Peppas L. Mechanical properties of hydrogels and their experimental determination. Biomaterials. 1996;17:1647-57.

[33] Bohner M. Design of ceramic-based cements and putties for bone graft substitution. Eur Cell Mater. 2010;20:1-12.

[34] Venkatesan J, Bhatnagar I, Manivasagan P, Kang KH, Kim SK. Alginate composites for bone tissue engineering: a review. Int J Biol Macromol. 2015;72:269-81.

[35] Lee KY, Mooney DJ. Alginate: properties and biomedical applications. Prog Polym Sci. 2012;37:106-26.

[36] Morch YA, Donati I, Strand BL, Skjak-Braek G. Effect of Ca2+, Ba2+, and Sr2+ on alginate microbeads. Biomacromolecules. 2006;7:1471-80.

[37] Oliveira SM, Almeida IF, Costa PC, Barrias CC, Ferreira MR, Bahia MF, et al. Characterization of polymeric solutions as injectable vehicles for hydroxyapatite microspheres. AAPS PharmSciTech. 2010;11:852-8.

[38] Olderoy MO, Xie M, Andreassen JP, Strand BL, Zhang Z, Sikorski P. Viscoelastic properties of mineralized alginate hydrogel beads. J Mater Sci Mater Med. 2012;23:1619-27.

[39] Oliveira SM, Barrias CC, Almeida IF, Costa PC, Ferreira MR, Bahia MF, et al. Injectability of a bone filler system based on hydroxyapatite microspheres and a vehicle with in situ gel-forming ability. J Biomed Mater Res B Appl Biomater. 2008;87:49-58.

[40] Ito T, Saito M, Uchino T, Senna M, Iafisco M, Prat M, et al. Preparation of injectable auto-forming alginate gel containing simvastatin with amorphous calcium phosphate as a controlled release medium and their therapeutic effect in osteoporosis model rat. J Mater Sci Mater Med. 2012;23:1291-7.

[41] Habib M, Baroud G, Gitzhofer F, Bohner M. Mechanisms underlying the limited injectability of hydraulic calcium phosphate paste. Part II: particle separation study. Acta Biomater. 2010;6:250-6.

[42] Khanarian NT, Jiang J, Wan LQ, Mow VC, Lu HH. A hydrogel-mineral composite scaffold for osteochondral interface tissue engineering. Tissue Eng Part A. 2012;18:533-45.

[43] Rowley JA, Madlambayan G, Mooney DJ. Alginate hydrogels as synthetic extracellular matrix materials. Biomaterials. 1999;20:45-53.

[44] Krebs MD, Salter E, Chen E, Sutter KA, Alsberg E. Calcium phosphate-DNA nanoparticle gene delivery from alginate hydrogels induces in vivo osteogenesis. J Biomed Mater Res A. 2010;92:1131-8.

[45] Kolambkar YM, Dupont KM, Boerckel JD, Huebsch N, Mooney DJ, Hutmacher DW, et al. An alginate-based hybrid system for growth factor delivery in the functional repair of large bone defects. Biomaterials. 2011;32:65-74.

[46] Grellier M, Granja PL, Fricain JC, Bidarra SJ, Renard M, Bareille R, et al. The effect of the co-immobilization of human osteoprogenitors and endothelial cells within alginate microspheres on mineralization in a bone defect. Biomaterials. 2009;30:3271-8.

[47] Abbah SA, Lu WW, Chan D, Cheung KM, Liu WG, Zhao F, et al. In vitro evaluation of alginate encapsulated adipose-tissue stromal cells for use as injectable bone graft substitute. Biochem Biophys Res Commun. 2006;347:185-91.

[48] Chang SC, Chung HY, Tai CL, Chen PK, Lin TM, Jeng LB. Repair of large cranial defects by hBMP-2 expressing bone marrow stromal cells: comparison between alginate and collagen type I systems. J Biomed Mater Res A. 2010;94:433-41.

[49] Marie PJ, Felsenberg D, Brandi ML. How strontium ranelate, via opposite effects on bone resorption and formation, prevents osteoporosis. Osteoporos Int. 2011;22:1659-67.

[50] Grynpas MD, Hamilton E, Cheung R, Tsouderos Y, Deloffre P, Hott M, et al. Strontium increases vertebral bone volume in rats at a low dose that does not induce detectable mineralization defect. Bone. 1996;18:253-9.

[51] Bonnelye E, Chabadel A, Saltel F, Jurdic P. Dual effect of strontium ranelate: stimulation of osteoblast differentiation and inhibition of osteoclast formation and resorption in vitro. Bone. 2008;42:129-38.

[52] Yang F, Yang D, Tu J, Zheng Q, Cai L, Wang L. Strontium enhances osteogenic differentiation of mesenchymal stem cells and in vivo bone formation by activating Wnt/catenin signaling. Stem Cells. 2011;29:981-91.

[53] Baron R, Tsouderos Y. In vitro effects of S12911-2 on osteoclast function and bone marrow macrophage differentiation. Eur J Pharmacol. 2002;450:11-7.

[54] Peng S, Liu XS, Huang S, Li Z, Pan H, Zhen W, et al. The cross-talk between osteoclasts and osteoblasts in response to strontium treatment: involvement of osteoprotegerin. Bone. 2011;49:1290-8.

[55] Baron R, Tsouderos Y. In vitro effects of S12911-2 on osteoclast function and bone marrow macrophage differentiation. European Journal of Pharmacology. 2002;450:11-7.

[56] Bonnelye E, Chabadel A, Saltel F, Jurdic P. Dual effect of strontium ranelate: Stimulation of osteoblast differentiation and inhibition of osteoclast formation and resorption in vitro. Bone. 2008;42:129-38.

[57] Takahashi N, Sasaki T, Tsouderos Y, Suda T. S 12911-2 Inhibits Osteoclastic Bone Resorption In Vitro. Journal of Bone and Mineral Research. 2003;18:1082-7.

[58] Hurtel-Lemaire AS, Mentaverri R, Caudrillier A, Cournarie F, Wattel A, Kamel S, et al. The Calcium-sensing Receptor Is Involved in Strontium Ranelate-induced Osteoclast Apoptosis: NEW INSIGHTS INTO THE ASSOCIATED SIGNALING PATHWAYS. Journal of Biological Chemistry. 2009;284:575-84.

[59] Marie PJ, Felsenberg D, Brandi ML. How strontium ranelate, via opposite effects on bone resorption and formation, prevents osteoporosis. Osteoporosis International. 2011;22:1659-67.

[60] Atkins GJ, Welldon KJ, Halbout P, Findlay DM. Strontium ranelate treatment of human primary osteoblasts promotes an osteocyte-like phenotype while eliciting an osteoprotegerin response. Osteoporosis International. 2009;20:653-64.

[61] Brennan TC, Rybchyn MS, Green W, Atwa S, Conigrave AD, Mason RS. Osteoblasts play key roles in the mechanisms of action of strontium ranelate. British Journal of Pharmacology. 2009;157:1291-300.

[62] Caverzasio J. Strontium ranelate promotes osteoblastic cell replication through at least two different mechanisms. Bone. 2008;42:1131-6.

[63] Chattopadhyay N, Quinn SJ, Kifor O, Ye C, Brown EM. The calcium-sensing receptor (CaR) is involved in strontium ranelate-induced osteoblast proliferation. Biochemical Pharmacology. 2007;74:438-47.

[64] Barbara A, Delannoy P, Denis BG, Marie PJ. Normal matrix mineralization induced by strontium ranelate in MC3T3-E1 osteogenic cells. Metabolism. 2004;53:532-7.

[65] Choudhary S, Halbout P, Alander C, Raisz L, Pilbeam C. Strontium Ranelate Promotes Osteoblastic Differentiation and Mineralization of Murine Bone Marrow Stromal Cells: Involvement of Prostaglandins. Journal of Bone and Mineral Research. 2007;22:1002-10.

[66] Zhu L-L, Zaidi S, Peng Y, Zhou H, Moonga BS, Blesius A, et al. Induction of a program gene expression during osteoblast differentiation with strontium ranelate. Biochemical and Biophysical Research Communications. 2007;355:307-11.

[67] Fromigué O, Haÿ E, Barbara A, Marie PJ. Essential Role of Nuclear Factor of Activated T Cells (NFAT)-mediated Wnt Signaling in Osteoblast Differentiation Induced by Strontium Ranelate. Journal of Biological Chemistry. 2010;285:25251-8.

[68] Delannoy P, Bazot D, Marie PJ. Long-term treatment with strontium ranelate increases vertebral bone mass without deleterious effect in mice. Metabolism. 2002;51:906-11.

[69] Buehler J, Chappuis P, Saffar JL, Tsouderos Y, Vignery A. Strontium ranelate inhibits bone resorption while maintaining bone formation in alveolar bone in monkeys (Macaca fascicularis). Bone. 2001;29:176-9.

[70] Ammann P, Shen V, Robin B, Mauras Y, Bonjour JP, Rizzoli R. Strontium ranelate improves bone resistance by increasing bone mass and improving architecture in intact female rats. J Bone Miner Res. 2004;19:2012-20.

[71] Ammann P, Badoud I, Barraud S, Dayer R, Rizzoli R. Strontium ranelate treatment improves trabecular and cortical intrinsic bone tissue quality, a determinant of bone strength. J Bone Miner Res. 2007;22:1419-25.

[72] Bain SD, Jerome C, Shen V, Dupin-Roger I, Ammann P. Strontium ranelate improves bone strength in ovariectomized rat by positively influencing bone resistance determinants. Osteoporos Int. 2009;20:1417-28.

[73] Peng S, Liu XS, Wang T, Li Z, Zhou G, Luk KD, et al. In vivo anabolic effect of strontium on trabecular bone was associated with increased osteoblastogenesis of bone marrow stromal cells. J Orthop Res. 2010;28:1208-14.

[74] Meunier PJ, Roux C, Seeman E, Ortolani S, Badurski JE, Spector TD, et al. The effects of strontium ranelate on the risk of vertebral fracture in women with postmenopausal osteoporosis. N Engl J Med. 2004;350:459-68.

[75] Reginster JY, Seeman E, De Vernejoul MC, Adami S, Compston J, Phenekos C, et al. Strontium ranelate reduces the risk of nonvertebral fractures in postmenopausal women with osteoporosis: Treatment of Peripheral Osteoporosis (TROPOS) study. J Clin Endocrinol Metab. 2005;90:2816-22.

[76] Abrahamsen B, Grove EL, Vestergaard P. Nationwide registry-based analysis of cardiovascular risk factors and adverse outcomes in patients treated with strontium ranelate. Osteoporosis International. 2014;25:757-62.

[77] Cooper C, Fox KM, Borer JS. Ischaemic cardiac events and use of strontium ranelate in postmenopausal osteoporosis: a nested case–control study in the CPRD. Osteoporosis International. 2014;25:737-45.

[78] Reginster JY, Neuprez A, Dardenne N, Beaudart C, Emonts P, Bruyere O. Efficacy and safety of currently marketed anti-osteoporosis medications. Best Practice & Research Clinical Endocrinology & Metabolism. 2014;28:809-34.

[79] Thormann U, Ray S, Sommer U, Elkhassawna T, Rehling T, Hundgeburth M, et al. Bone formation induced by strontium modified calcium phosphate cement in critical-size metaphyseal fracture defects in ovariectomized rats. Biomaterials. 2013;34:8589-98.

[80] Baier M, Staudt P, Klein R, Sommer U, Wenz R, Grafe I, et al. Strontium enhances osseointegration of calcium phosphate cement: a histomorphometric pilot study in ovariectomized rats. J Orthop Surg Res. 2013;8:16.

[81] Liu P, Wang N, Hao Y, Zhao Q, Qiao Y, Li H, et al. Entangled titanium fibre balls combined with nano strontium hydroxyapatite in repairing bone defects. Med Princ Pract. 2014;23:264-70.

CHAPTER II

IN VIVO AND CLINICAL APPLICATION OF STRONTIUM-ENRICHED BIOMATERIALS FOR BONE REGENERATION

Article 1

Published in Bone and Joint Research. 2017 Jun;6(6):366-375.

doi: 10.1302/2046-3758.66.BJr- 2016-0311.r1

In vivo and clinical application of strontium-enriched biomaterials for bone regeneration

Nuno Neves[a,b,c,d], Daniela Linhares[d,e], Gilberto Costa[c,d], Cristina C Ribeiro[a,b,f], Mário A Barbosa[a,b,g]

[a]i3S - Instituto de Investigação e Inovação em Saúde, Universidade do Porto, Rua Alfredo Allen, 208, 4200-135 Porto, Portugal

[b]INEB - Instituto de Engenharia Biomédica, Universidade do Porto, Rua Alfredo Allen, 208, 4200-135 Porto, Portugal

[c]FMUP - Faculdade de Medicina da Universidade do Porto, Departamento de Cirurgia, Serviço de Ortopedia, Alameda Prof. Hernâni Monteiro, 4200-319 Porto, Portugal

[d]CHSJ - Centro Hospitalar de São João, Orthopedic Department, Alameda Prof. Hernâni Monteiro, 4200-319 Porto, Portugal

[e]MEDCIDS - Faculdade de Medicina da Universidade do Porto, Alameda Prof. Hernâni Monteiro, 4200-319 Porto, Portugal

[f]ISEP - Instituto Superior de Engenharia do Porto, Instituto Politécnico do Porto, Rua Dr. António Bernardino de Almeida 431, 4249-015 Porto, Portugal

[g]ICBAS-Instituto de Ciências Biomédicas Abel Salazar, Universidade do Porto, Rua de Jorge Viterbo Ferreira 228, 4050-313 Porto, Portugal

Abstract

Objectives

This systematic review aimed to assess the in vivo and clinical effect of strontium (Sr)- enriched biomaterials in bone formation and/or remodelling.

Methods

A systematic search was performed in PubMed, followed by a two-step selection process. We included in vivo original studies on Sr-containing biomaterials used for bone support or regeneration, comparing at least two groups that only differ in Sr addition in the experimental group.

Results

A total of 572 references were retrieved and 27 were included. Animal models were used in 26 articles, and one article described a human study. Osteoporotic models were included in 11 papers. All articles showed similar or increased effect of Sr in bone formation and/or regeneration, in both healthy and osteoporotic models. No study found a decreased effect. Adverse effects were assessed in 17 articles, 13 on local and four on systemic adverse effects. From these, only one reported a systemic impact from Sr addition. Data on gene and/or protein expression were available from seven studies.

Conclusions

This review showed the safety and effectiveness of Sr-enriched biomaterials for stimulating bone formation and remodelling in animal models. The effect seems to increase over time and is impacted by the concentration used. However, included studies present a wide range of study methods. Future work should focus on consistent models and guidelines when developing a future clinical application of this element.

Keywords: Biomaterials, Strontium, Bone

Introduction

The treatment of fractures carries important challenges, especially when impaired bone healing or bone loss is present. Osteoporosis is increasingly found in Western countries as the population ages, leading to a significant rise in the incidence of specific fractures, where these problems are particularly evident [1]. New treatment options are needed to overcome the challenges associated with management of this condition.

Biological and synthetic bone grafts have been used to manage bone defects, and autografts are the current benchmark [2]. However, due to their limited availability, the morbidity associated with harvest surgery and the relatively poor performance of synthetic materials, especially under osteoporotic conditions, there is a need for the development of effective and safer alternatives [3, 4]. One proposed strategy has been the addition of osteoinductive factors or osteoprogenitor cells to a bone substitute, in order to improve osteogenesis, particularly when impaired healing response is expected [5-7].

Strontium (Sr) is a trace element that simultaneously stimulates bone formation and inhibits bone resorption [8-10]. Nevertheless, the cardiovascular safety of oral Sr ranelate is still a matter of concern as a small but significant increase in non-fatal myocardial infarctions has been reported [11-13], leading to strict indications and restrictions for its use [11].

Several pre-clinical studies, performed in both normal and osteoporotic animal models, were consistent with previous in vitro studies, showing the beneficial effect of Sr ranelate in increasing bone architecture and bone strength [14-16]. Accordingly, in order to enhance bone repair, Sr has recently been incorporated into different bone substitutes. This strategy aims to achieve a safer use of its osteoanabolic and anti-osteoclastic activity, as high concentrations are achieved locally, improving bone formation with less systemic impact. However, in vivo studies are scarce, and most reports do not present an adequate control group. Whether Sr-enriched materials are

effective and safe is still a matter of debate, and more information on local Sr use is needed, with uniform criteria.

The aim of this study was to systematically review the in vivo effect of Sr in bone formation and/or remodelling, when incorporated into biomaterials.

Materials and Methods

A systematic search was performed in Pubmed and Scopus, using as a search strategy a combination of “Strontium”, “Bone regeneration”, “osteogenesis” (and similar terms such as ("Bone Substitutes" or Bone) and “Biomaterials” (and equivalents such as "Biocompatible materials" or "materials Testing" or "Tissue Scaffolds" or "Biomimetic materials"). The search was limited by english language, human or other animal species (in Pubmed) and articles published after 1990 until July 2015. Additional papers were retrieved by non-systematic searches of relevant sources and screening of all retrieved article references (Fig. 1).

Increased bone regeneration was defined based on increased bone formation and/or increased bone remodelling. Two comparison groups were previously defined, as an experimental group (E), which received a Sr-enriched biomaterial for evaluation of bone support or regeneration, and a control group (C) that received a similar Sr-free material. The groups had to differ only in Sr addition to the biomaterial in order to be included. Subgroups were also defined when specific conditions were present in both experimental and control groups (such as osteoporosis).

The study was conducted in two phases (Fig. 1). In each phase, two independent reviewers (NN and DL) analysed the references and pooled according to predefined inclusion – A) studies with original data, B) on Sr doped materials, C) used for bone support or regeneration, D) performed in vivo – and exclusion criteria – E) articles without a control group only different from experimental on Sr addition to the biomaterial, F) on Sr usage only as a substitute on implant coating material, and G) if full-text not available (Fig. 1). In phase one, titles and abstracts were screened, and articles proceeded to the next phase upon inclusion of at least one reviewer. In phase two, full texts were assessed and disagreements were discussed between reviewers. When the full text was not available, authors were contacted and asked for a full-text copy. There was no article excluded due to unavailability of its full text.

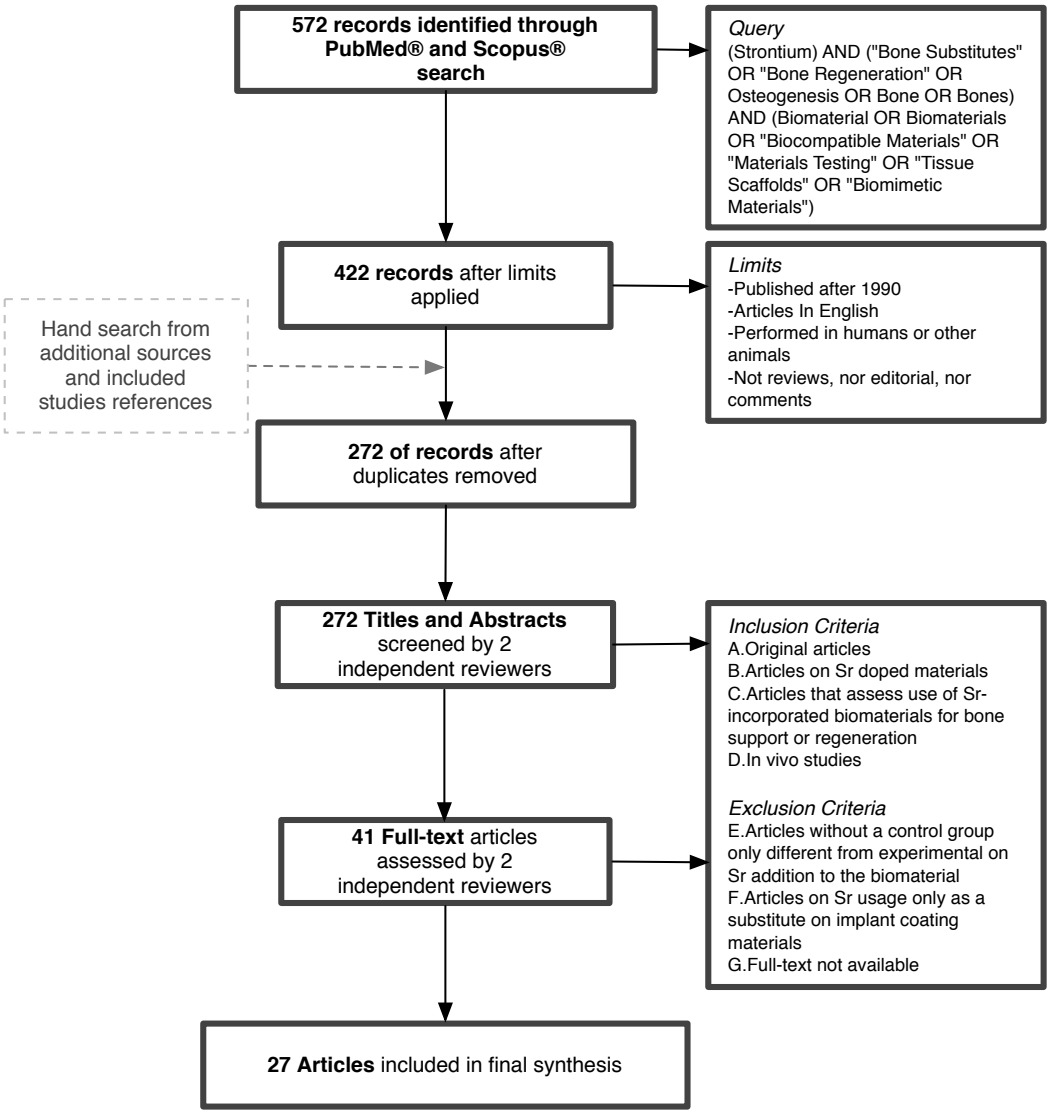

Fig 1. Flow diagram showing the study screening process.

Using an electronic form pre-developed by the authors, two investigators (NN and DL) performed data extraction. Qualitative results on the effect of Sr on bone regeneration were extracted independently of technique used for assessing Sr effect in each group. General results on implant effect were retrieved from individual papers, with data presented according to the amount of Sr in each biomaterial, time between material implantation and the analysis, and presence of concomitant conditions. The reported effect of Sr on bone formation, bone remodelling and its adverse effects were converted in a graphic summary table. Increased bone

formation was considered as higher reported bone formation, total bone volume or other similar reference. Enhanced bone remodelling was defined as advanced maturation stage, higher biomaterial degradation, and central versus peripheral bone formation or similar.

When available, data on significance from each study were also gathered, with a statistically significant value defined as $p<0.05$. Data on gene or protein expression were collected upon availability.

This systematic review was conducted based on Preferred reporting Items for Systematic reviews and meta-analyses (PRISMA) statement guidelines [17]. The PRISMA statement checklist is available as Supplementary material.

Results

A total of 572 references were retrieved after a literature search in Pubmed (210 references), and in Scopus (362 references), downgraded to 272 records after the application of exclusion criteria, the removal of duplicates, and the addition of hand and reference searches. In the title and abstracts selection phase, 231 records were excluded, mainly in vitro studies and studies on Sr's usage as a coating material, rather than as an implant for bone support or regeneration. In the full text selection phase, 41 papers were included. Four full texts were not available but were retrieved after contact with the authors. From these, 14 papers were excluded, mostly due to absence of control groups that received a Sr-free material, otherwise similar to the experimental material, and 27 articles were included in the final review (Fig. 1) [15, 16, 18-42].

General article information is available in Table I and general results on implant effect on Supplementary Table I. Rat models were used in 17 studies, nine were in rabbits and one in humans. The population of included studies ranged from four to 72 animals (Table I). Apart from two articles, the primary goal of the papers was to assess the effect of Sr-enriched materials in the models studied. The majority of bone defects were created in long bones, mainly in the femur (n = 18). Most of the defects were drilled and bilateral, with some studies using the same animal in the control and experimental groups. Three studies used segmental defects (Table I).

The major concomitant condition studied in the animal models was osteoporosis; two studies included models with and without osteoporosis, and nine included only osteoporotic animals. One study was performed on animals with osteonecrosis. In the remaining ten studies, all animals were healthy (Table I). The single article concerning humans included subjects who underwent a craniotomy due to different neoplastic and vascular conditions.

Time from implantation to analysis varied among the different studies, ranging from six days to 12 months. The studies used different materials. (Table I). Two sets

of studies used similar materials; eight on bioactive glass and five on hydroxyapatite (HA)/Calcium phosphate (CP) cements. Sr concentration in the E group ranged from 0.1% to 22% (Supplementary Table I). All but three studies performed histologic and/or histomorphometric analysis. Radiological analysis such as micro-CT, PET scan, radiograph or scintigraphy were used in 12 papers for imaging (Table I). Gene analysis and immunohistochemistry were available in two [21, 31] and six [16, 31, 34, 38, 40, 41] papers, respectively. Data on protein or gene expression are displayed in Figure 2.

ID	Animal	n		Concomitant conditions	Defect			Material		Analysis
		E	C		Type	mm	Location	E	C	
Banarjee [18]	Sprague Dawley rats	8	4	H	Bilateral drilled	3	Distal Femur	ß-TCP-MgO/SrO cylinders	ß-TCP cylinders	Hist
Bose [19]	Sprague Dawley rats	4	4	H	Bilateral drilled	3	Distal Femur	ß-TCP-MgO/SrO cylinders	ß-TCP cylinders	Hist
Boyd [20]	Wistar rats	12	12	O/H	Unilateral drilled	1	Midshaft Femur	Sr-Bioactive glass	Bioactive glass	Hist
Cardemil [21]	Sprague Dawley rats	32	32	O/H	Bilateral drilled	2.3	Distal Femur	Sr-CP granules	HA granules	Hist*; G
Cheng [22]	Sprague Dawley rats	22	21	O	Unilateral wedge	4	Distal Femur	Sr-CPC Xerogel particles Sr-Fe foam	CPC Xerogel particles Fe foam	PET
Cheng [23]	Sprague Dawley rats	7	7	O	Unilateral wedge	4	Distal Femur	Sr-CPC	CPC	PET
Dagang [24]	New Zealand White rabbits	2	2	H	Unilateral drilled	2.2	Distal Femur	Sr-HA cement	HA cement	Hist
Gorustovich [25]	Wistar rats	15	15	H	Bilateral drilled	1.5	Tibia	Sr-Bioactive glass	Bioactive glass	Hist*
Gu [26]	New Zealand White rabbits	12	12	H	Unilateral segmental	15	Radius	Sr-CPP scaffold	Sr-CPP scaffold	Hist*
Lin [29]	Fisher rats	3	3	O	Drilled (2 defects)	5	Calvarius	Sr-Ca Silicate scaffold	Ca Silicate scaffold	Hist*; µ-CT
Mohan [30]	New Zealand White rabbits	6	6	H	Unilateral segmental	15	Midshaft Ulna	Sr-CP cylinders	HA cylinders	Hist*; µ-CT
Thormann [16]	Sprague Dawley rats	15	15	O	Unilateral wedge	4	Distal Femur	Sr-CPC	CPC	Hist*; G; Immuno
Tian [31]	New Zealand White rabbits	24	24	H	Unilateral segmental	15	Radius	Sr-CPP scaffold	CPP scaffold	Hist*; X-ray; Immuno
Wei [32]	Wistar rats	6	6	O	Bilateral drilled	3	Distal Femur	Sr Bioactive glass	Bioactive glass	Hist*; µ-CT
Xie [33]	New Zealand white rabbits	NI	NI	H	Unilateral	15	Femur	K/Sr-CPP scaffold	CPP scaffold	Hist*;
Zhao [35]	Sprague Dawley rats	6	6	H	Drilled (2 defects)	5	Calvarius	Sr Bioactive glass	Sr Bioactive glass	Hist*; µ-CT
Zhang [34]	Wistar rats	NI	NI	O	Bilateral drilled	3	Distal Femur	Sr Bioactive glass	Bioactive glass	Hist*; µ-CT; G; Immuno
Baier [15]	Sprague Dawley rats	30	30	O	Unilateral drilled	2	Distal Femur	Sr-CPC	CPC	Hist*
Izci [27]	Humans	4	4	Other†	Unilateral drilled	15	Cranium	Si-Sr-HA peg	Si-HA peg	µ-CT; Scintigraphy
Li [28]	Wistar rats	20	20	H	Bilateral drilled	3	Proximal Tibia	Sr-CaS paste	CaS paste	Hist*; µ-CT; X-ray

ID	Animal	n		Concomitant conditions	Defect			Material		Analysis
		E	C		Type	mm	Location	E	C	
Jebahi [36]	Wistar rats	5	5	O	Unilateral drilled	3	Distal Femur	Sr Bioactive glass	Bioactive glass	Hist*
Jebahi [37]	Wistar rats	5	5	O	Unilateral drilled	3	Distal Femur	Sr Bioactive glass	Bioactive glass	Hist*
Kang [38]	Japanese White rabbits	18	18	ON	Unilateral drilled	3	Proximal Femur	Sr-CPP scaffold and MNCs	CPP scaffold and MNCs	Hist*; X-ray; Immuno
Tarafder [39]	Sprague Dawley rats	4	4	H	Bilateral drilled	3	Distal Femur	ß-TCP-MgO/SrO cylinders	ß-TCP cylinders	Hist*
Tarafder [40]	New Zealand White rabbits	2	2	H	Bilateral drilled	5.5	Distal Femur	ß-TCP-MgO/SrO cylinders	ß-TCP cylinders	Hist*; Immuno
Xie [41]	New Zealand White rabbits	9	9	H	Unilateral	15	Femur Shaft	K/Sr-CPP scaffold	CPP	Hist*; X-ray; Immuno
Zhang [42]	New Zealand White rabbits	6	6	H	Unilateral drilled	6	Distal Femur	Sr-Borate Bioactive glass	Borate Bioactive glass	Hist*

Table I. Description of the sample and methods of the studies included

Results stated by each paper on the effect of the Sr-enriched biomaterial in bone formation and/or remodelling are displayed in Supplementary Table I. Although five studies reported analysis with multiple Sr concentrations, only in three did the authors gather information on the comparison between materials with different Sr content. In two studies, a significant superior overall effect was found with materials enriched with higher Sr concentration; the other study that looked at various concentrations found non-significant differences. Only one article reported the differential effect between healthy specimens and those with osteoporosis, finding an increased effect in osteoporotic animals (Supplementary Table I).

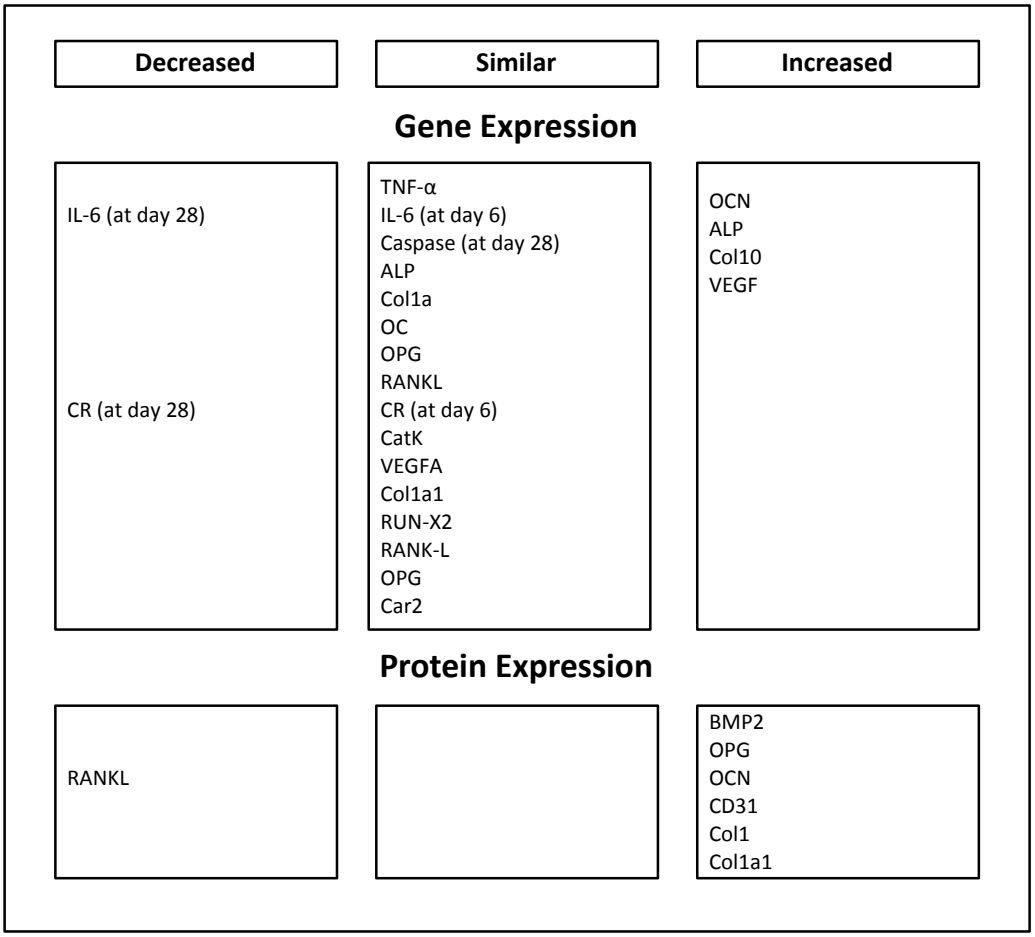

Fig. 2. Summary of study results on gene and protein expression. When different results from different study times were available, they were stated.

A graphic analysis on the result of the effect of the studied biomaterial in bone formation and remodelling, along with a summary of adverse effects reported by each paper, is presented in Table II. Two articles studying bone formation reported a similar effect in the E and C groups; another one reported similar effects only in osteoporotic animals but an increased effect in healthy ones [20]. Baier et al [15] only found significant differences in the third month in both bone formation and remodelling. Cheng et al [22] studied three materials, with different compositions, but only one material, calcium phosphate cement (CPC), resulted in an increased effect on the experimental group. Apart from these, all other studies with analysis on bone formation found an increased effect of enriched material (Tables II and III). Of the

studies with reports on bone remodelling, four showed similar results in experimental and control, four found an increased effect in experimental only in late study phases, and 17 reported an increased effect in the experimental group in all studied times (Table III).

Article	Strontium content	Time	Bone formation	Bone remodelling	Adverse reaction	Inflammatory reaction
Bose, 2011 [18]	1 wt%	4 wks	Increased	NI		
		8 wks	Increased	NI		
		12 wks	NI	Increased		
		16 wks	NI	Increased		
Tian, 2009 [31]	1 wt%	4 wks	Increased *	Similar	L ↔	No
		12 wks	Increased *	Similar		
		16 wks	Increased *	Similar		
Xie, 2012 [33]	2 wt%	4 wks	Increased	Similar		
		8 wks	Increased	Similar		
		12 wks	Increased	Increased		
		Overall	Increased	Increased	L ↔	No
Dagang, 2008 [24]	5/10 wt%	4/8/12/24 wks	Similar	Increased	L ↔	No
Gorustovich, 2010 [25]	6 wt%	30 days	NI	Similar	L ↔	No
Gu, 2013 [26]	11.5 Ca/Sr MR	4 wks	NI	Increased	L ↔	No
		8 wks	NI	Increased	L ↔	No
		16 wks	Increased	Increased	L ↔	No
		Overall	Increased	Increased		
Banarjee, 2010 [18]	0.25/1 wt%	4/16 wks	NI	Increased		
Li, 2014 [28]	5/10 wt%	4 wks	Increased	Similar		
		8 wks	Increased	NI		
		12 wks	Increased	Increased		
Mohan, 2012 [30]	1.67 (Ca+Sr)/P MR	4/12 wks	Increased *	Increased *	L ↔	No
Zhao, 2015 [35]	10 wt%	8 wks	Increased *	Increased *		
Izci, 2013 [27]	NI	3/6/12 mths	Increased	Similar	L ↔	No
Kang, 2015 [38]	11.5 Ca/Sr MR	4/8/12 wks	Increased *	Increased *	L ↔	No
Tarafder, 2013 [39]	1 wt%	4 wks	Increased *	Increased *		
		8 wks	Increased *	Increased *	S (Similar Mg and Sr excretion in urine)	
		12 wks	Increased *	Increased		
		16 wks	Similar	NI		
Tarafder, 2014 [40]	1 wt%	8/12 wks	Increased *	Increased *		
Xie, 2013 [41]	11.5 Ca/Sr MR	4 wks	Similar	Increased	L ↔	No
		8 wks	Increased	Increased	L ↔	No
		12 wks	Increased	Increased	L ↔	No
Zhang, 2015 [42]	9 mol% SrO	4/8 wks	Increased *	Increased *	L ↔	No

Article	Strontium content	Time	Bone formation	Bone remodelling	Adverse reaction	Inflammatory reaction
Boyd, 2009 [20]	0.14 SrO Mol Fract	4 wks	NI	Similar	L ↔	No
	0.28 SrO Mol Fract	4 wks	Increased	NI	L ↔	No
			Similar	NI		
Cardemil, 2013 [21]	NI	6 days	Similar	NI	L ↔	Yes
		28 days	Similar	Increased *		
		6 days	Similar	NI		
		28 days	Similar	Increased *		
Wei, 2014 [32]	5 wt%	2 wks	Similar	Similar		
		4 wks	Increased *	NI		
		8 wks	Increased *	Increased		
Thormann, 2013 [16]	0.123 Sr/Ca MR	6 wks	Increased *	Increased *		
Zhang, 2013 [34]	2.5 wt%	2 wks	Increased *	Increased *		
		4 wks	Increased *	Increased *	S Increased * (Significant Sr increase in blood and urine samples)	
		8 wks	Increased *	Increased/ Similar		
	5 wt%	2 wks	Increased *	Increased *		
		4 wks	Increased *	Increased *		
Baier, 2013 [15]	NI	1 mth	Similar	Similar		
		3 mths	Similar	Similar	S (Similar spine and contralateral BMD)	
		6 mths	Increased*	Increased *		
Lin, 2013 [29]	10 wt%	4 wks	Increased *	Increased *		
Cheng, 2014 [22]	CPC – 8.36 wt%	6 wks	Increased	NI		
	Xerogel – 20 wt%		Similar	NI		
	Iron Foam – 22 wt%		Similar	NI		
Cheng, 2014 [23]	8.36 wt%	6 wks	Increased	NI		
Jebahi, 2012 [36]	0.1%	60 days	Increased	Increased	S (Similar blood cell counts and similar Ca and P blood levels)	
Jebahi, 2013 [37]	0.1%	90 days	Increased *	Increased *	L ↔	No

Table II. Summary of general results on bone formation and bone remodelling from individual studies. Results are presented according to the content of Sr used in the biomaterial and the average time from implantation to evaluation
*Shaded cells represent results from osteoporotic models. *Statistically significant difference between experimental and control wt%, weight percentage; MR, molar ratio; Mol Fract, Molar Fraction; d, days; w, weeks; m, months; NI, No Information; L, local; S, Systemic; CPC, Calcium Polyphosphate Cement; BMD, Bone mineral Density ↔ Similar in experimental and control*

No study found a decreased effect of Sr addition in bone formation and/or regeneration when compared with controls. Overall, two articles had no report on bone remodelling, and another two did not report on bone formation.

Of the 17 articles with results on adverse effects of the implanted biomaterial, 13 reported similar local secondary effects in experimental and control. From these,

12 found no inflammatory reaction and one showed increased inflammation in both experimental and control. One article reported increased systemic effects of Sr application, with significantly raised levels of this ion in urine and blood samples, and the other three articles found no differences in systemic effects of Sr application.

Time (wks)	Healthy					Osteoporosis				
	No of articles	Bone formation		Bone remodelling		No of articles	Bone formation		Bone remodelling	
		Increased*	Similar†	Increased*	Similar†		Increased*	Similar†	Increased*	Similar†
1	1	1	0	0	0	1	1	0	0	0
2	0	0	0	0	0	2	1	1	1	1
4	14	3	8	5	8	6	3	3	1	3
6	0	0	0	0	0	3	2‡	3‡	0	1
8	10	1	8	1	7	3	0	3	0	3
12	10	1	8	2	7	2	1	1	1	1
16	5	1	2	1	3	0	0	0	0	0
24	2	1	1	1	1	1	0	1	0	1
48	1	0	1	1	0	0	0	0	0	0

Table III. Number of studies stating a specific result on bone formation and bone remodelling according to the time from implantation to evaluation. The single article on osteonecrosis was excluded from this analysis. *†experimental versus control; *experimental versus control; ‡Cheng, 2014 [35] have different materials*

Discussion

This is the first systematic review that summarizes the in vivo effect in bone formation and remodelling of Sr-enriched biomaterials. Overall, Sr improves bone formation and remodelling, leading to a higher response when compared with similar Sr-free materials. Sr effect is present even in osteoporotic environments and some studies report greater effects in these models (Supplementary Table I). Our results are in agreement with other reviews on other enriching elements [43, 44] and with previous in vitro results on Sr [9, 45-50].

Bone formation and remodelling: timing, models and health status

From the 25 articles with results on bone formation, 23 report some kind of improvement in the experimental group. Although not all state a benefit in all study points, we observed that the Sr effect appears mostly in the later stages of each study. In fact, a tendency to an increase in the number of studies reporting a stronger effect of Sr in bone formation in later study points is observed when analysing studies according to the time of evaluation, as seen in Table III. Conclusions from studies with earlier assessment points therefore may be premature to differentiate the bone reaction between experimental and control. This may explain why Cardemil et al [21] found no differences, since the study ended just four weeks after implantation. However, some authors reported a significant improvement in experimental even at weeks two and four. One can argue that response to Sr may be influenced by the amount of time that the bone is exposed to this component.

Few studies report similar effects on bone formation in experimental and control, and for each study time the number of studies reporting increased effect in experimental versus control is at least similar to the number of studies stating equal effects. When considering bone remodelling, fewer results are available, and the number of studies reporting increased bone formation and remodelling in experimental is only superior after six weeks. These results on bone formation and

remodelling are valid, independent of the model's health status. This confirms previous reports on Sr, as a stimulator of bone differentiation and osteogenesis [9, 45-50]. However, the optimal conditions for its usage are yet to be determined, in order to maximize its beneficial effects. Moreover, no study showed decreased bone formation or remodelling in experimental, in any time period, for either healthy or diseased models. The presence of a beneficial effect of Sr even in osteoporotic models, may enhance its therapeutic value, since osteogenesis impairment is a major challenge in this condition [4].

Biomaterials

We decided to consider Strontium Calcium Phosphate (SrCaPO4) and Sr-HA as similar materials, since SrCaPO4 results from incorporation of Sr into HA [40]. However, it is known that incorporation of Sr into HA may impact its solubility [21], which may partially explain why only articles using biomaterials with Sr-HA showed no improved effect in E. Although Mohan et al [30] found a significant improvement in E using HA as a base material, we cannot make any comparison with the two other articles using HA since different defect models were used.

The rate of Sr release from the biomaterial was also identified as a possible factor impacting its activity, since osteoblast-like cells use the strontium released from the biomaterial to synthesize their mineralised extracellular matrix [51]. Thormann et al [16] showed higher Sr concentrations in zones of increased bone formation, supporting this finding. More studies on the relationship between Sr concentrations and bone formation are needed to clarify this theory.

Sr content

Our study also showed that even small amounts of Sr might be enough to have an impact on both bone formation and remodelling since some authors found significant differences with only 0.1% of this component [36, 37]. However, two of the

three authors who specifically compared different Sr percentages found an increased overall response with higher concentrations [23, 24], confirming previous in vitro reports [52]. The other author reported similar results between E and C [28]. All three authors agree that the optimum dose of Sr is yet to be discovered, since it can impact both the bone response and material properties [24, 28, 34].

Gene expression

The available information on Sr impact on gene expression can be seen in Figure 2. Broadly speaking, little variation was found but a decrease in the pro-inflammatory cytokine Il-6, a stimulator of osteoclast recruitment and bone reabsorption, related to altered bone metabolism, may help to explain the Sr effect as a promoter of bone formation and remodelling [53]. The increase in genes and proteins involved in these processes, such as osteocalcin and bone morphogenetic protein supports our reported results of Sr's bone forming effects [53].

Side effects

As previously stated, Sr systemic side effects were responsible for a downgrading of its interest for the scientific community, and for a move to local application of this component [11-13]. Our review found only four studies on the systemic repercussion of local Sr application. While one study reported increased levels of Sr in both urine and blood samples [34], another showed similar urinary excretion of this element [39]. The other two studies found no difference between experimental and control groups [15, 36]. One study reported increased values of serum Sr, but no comparison with C was performed, and the authors state that the concentration was 100 times lower than that needed to produce systemic effects [15]. Nevertheless, the pathological effects of these findings are not well known and still a matter of debate for future studies. A total of 13 reported on local effects, but no differences were found from C, and only one study found an increased

inflammatory reaction, both in experimental and control. Also, the short follow-up of most included studies impacts the ability to trace reliable conclusions on the adverse long-term effect of Sr.

Methodologies and limitations

The methods of the included studies were highly variable. First, different animal models were used, and only nine studies presented the same animal species. This can impact the results since it is known that both bone architecture and the regeneration process are different among species, posing problems when it comes to comparisons between studies [54, 55]. Also, all studies in animals used small species, with known differences in bone macroscopic, microscopic and remodelling properties when compared with humans [55]. Although larger animals, like dog and sheep, present a more reliable model, they may pose more ethical, housing, handling and availability issues [54, 55]. These variations between species may, at least partially, explain the different responses to the biomaterial found in the included studies. Only one article studied the application of Sr-enriched biomaterials in humans [27]. Although achieving an increased effect of Sr, the constraints of study design impact our ability to draw reliable conclusions. Even in the same species, defects differ in size, type and location. All studies that created a segmental defect found an increased effect of Sr on both bone formation and remodelling independent of the study time. This did not happen with other types of defect. One may suppose that segmental defects, with a greater impact on bone macrostructure, may influence either bone response, with the possibility of stimulation of a quicker reaction, or the ability to retrieve reliable results in the early stages. Guidelines are not available regarding the appropriate defect needed for each case, and a recent study pointed out that differences in defect creation impact the bone response [54]. More accurate and homogeneous lines of conduct are essential for the future design of comparable and reproducible study models.

As stated before, time to healing evaluation is variable among studies. Previous reports stated that fracture consolidation with a neocortex consisting of woven and lamellar bone is usually completed in an average of five to six weeks. However, different models, and even different bone defects, can alter this timeline [56].

Different methods for evaluation of response were found. Qualitative measurements, such as histology or imaging techniques, are observer-dependent subjective analyses, introducing bias to the reported results [57]. This may explain why Dagang, Kewei and Yong [24] found no significant differences between E and C since this study performed only a histological analysis. Our review has other limitations. Only 27 studies were retrieved. From these, 20 presented numeric results from histological analysis, but a quantitative synthesis of data was not possible since only a few performed comparable measurements of bone formation and/or remodelling. These studies, along with those with only qualitative data, were included in the review, allowing a broad qualitative assessment of published studies but no meta-analysis was performed. The definition of bone formation and bone remodelling was subjective and different in each study. Two reviewers performed the selection of relevant results but the absence of strict definitions increases the risk of bias. Many studies, especially those with only qualitative data assessment, did not present the significance of the comparisons, increasing the subjectivity of their interpretation.

Future studies must follow appropriate protocols, and guidelines on results assessment for each technique should be drafted. The application of Sr in larger animal models, with longer follow-up times, is needed, with an appropriate monitoring of long-term local and systemic side effects. More studies on the comparison between diseased and healthy models, and between different Sr concentrations, would be of great importance to better understand the potentiality of this element.

In conclusion, Sr is an apparently safe and effective doping material for stimulating bone formation and remodelling. Its effect may be more pronounced and

variable over time according to the concentration applied. Additionally, its benefit in osteoporotic models raises the possibility of its therapeutic value. However, the plethora of methods, measurements and protocols found in individual studies impacts the ability to perform a reliable data synthesis and analysis on Sr effect. It is important to develop adequate models and follow consistent guidelines of research in future studies, in order to better define the therapeutic application of this element.

Article focus

- Systematic review
- Assess the in vivo effect of Sr-enriched biomaterials in bone formation and/or remodelling

Key messages

- Increased bone formation and/or remodelling in biomaterials enriched with Sr
- Sr effect is impacted by time and concentration

Strengths and Limitations

- First systematic review of Sr-enriched biomaterials
- Inclusion of studies with heterogeneous methods may impact comparability

Supplementary Material

ID	Strontium content	Time	Results
Bose [19]	1 wt%	4 wks	Increased bone formation in E *versus* C
		8 wks	Increased bone formation in E *versus* C
		12 wks	Presence of bone remodelling in E *versus* no bone remodelling in C
		16 wks	Bone remodelling with compact interface bone-implant in E *versus* fibrous interface in C
Tian [31]	1 wt%	4 wks	Similar observation of new bone in the margins of the implant, with no new bone formation in the centre in E and C. Increased number of osteoblasts (measurement of active bone formation) and presence of woven type of new bone in E *versus* C
		12 wks	Increased newly formed bone in E *versus* C; Presence of active osteoblasts in E and numerous osteoblasts in C; Presence of degradation of the scaffold in E
		16 wks	Presence of new bone regenerated and penetrated through the interconnective pores in E *versus* no new bone and only fibrous tissue in the centre of the scaffolds and increased quantity and density of the defected area in C
		Overall	Significantly increased percentage of new bone volume in E; Similar degradability and degradation rate in E and C Radiograph: Illegible bone boundary with implant in E and C
Xie [33]	2 wt%	4 wks	Increased bone volume in E *versus* C; Clearly visible interfaces of all the scaffolds in E and C
		8 wks	Increased bone volume in E *versus* C; Presence of new bone formation in the centre and similar degradation in E and C
		12 wks	Increased bone volume in E *versus* C; Large new bone in the centre of scaffolds with trabecular structure encasing the scaffold in E *versus* new bone regenerated and penetrated through the interconnective pores to the margin in C
		Overall	Incorporation of Sr decreased significantly the number of osteoclasts;
Dagang [24]	5 wt%	4/8/12/24 wks	Higher degradability and mature bone (measured by haversian canals) in E *versus* C; similar/no inflammation reaction, no fibrous membrane on the interface, slight surface absorption in E and C. No significant differences in newly formed bone.
	10 wt%		Higher degradability, mature bone (measured by haversian canals) and surface absorption (obvious absorption pores) in E *versus* C; similar no inflammation reaction, no fibrous membrane on the interface in E and C. No significant differences in newly formed bone. Sr 10% *versus* Sr 5%: higher degradation and higher absorption pores
Gorustovich [25]	6 wt%	30 days	Similar affinity index (direct contact area), no fibrous layer, no macrophage and no inflammatory cells in the interface in E and C; EDX analysis with similar bond to bone through a calcium-phosphorus interface in E and C
Gu [26]	11.5 Ca/Sr MR	4 wks	Newly formed bone within and surrounding all the scaffolds in E *versus* only around the scaffolds in C
		8 wks	Presence of woven bone in E
		16 wks	Similar repair of most of the defect in E and C; greater ratio of newly formed bone/residual materials in E *versus* C
		Overall	Superior osteogenic capacity in E; Scaffold/bone boundary became illegible in E
Banarjee [18]	0.25/1 wt%	4 to 16 wks	Presence of new bone on the pre-existing cortical bone and on the implant in E *versus* only on the pre-existing cortical bone in C
Li [28]	5 wt%	4 wks	Immature bone trabeculae and cancellous bone in E *versus* original repair in the defect area in C. Radiograph: presence of reabsorption in experimental and control
		8 wks	Well organised mature bone trabeculae in E *versus* immature bone trabeculae in C
		12 wks	Complete cortical repair in E *versus* cortical bone tissue with many voids in C. Radiograph: implant was not noted radiographically and the cortex closed in E and C; Slower resorption rates and more compact bone repair in E *versus* C
	10 wt%	4 wks	Well differentiated bone trabeculae in E *versus* original repair in the defect area in C. Radiograph: Presence of reabsorption in E and C
		8 wks	Regeneration of incomplete cortical surface at the same level of the adjacent cortical plate in E *versus* immature bone trabeculae in C
		12 wks	Complete cortical repair in E *versus* cortical bone tissue with many voids in C. Radiograph: Implant was not noted radiographically and the cortex closed in E and C; Slower resorption rates and more compact bone repair in E *versus* C
	Overall	Overall	Micro-CT new bone formation and sporadic trabecular bone in the marrow canal in E and C; Improved new cortex formation in E *versus* C; significantly higher BMD and bone volume (relation BV/TV) in E *versus* C Sr 10% *versus* 5%: Non-significant difference in BMD and bone volume (relation BV/TV) in E *versus* C

ID	Strontium content	Time	Results
Mohan [30]	1.67 (Ca+Sr)/P MR	4 wks	Significantly more newly formed bone in E *versus* C
		12 wks	Significantly more newly formed bone and material degradation in E *versus* C. Increased prominence of mature lamellar bone in E *versus* C
		Overall	Micro-CT: Increased bone volume, fraction trabecular number, trabecular thickness and bone density in E *versus* C
Zhao [35]	10 wt%	8 wks	Significantly higher mineralisation levels and new bone area in E *versus* C; Significantly lower material residual area in E *versus* C Micro-CT: Significantly superior bone volume (relation BV/TV), BMD and significantly higher blood vessel area and blood vessel number in E *versus* C
Izci [27]	NI	3/6/12 mths	Scintigraphy: Superior osteoblastic activity in E *versus* C. Micro-CT: Osseo-integration in E and C
Kang [38]	11.5 Ca/Sr MR	4 wks	Significantly more newly formed bone in E *versus* C
		12 wks	Significantly higher defect repair and newly formed bone in E *versus* C. Radiograph: significantly higher trapdoor cartilage and defect repair in E *versus* C
Tarafder [39]	1 wt%	4 wks	Significantly higher bone area fraction (total newly formed bone area/total area) and osteoid area fraction (osteoid area/total area) in E *versus* C
		8 wks	Significantly higher bone area fraction and osteoid area fraction in E *versus* C
		12 wks	Significantly higher bone area fraction in E *versus* C. Completely mineralised bone formation in E *versus* presence of osteoid in C
		16wks	Similar bone area fraction in E *versus* C
Tarafder [40]	1 wt%	8 wks	Osteoid-like new bone formation E *versus* no osteoid-like new bone formation in C; Significantly higher bone area fraction (total newly formed bone area/total area) and osteoid area fraction (osteoid area/total area) in E *versus* C
		12wks	Significantly higher bone area fraction in E *versus* C; Significantly higher haversian canal area (haversian canal area/total area) in E *versus* C
Xie [41]	11.5 Ca/Sr MR	4 wks	Similar newly formed bone in E *versus* C; Similar new bone formation in the margins with no new bone in the centre of the implant in E and C; Higher degradability in E *versus* C
		8 wks	Higher newly formed bone in E *versus* C; Sporadic new bone formation in the centre of the implant in E *versus* no new bone in the centre in C
		12 wks	Higher newly formed bone in E *versus* C; Similar close union between implant and host bone in E and C; Trabecular bone in the centre of the implant in E *versus* only on the margins in C
Zhang [42]	9 mol% SrO	4/8 wks	Significantly higher bone-implant contact index in E *versus* C; Significantly lower Tb.Pf (Trabecular Bone Pattern Factor) in E *versus* C. Micro-CT: Significantly higher bone volume (relation BV/TV) in E *versus* C
Boyd [20]	0.14 SrO Mol Fract	4 wks	Mixed response of bone and fibrous tissue and no medullary inflammation in E and C
	0.28 SrO Mol Fract	4 wks	Presence of direct bone formation and no medullary inflammation in E
			Cortical healing in 3 of 6 of E and 2 of 6 of C; Similar bone marrow bone formation in E and C
Cardemil [21]	NI	6 days	Presence of local inflammatory reaction, with more new blood vessels and similar osteogenesis in E *versus* C
		28 days	Non-significantly higher proportion of bone at the centre of the defect in C *versus* significantly higher proportion of bone at the periphery of the defect in E; Significantly greater decrease in percentage of granule area in E *versus* C; less easily distinguished bone-granule interface in E; Bone formation in E and C
		6 days	Idem 6d
		28 days	Significantly higher proportion of bone at the centre of the defect in C *versus* significantly higher proportion of bone at the periphery of the defect in E; Significantly greater decrease in percentage of granule area in E *versus* C; less easily distinguished bone-granule interface in E; Bone formation in E and C Osteoporotic *versus* non-osteoporotic in E: trend to higher total-bone percentage; Significantly higher percentage of bone at the periphery
Wei [32]	5 wt%	2 wks	Similar new bone formation, presence of bone regeneration and woven trabecula in E and C
		4 wks	Significantly more new bone in E *versus* C
		8wks	Significantly more new bone, and superior bone thickness in E *versus* C
		Overall	Higher degradation rate and rate of new bone formed in E *versus* C Micro-CT: Increased bone volume fraction in E *versus* C
Thormann [16]	0.123 Sr/Ca MR	6 wks	Statistically higher new bone formation in E (also increased fragmentation and osteoid formation) *versus* C; Significantly more bone formation at the bone-biomaterial interface region in E *versus* C; Significantly higher TRAP-positive cells in E *versus* C

ID	Strontium content	Time	Results
Zhang [34]	2.5 wt%	2 wks	Similar percentage of bone regeneration in E and C; Micro-CT: Significantly superior bone volume (relation BV/TV), trabecular number and trabecular thickness and significantly inferior trabecular separation in E *versus C*
		4 wks	Significantly higher percentage of bone regeneration in E *versus* C; Presence of maturing trabecula forming lamellar bone with osteoclasts involving the bone remodelling in E *versus* dispersed or scattered newly formed bone in C. Micro-CT: Significantly superior bone volume (relation BV/TV), trabecular number and trabecular thickness and significantly inferior trabecular separation in E *versus* C
		8 wks	Significantly higher percentage of bone regeneration in E *versus* C; Greater amount and thickness of trabecula, with plenty of osteocytes clearly visible in the mineralised bone matrix in E *versus* C Micro-CT: Significantly superior bone volume (relation BV/TV), and trabecular thickness, similar trabecular number and trabecular separation in E *versus* C
	5 wt%	2 wks	Similar percentage of bone regeneration in E and C Micro-CT: Significantly superior bone volume (relation BV/TV), trabecular number and trabecular thickness and significantly inferior trabecular separation in E *versus* C Sr 5% *versus* Sr 2.5%: Similar percentage of bone regeneration; Micro-CT: Significantly superior bone volume (relation BV/TV), trabecular number and trabecular thickness, and significantly inferior trabecular separation in E *versus* C
		4 wks	Significantly higher percentage of bone regeneration in E *versus* C. Micro-CT: Significantly superior bone volume (relation BV/TV), trabecular number and trabecular thickness, and significantly inferior trabecular separation in E *versus* C Sr 5% *versus* Sr 2.5%: Micro-CT: Significantly superior bone volume (relation BV/TV), trabecular number and trabecular thickness, and significantly inferior trabecular separation in E *versus* C
		8 wks	Significantly higher percentage of bone regeneration in E *versus* C. Micro-CT: Significantly superior bone volume (relation BV/TV), and trabecular thickness, similar trabecular number and significantly inferior trabecular separation in E *versus* C. Sr 5% *versus* Sr 2.5%: Significantly higher percentage of bone regeneration; Micro-CT: Significantly superior bone volume (relation BV/TV) and trabecular thickness, similar trabecular number and trabecular separation in E *versus* C
Baier [15]	NI	1 mth	Similar circumferential contact index, ingrowth index, implant discontinuities and implant discontinuities containing newly formed bone in E and C
		3 mths	Significantly higher circumferential contact index, ingrowth index, implant discontinuities and implant discontinuities containing newly formed bone in E *versus* C
		6 mths	Non-significantly higher circumferential contact index in E *versus* C; Significantly higher ingrowth index, implant discontinuities and implant discontinuities containing newly formed bone in E *versus* C
Lin [29]	10 wt%	4 wks	Significantly higher mineralised tissue, newly formed bone and blood vessels in E *versus* C; Significantly lower remnant scaffold area in E *versus* C. Micro-CT: Increased newly formed bone area, significantly increased new bone mineral density, higher bone volume/total volume ratio and higher trabecular thickness in E *versus* C
Cheng [22]	CPC – 8.36 wt% Xerogel – 20 wt% Iron Foam – 22 wt%	6 wks	PET scan: Significant increase in bone formation in the biomaterial-bone interface in E *versus* C; Non-significant differences in defect region in E *versus* C PET scan: No significant differences in bone formation in E *versus* C PET scan: No significant differences in bone formation in E *versus* C
Cheng [23]	8.36 wt%	6 wks	PET scan: Increased bone formation in E *versus* C
Jebahi [36]	0.1 wt%	60 days	Similar presence of newly formed bone in E and C; Highly cellular layer, more advanced ossification and more bone regeneration in E *versus* sparser osteoid deposition in C
Jebahi [37]	0.1 wt%	90 days	Significantly superior bone volume (relation BV/TV), osteoblast number and Ob.S/BS in E *versus* C; Significantly lower Oc.S/BS and OV/BV in E *versus* C; Similar mineralising surface (MS/CS) in E and C; EDX analysis showed higher bioactivity in bone-implant surface E *versus* C

Supplementary Table I. Studies showing individual results of Sr effect on bone formation and/or bone remodelling. Results are presented according to the content of Sr used in the biomaterial and the average time from implantation to evaluation. *E, Experimental; C, Control; w, weeks; d, days; m, months; wt%, weight percentage; MR, Molar Ratio; Mol Fract, Molar Fraction; CT, Computed Tomography; PET, Positron-Emission Tomography; EDX, Energy-dispersive X-ray analysis; BMD, Bone Mineral Density; BV/TV, Bone Volume/Total Volume; Ob.S/BS, Osteoblast/Bone Surface; OV/BV, Osteoid/Bone Surface; Oc.S/BS, Osteoclast/Bone Surface; MS/CS, Mineralising Surface. When available, comparisons among study times or Sr doses are presented. Unless stated otherwise, results are from histology and/or histomorphometric analysis. Shaded cells represent results from osteoporotic models.*

Section/topic	#	Checklist item	Reported on page #
TITLE			
Title	1	Identify the report as a systematic review, meta-analysis, or both.	1
ABSTRACT			
Structured summary	2	Provide a structured summary including, as applicable: background; objectives; data sources; study eligibility criteria, participants, and interventions; study appraisal and synthesis methods; results; limitations; conclusions and implications of key findings; systematic review registration number.	1
INTRODUCTION			
Rationale	3	Describe the rationale for the review in the context of what is already known.	1/2
Objectives	4	Provide an explicit statement of questions being addressed with reference to participants, interventions, comparisons, outcomes, and study design (PICOS).	2
METHODS			
Protocol and registration	5	Indicate if a review protocol exists, if and where it can be accessed (e.g., Web address), and, if available, provide registration information including registration number.	N/A
Eligibility criteria	6	Specify study characteristics (e.g., PICOS, length of follow-up) and report characteristics (e.g., years considered, language, publication status) used as criteria for eligibility, giving rationale.	2/Figure 1
Information sources	7	Describe all information sources (e.g., databases with dates of coverage, contact with study authors to identify additional studies) in the search and date last searched.	2/Figure 1
Search	8	Present full electronic search strategy for at least one database, including any limits used, such that it could be repeated.	2/Figure 1
Study selection	9	State the process for selecting studies (i.e., screening, eligibility, included in systematic review, and, if applicable, included in the meta-analysis).	2/Figure 1
Data collection process	10	Describe method of data extraction from reports (e.g., piloted forms, independently, in duplicate) and any processes for obtaining and confirming data from investigators.	2/3
Data items	11	List and define all variables for which data were sought (e.g., PICOS, funding sources) and any assumptions and simplifications made.	2-4
Risk of bias in individual studies	12	Describe methods used for assessing risk of bias of individual studies (including specification of whether this was done at the study or outcome level), and how this information is to be used in any data synthesis.	N/A
Summary measures	13	State the principal summary measures (e.g., risk ratio, difference in means).	2/5
Synthesis of results	14	Describe the methods of handling data and combining results of studies, if done, including measures of consistency (e.g., I^2) for each meta-analysis.	5
Risk of bias across studies	22	Present results of any assessment of risk of bias across studies (see Item 15).	N/A
Additional analysis	23	Give results of additional analyses, if done (e.g., sensitivity or subgroup analyses, meta-regression [see Item 16]).	2
RESULTS			
Study selection	17	Give numbers of studies screened, assessed for eligibility, and included in the review, with reasons for exclusions at each stage, ideally with a flow diagram.	2/3/Figure 1
Study characteristics	18	For each study, present characteristics for which data were extracted (e.g., study size, PICOS, follow-up period) and provide the citations.	3/4
Risk of bias within studies	19	Present data on risk of bias of each study and, if available, any outcome level assessment (see item 12).	N/A
Results of individual studies	20	For all outcomes considered (benefits or harms), present, for each study: (a) simple summary data for each intervention group (b) effect estimates and confidence intervals, ideally with a forest plot.	Table 2
Synthesis of results	21	Present results of each meta-analysis done, including confidence intervals and measures of consistency.	N/A
Risk of bias across studies	22	Present results of any assessment of risk of bias across studies (see Item 15).	N/A
Additional analysis	23	Give results of additional analyses, if done (e.g., sensitivity or subgroup analyses, meta-regression [see Item 16]).	Table 3

Section/topic	#	Checklist item	Reported on page #
DISCUSSION			
Summary of evidence	24	Summarize the main findings including the strength of evidence for each main outcome; consider their relevance to key groups (e.g., healthcare providers, users, and policy makers).	7/8
Limitations	25	Discuss limitations at study and outcome level (e.g., risk of bias), and at review-level (e.g., incomplete retrieval of identified research, reporting bias).	7/8
Conclusions	26	Provide a general interpretation of the results in the context of other evidence, and implications for future research.	7-9
FUNDING			
Funding	27	Describe sources of funding for the systematic review and other support (e.g., supply of data); role of funders for the systematic review.	10

Supplementary Table ii. Prisma Statement Checklist. *N/A: Non-Applicable. From: Moher D, Liberati A, Tetzlaff J, Altman DG, The PRISMA Group (2009). Preferred Reporting Items for Systematic Reviews and Meta-Analyses: The PRISMA Statement. PLoS Med 6(7): e1000097. doi:10.1371/journal.pmed1000097.*

References

[1] Alves SM, Economou T, Oliveira C, Ribeiro AI, Neves N, Gomez-Barrena E, et al. Osteoporotic hip fractures: bisphosphonates sales and observed turning point in trend. A population-based retrospective study. Bone. 2013;53:430-6.

[2] Matassi F, Nistri L, Chicon Paez D, Innocenti M. New biomaterials for bone regeneration. Clin Cases Miner Bone Metab. 2011;8:21-4.

[3] Lin K, Liu P, Wei L, Zou Z, Zhang W, Qian Y, et al. Strontium substituted hydroxyapatite porous microspheres: Surfactant-free hydrothermal synthesis, enhanced biological response and sustained drug release. Chemical Engineering Journal. 2013;222:49-59.

[4] Goldhahn J, Scheele WH, Mitlak BH, Abadie E, Aspenberg P, Augat P, et al. Clinical evaluation of medicinal products for acceleration of fracture healing in patients with osteoporosis. Bone. 2008;43:343-7.

[5] Liu HY, Wu AT, Tsai CY, Chou KR, Zeng R, Wang MF, et al. The balance between adipogenesis and osteogenesis in bone regeneration by platelet-rich plasma for age-related osteoporosis. Biomaterials. 2011;32:6773-80.

[6] Cao L, Liu G, Gan Y, Fan Q, Yang F, Zhang X, et al. The use of autologous enriched bone marrow MSCs to enhance osteoporotic bone defect repair in long-term estrogen deficient goats. Biomaterials. 2012;33:5076-84.

[7] Cho SW, Sun HJ, Yang JY, Jung JY, Choi HJ, An JH, et al. Human adipose tissue-derived stromal cell therapy prevents bone loss in ovariectomized nude mouse. Tissue Eng Part A. 2012;18:1067-78.

[8] Marie PJ, Felsenberg D, Brandi ML. How strontium ranelate, via opposite effects on bone resorption and formation, prevents osteoporosis. Osteoporos Int. 2011;22:1659-67.

[9] Bonnelye E, Chabadel A, Saltel F, Jurdic P. Dual effect of strontium ranelate: Stimulation of osteoblast differentiation and inhibition of osteoclast formation and resorption in vitro. Bone. 2008;42:129-38.

[10] Baron R, Tsouderos Y. In vitro effects of S12911-2 on osteoclast function and bone marrow macrophage differentiation. Eur J Pharmacol. 2002;450:11-7.

[11] Reginster JY, Neuprez A, Dardenne N, Beaudart C, Emonts P, Bruyere O. Efficacy and safety of currently marketed anti-osteoporosis medications. Best Pract Res Clin Endocrinol Metab. 2014;28:809-34.

[12] Cooper C, Fox KM, Borer JS. Ischaemic cardiac events and use of strontium ranelate in postmenopausal osteoporosis: a nested case-control study in the CPRD. Osteoporos Int. 2014;25:737-45.

[13] Abrahamsen B, Grove EL, Vestergaard P. Nationwide registry-based analysis of cardiovascular risk factors and adverse outcomes in patients treated with strontium ranelate. Osteoporos Int. 2014;25:757-62.

[14] Hulsart-Billstrom G, Xia W, Pankotai E, Weszl M, Carlsson E, Forster-Horvath C, et al. Osteogenic potential of Sr-doped calcium phosphate hollow spheres in vitro and in vivo. J Biomed Mater Res A. 2013;101:2322-31.

[15] Baier M, Staudt P, Klein R, Sommer U, Wenz R, Grafe I, et al. Strontium enhances osseointegration of calcium phosphate cement: a histomorphometric pilot study in ovariectomized rats. Journal of Orthopaedic Surgery and Research. 2013;8:16-.

[16] Thormann U, Ray S, Sommer U, Elkhassawna T, Rehling T, Hundgeburth M, et al. Bone formation induced by strontium modified calcium phosphate cement in critical-size metaphyseal fracture defects in ovariectomized rats. Biomaterials. 2013;34:8589-98.

[17] Liberati A, Altman DG, Tetzlaff J, Mulrow C, Gotzsche PC, Ioannidis JP, et al. The PRISMA statement for reporting systematic reviews and meta-analyses of studies that evaluate healthcare interventions: explanation and elaboration. BMJ. 2009;339:b2700.

[18] Banerjee SS, Tarafder S, Davies NM, Bandyopadhyay A, Bose S. Understanding the influence of MgO and SrO binary doping on the mechanical and biological properties of beta-TCP ceramics. Acta Biomater. 2010;6:4167-74.

[19] Bose S, Tarafder S, Banerjee SS, Davies NM, Bandyopadhyay A. Understanding in vivo response and mechanical property variation in MgO, SrO and SiO(2) doped beta-TCP. Bone. 2011;48:1282-90.

[20] Boyd D, Carroll G, Towler MR, Freeman C, Farthing P, Brook IM. Preliminary investigation of novel bone graft substitutes based on strontium-calcium-zinc-silicate glasses. J Mater Sci Mater Med. 2009;20:413-20.

[21] Cardemil C, Elgali I, Xia W, Emanuelsson L, Norlindh B, Omar O, et al. Strontium-doped calcium phosphate and hydroxyapatite granules promote different inflammatory and bone remodelling responses in normal and ovariectomised rats. PLoS One. 2013;8:e84932.

[22] Cheng C, Alt V, Pan L, Thormann U, Schnettler R, Strauss LG, et al. Application of F-18-sodium fluoride (NaF) dynamic PET-CT (dPET-CT) for defect healing: a comparison of biomaterials in an experimental osteoporotic rat model. Med Sci Monit. 2014;20:1942-9.

[23] Cheng C, Alt V, Pan L, Thormann U, Schnettler R, Strauss LG, et al. Preliminary evaluation of different biomaterials for defect healing in an experimental osteoporotic rat model with dynamic PET-CT (dPET-CT) using F-18-sodium fluoride (NaF). Injury. 2014;45:501-5.

[24] Dagang G, Kewei X, Yong H. The influence of Sr doses on the in vitro biocompatibility and in vivo degradability of single-phase Sr-incorporated HAP cement. J Biomed Mater Res A. 2008;86:947-58.

[25] Gorustovich AA, Steimetz T, Cabrini RL, Porto Lopez JM. Osteoconductivity of strontium-doped bioactive glass particles: a histomorphometric study in rats. J Biomed Mater Res A. 2010;92:232-7.

[26] Gu Z, Zhang X, Li L, Wang Q, Yu X, Feng T. Acceleration of segmental bone regeneration in a rabbit model by strontium-doped calcium polyphosphate scaffold through stimulating VEGF and bFGF secretion from osteoblasts. Mater Sci Eng C Mater Biol Appl. 2013;33:274-81.

[27] Izci Y, Secer HI, Ilica AT, Karacalioglu O, Onguru O, Timucin M, et al. The efficacy of bioceramics for the closure of burr-holes in craniotomy: case studies on 14 patients. J Appl Biomater Funct Mater. 2013;11:e187-96.

[28] Li X, Xu CP, Hou YL, Song JQ, Cui Z, Wang SN, et al. A novel resorbable strontium-containing alpha-calcium sulfate hemihydrate bone substitute: a preparation and preliminary study. Biomed Mater. 2014;9:045010.

[29] Lin K, Xia L, Li H, Jiang X, Pan H, Xu Y, et al. Enhanced osteoporotic bone regeneration by strontium-substituted calcium silicate bioactive ceramics. Biomaterials. 2013;34:10028-42.

[30] Mohan BG, Shenoy SJ, Babu SS, Varma HK, John A. Strontium calcium phosphate for the repair of leporine (Oryctolagus cuniculus) ulna segmental defect. J Biomed Mater Res A. 2013;101:261-71.

[31] Tian M, Chen F, Song W, Song Y, Chen Y, Wan C, et al. In vivo study of porous strontium-doped calcium polyphosphate scaffolds for bone substitute applications. J Mater Sci Mater Med. 2009;20:1505-12.

[32] Wei L, Ke J, Prasadam I, Miron RJ, Lin S, Xiao Y, et al. A comparative study of Sr-incorporated mesoporous bioactive glass scaffolds for regeneration of osteopenic bone defects. Osteoporos Int. 2014;25:2089-96.

[33] Xie H, Wang Q, Ye Q, Wan C, Li L. Application of K/Sr co-doped calcium polyphosphate bioceramic as scaffolds for bone substitutes. J Mater Sci Mater Med. 2012;23:1033-44.

[34] Zhang Y, Wei L, Chang J, Miron RJ, Shi B, Yi S, et al. Strontium-incorporated mesoporous bioactive glass scaffolds stimulating in vitro proliferation and

differentiation of bone marrow stromal cells and in vivo regeneration of osteoporotic bone defects. Journal of Materials Chemistry B. 2013;1:5711-22.

[35] Zhao S, Zhang J, Zhu M, Zhang Y, Liu Z, Tao C, et al. Three-dimensional printed strontium-containing mesoporous bioactive glass scaffolds for repairing rat critical-sized calvarial defects. Acta Biomater. 2015;12:270-80.

[36] Jebahi S, Oudadesse H, el Feki H, Rebai T, Keskes H, Pellen P, et al. Antioxidative/oxidative effects of strontium-doped bioactive glass as bone graft. In vivo assays in ovariectomised rats. Journal of Applied Biomedicine. 2012;10:195-209.

[37] Jebahi S, Oudadesse H, Elleuch J, Tounsi S, Keskes H, pellen P, et al. The potential restorative effects of strontium-doped bioactive glass on bone microarchitecture after estrogen-deficieny induced osteoporosis: Physicochemical and histomorphometric analyses. Journal of the Korean Society for Applied Biological Chemistry. 2013;56:533-40.

[38] Kang P, Xie X, Tan Z, Yang J, Shen B, Zhou Z, et al. Repairing defect and preventing collapse of femoral head in a steroid-induced osteonecrotic of femoral head animal model using strontium-doped calcium polyphosphate combined BM-MNCs. Journal of materials science Materials in medicine. 2015;26:80.

[39] Tarafder S, Davies NM, Bandyopadhyay A, Bose S. 3D printed tricalcium phosphate bone tissue engineering scaffolds: Effect of SrO and MgO doping on in vivo osteogenesis in a rat distal femoral defect model. Biomaterials Science. 2013;1:1250-9.

[40] Tarafder S, Dernell WS, Bandyopadhyay A, Bose S. SrO- and MgO-doped microwave sintered 3D printed tricalcium phosphate scaffolds: Mechanical properties and in vivo osteogenesis in a rabbit model. Journal of Biomedical Materials Research - Part B Applied Biomaterials. 2014;103:679-90.

[41] Xie H, Wang J, Li C, Gu Z, Chen Q, Li L. Application of strontium doped calcium polyphosphate bioceramic as scaffolds for bone tissue engineering. Ceramics International. 2013;39:8945-54.

[42] Zhang Y, Cui X, Zhao S, Wang H, Rahaman MN, Liu Z, et al. Evaluation of injectable strontium-containing borate bioactive glass cement with enhanced osteogenic capacity in a critical-sized rabbit femoral condyle defect model. ACS Applied Materials and Interfaces. 2015;7:2393-403.

[43] Bose S, Roy M, Bandyopadhyay A. Recent advances in bone tissue engineering scaffolds. Trends in biotechnology. 2012;30:546-54.

[44] Qiu Z-Y, Noh I-S, Zhang S-M. Silicate-doped hydroxyapatite and its promotive effect on bone mineralization. Frontiers of Materials Science. 2013;7:40-50.

[45] Chattopadhyay N, Quinn SJ, Kifor O, Ye C, Brown EM. The calcium-sensing receptor (CaR) is involved in strontium ranelate-induced osteoblast proliferation. Biochem Pharmacol. 2007;74:438-47.

[46] Atkins GJ, Welldon KJ, Halbout P, Findlay DM. Strontium ranelate treatment of human primary osteoblasts promotes an osteocyte-like phenotype while eliciting an osteoprotegerin response. Osteoporos Int. 2009;20:653-64.

[47] Brennan TC, Rybchyn MS, Green W, Atwa S, Conigrave AD, Mason RS. Osteoblasts play key roles in the mechanisms of action of strontium ranelate. Br J Pharmacol. 2009;157:1291-300.

[48] Choudhary S, Halbout P, Alander C, Raisz L, Pilbeam C. Strontium ranelate promotes osteoblastic differentiation and mineralization of murine bone marrow stromal cells: involvement of prostaglandins. J Bone Miner Res. 2007;22:1002-10.

[49] Zhu LL, Zaidi S, Peng Y, Zhou H, Moonga BS, Blesius A, et al. Induction of a program gene expression during osteoblast differentiation with strontium ranelate. Biochem Biophys Res Commun. 2007;355:307-11.

[50] Fromigue O, Hay E, Barbara A, Marie PJ. Essential role of nuclear factor of activated T cells (NFAT)-mediated Wnt signaling in osteoblast differentiation induced by strontium ranelate. J Biol Chem. 2010;285:25251-8.

[51] Kokesch-Himmelreich J, Schumacher M, Rohnke M, Gelinsky M, Janek J. ToF-SIMS analysis of osteoblast-like cells and their mineralized extracellular matrix on strontium enriched bone cements. Biointerphases. 2013;8:17.

[52] Christoffersen J, Christoffersen MR, Kolthoff N, Bärenholdt O. Effects of strontium ions on growth and dissolution of hydroxyapatite and on bone mineral detection. Bone. 1997;20:47-54.

[53] Rahman MS, Akhtar N, Jamil HM, Banik RS, Asaduzzaman SM. TGF-β/BMP signaling and other molecular events: regulation of osteoblastogenesis and bone formation. Bone Res. 2015;3:15005-.

[54] Li Y, Chen S-K, Li L, Qin L, Wang X-L, Lai Y-X. Bone defect animal models for testing efficacy of bone substitute biomaterials. Journal of Orthopaedic Translation. 2015;3:95-104.

[55] Pearce AI, Richards RG, Milz S, Schneider E, Pearce SG. Animal models for implant biomaterial research in bone: a review. Eur Cell Mater. 2007;13:1-10.

[56] Chakkalakal DA, Strates BS, Mashoof AA, Garvin KL, Novak JR, Fritz ED, et al. Repair of segmental bone defects in the rat: an experimental model of human fracture healing∗. Bone. 1999;25:321-32.

[57] Tadrous PJ. On the concept of objectivity in digital image analysis in pathology. Pathology. 2010;42:207-11.

CHAPTER III

STRONTIUM-RICH INJECTABLE HYBRID SYSTEM FOR BONE REGENERATION

Article 2

Published in Materials Science and Engineering C: Materials for Biological Applications. 2016 Feb;59:818-827

doi: 10.1016/j.msec.2015.10.038

Strontium-rich injectable hybrid system for bone regeneration

Nuno Neves[a,b,c], Bruno B. Campos[d], Isabel F. Almeida[e], Paulo C. Costa[e], Abel Trigo Cabral[c], Mário A. Barbosa[a,b,f], Cristina C. Ribeiro[a,b,g, #]

[a]i3S - Instituto de Investigação e Inovação em Saúde, Universidade do Porto, Portugal

[b]INEB - Instituto de Engenharia Biomédica, Universidade do Porto, Rua do Campo Alegre 823, 4150-180 Porto, Portugal

[c]FMUP - Faculdade de Medicina da Universidade do Porto, Departamento de Cirurgia, Serviço de Ortopedia, Alameda Prof. Hernâni Monteiro, 4200-319 Porto, Portugal

[d]FCUP - Faculdade de Ciências da Universidade do Porto, Centro de Investigação em Química, Departamento de Química e Bioquímica, Rua do Campo Alegre 1021/1055, 4169-007 Porto, Portugal

[e]FFUP - Faculdade de Farmácia da Universidade do Porto, Laboratório de Tecnologia Farmacêutica, Departamento de Ciências do Medicamento, Rua de Jorge Viterbo Ferreira 228, 4050-313 Porto, Portugal

[f]ICBAS - Instituto de Ciências Biomédicas de Abel Salazar, Universidade do Porto, Rua de Jorge Viterbo Ferreira 228, 4050-313 Porto, Portugal

[g]ISEP – Instituto Superior de Engenharia do Porto, Instituto Politécnico do Porto, Rua Dr. António Bernardino de Almeida 431, 4249-015, Porto, Portugal

Abstract

Current challenges in the development of scaffolds for bone regeneration include the engineering of materials that can withstand normal dynamic physiological mechanical stresses exerted on the bone and provide a matrix capable of supporting cell migration and tissue ingrowth. The objective of the present work was to develop and characterize a hybrid polymer-ceramic injectable system that consists of an alginate matrix cross-linked *in situ* in the presence of strontium (Sr), incorporating a ceramic reinforcement in the form of Sr-rich microspheres. The incorporation of Sr in the microspheres and in the vehicle relies on the growing evidence that Sr has beneficial effects in bone remodeling and in the treatment of osteopenic disorders and osteoporosis. Sr-rich porous hydroxyapatite microspheres with a uniform size and a mean diameter of 555 μm were prepared, and their compression strength and friability tested. A 3.5% (w/v) ultrapure sodium alginate solution was used as the vehicle and its *in situ* gelation was promoted by the addition of calcium (Ca) or Sr carbonate and Glucone-δ-lactone. Gelation times varied with temperature and cross-linking agent, being slower for Sr than for Ca, but adequate for injection in both cases. Injectability was evaluated using a device employed in vertebroplasty surgical procedures, coupled to a texture analyser in compression mode. Compositions with 35% w of microspheres presented the best compromise between injectability and compression strength of the system, the force required to extrude it being lower than 100 N. Micro CT analysis revealed a homogeneous distribution of the microspheres inside the vehicle, and a mean inter-microspheres space of 220 μm. DMA results showed that elastic behavior of the hybrid is dominant over the viscous one and that the higher storage modulus was obtained for the 3.5%Alg-35%SrHAp-Sr formulation.

Keywords: Biomaterials; injectable bone substitute; strontium; alginate; hydroxyapatite

Introduction

Osteoporosis is a systemic disease that affects a significant part of the aging population in western countries. It results in progressive loss of mineralization and consequent changes in bone architecture leading to increased susceptibility to fractures. Because of the raise in expectancy of life, osteoporosis has become a serious public health issue that will probably be worsened in the near future. The treatment of bone defects in osteoporotic fractures remains a significant challenge. The use of calcium phosphate ceramics in bone regeneration, either alone or in combination with a polymeric phase, is now a common practice, since these materials provide good biological responses, based on their osteoconductive properties, and adequate mechanical properties [1-5]. The development of injectable materials for filling bone defects allows for the use of minimally invasive techniques. Most injectable ceramic materials consist of micro or nanoparticles suspended in appropriate vehicles [6-11]. Spherical particles are more suitable for implantation than non-homogeneous granules, since they conform better to irregular implant sites and present more predictable flowing properties during injection [12-15]. The space between particles is critical for the success of a scaffold for bone regeneration since blood vessels and cells should be able to invade the inter-particle network to promote bone formation throughout the filled defect. It is generally accepted that a size of 100-200 μm in diameter is suitable for bone in-growth [16].

The addition of inductive factors or osteoprogenitor cells is a current strategy to improve osteogenesis in osteoporosis [17-20]. Sr is a trace element that plays a dual role in bone metabolism, stimulating bone formation and inhibiting bone resorption [21-26]. *In vitro* pre-clinical studies indicate that Sr decreases bone resorption by directly inhibiting the differentiation, resorbing activity and apoptosis of osteoclasts [21, 25-27]. It was also observed that it enhanced the replication of preosteoblastic cells and osteogenic differentiation, reduced osteoblasts apoptosis and, secondarily,

promoted bone matrix synthesis [21, 24, 26, 28, 29]. At least three mechanisms are involved in the opposite effects of Sr: activation of the calcium-sensing receptor (CaSR), nuclear factor of activated Tc (NFATc)/Wnt signaling, and modulation of osteoprotegerin (OPG) and receptor activator of nuclear factor κ-B ligand (RANKL) [21]. The available *in vivo* data are consistent with the *in vitro* studies showing the beneficial effect of Sr in increasing bone architecture and bone strength in both intact and osteoporotic animal models [22, 30-35]. Sr has been used in clinical practice against osteoporosis as oral Sr ranelate, and has shown effectiveness in the prevention of both vertebral and non-vertebral osteoporotic fractures [21, 36, 37]. Incorporating Sr in calcium phosphate cements may be a strategy to achieve high Sr concentrations not in a systemic but in a local environment, using the osteoanabolic and anti-osteoclastic activity for enhancement of new bone formation [38-40].

Our group has developed an injectable system based on hydroxyapatite microspheres and an alginate-based vehicle with gel-forming ability [41]. We have extensively studied various types of microspheres, namely of calcium alginate [42], hybrid calcium phosphate/alginate [43] and calcium phosphates [44, 45].

In the present work we propose an injectable hybrid system that consists of a polymeric matrix cross-linked *in situ* with Sr, reinforced with Sr-rich calcium phosphate microspheres, to be used for bone regeneration. The reasoning behind this strategy is that our hybrid system will provide both a scaffold capable of supporting cell migration and tissue ingrowth and incorporate two Sr release kinetics, in order to guarantee an effective bone remodeling since the early stages of implantation.

Materials and Methods

1. Microspheres preparation and characterization

1.1. Microspheres preparation

HAp-microspheres and Sr-HAp microspheres were prepared using the droplet extrusion method combined with ionotropic gelation in the presence of Ca^{2+} and Sr^{2+} respectively. A homogeneous paste, obtained by dispersing the ceramic powder (HAp, Plasma Biotal) in a 3% (w/v) sodium alginate solution, was extruded drop-wise into a $CaCl_2$ or $SrCl_2$ cross-linking solution with a concentration of 0.1 M, where spherical-shaped particles were instantaneously formed due to the rapid establishment of Ca or Sr mediated junctions between polyguluronate chains on the polymer backbone.

Different ceramic-to-polymer solution ratios were tested, the 0.2 w/w being the one that resulted in more reproducible results. The size of the microspheres was controlled by regulating the extrusion flow rate using a syringe pump, and by applying a coaxial air stream (Encapsulation unit Var J1, *Nisco* Engineering AG). At completion of the gelation period the microspheres were recovered and rinsed in water. Finally, they were dried and sintered at 1100 ºC and 1200 ºC (Euroterm 2408 MLE, Termolab).

1.2. Microspheres characterization

HAp and Sr-HAp microspheres were characterized in terms of diameter (laser beam diffraction - Coulter LS, Beckman Coulter), porosity (mercury porosimetry - AutoPore IV, Micromeritics) and specific surface area (gas adsorption according to the Brunauer, Emmel and Teller-BET method - ASAP 2000, Micromeritics). Morphological and physic-chemical characterization of the microspheres was carried out using scanning electron microscopy (SEM-EDS), X-ray diffraction (XRD) and Fourier transform infrared spectroscopy (FTIR). The SEM/EDS exam was performed using a high resolution (Schottky) Environmental Scanning Electron Microscope with

X-ray Microanalysis and Electron Backscattered Diffraction analysis: Quanta 400 FEG ESEM/EDAX Genesis X4M. Samples were coated with an Au/Pd thin film, by sputtering, using the SPI Module Sputter Coater equipment. For FTIR and XRD analysis, microspheres were reduced to powder and analysed respectively as KBr pellets using a spectrophotometer (Spectrum 2000, Perkin Elmer) and as powder particles using a diffractometer (Philips X-Pert). Zeta potential of hydroxyapatite microspheres was determined from streaming potential measurements with a commercial electrokinetic analyser (EKA, Anton Paar GmbH) using a special cylindrical cell with a powder insert for granular or powder samples. The electrolyte used was 1 mM KCl and the pH was slowly changed from 3 to 10. Mechanical characterization of the microspheres (friability and rupture force) was performed using a friability tester and a texture analyser. Friability tests were implemented according to a procedure described in the European Pharmacopeia (7^{th} edition) with minor modifications. Briefly, 2 g of microspheres were loaded into a drum (F1, Sotax AG,) operating at 25 rpm. The fall height was 150 mm and the same microspheres were used for three cycles of 4 min each. After each cycle, the desegregated powder was blown out and the microspheres were collected and weighted again [41]. Friability was reported as percentage of total weight lost. Microspheres rupture force (hardness) was evaluated in a texture analyser (TA-XT2i, Stable Micro Systems). The load was applied vertically to individual microspheres, using a load cell of 5 kg and a cylindrical metallic probe with a diameter of 2 mm at a displacement rate of 0.1 mm/s. The rupture force was determined from the maximum force reached (breaking point). In each experiment, 10 microspheres were assayed and the mean value from at least three experiments was calculated.

2. Vehicle characterization

2.1. Alginate molecular weight determination

An ultra-pure sodium alginate (NovaMatrix, FMC Biopolymers) with >60% content of

guluronic *vs*. mannuronic acid units was used in the experiments. The molecular weight of the alginate was calculated by gel permeation chromatography/size exclusion chromatography (GPC/SEC). The analysis was performed at room temperature (circa 23 ºC), using a modular system, composed by an isocratic pump, a vacuum degasser and an autosampler module (GPC Max, Viscotek), a viscometer/right angle laser light scattering (RALLS) and a dual detector (T60, Viscotek), and a refractive index detector (K-5002, Knaeur), operating at the same wavelength as the RALLS detector (670 nm). Separations were performed in a set of PL aquagel- OH mixed columns. The mobile phase consisted of 0.1M $NaNO_3$ with 0.02% w/v NaN_3 and the flow-rate was maintained at 1.0 mL/min. Samples were dissolved in the mobile phase at 1 mg/mL, filtered, and 100 µL of sample were injected by the autosampler on an automatic injection valve equipped with a 200 µL loop. All modules were controlled and sample data analysed by the OmniSEC Triple Detection/Light Scattering GPC/SECModular GPCMax software. Samples were analyzed in quadruplicate.

2.2. Gel formation

Internal gelation of the Na alginate solution was promoted using a method previously described by Kuo and Ma [46] with minor modifications, described elsewhere [41]. Briefly, a Ca or Sr salt with limited solubility, in this case $CaCO_3$ or $SrCO_3$, was mixed with the alginate solution and used as a source of Ca or Sr ions respectively. The release of Ca or Sr into the solution was promoted by the generation of an acidic pH with Glucone-δ-lactone (GDL, Sigma), a slowly dissociating acid, which was also incorporated in the solution. Once released, Ca or Sr ions can participate in the interchain ionic binding between carboxyl groups (COO^-) of guluronic acids blocks in the polymer chain, giving rise to a cross-linked gel. The $CaCO_3$/GDL or $SrCO_3$/GDL ratio was set at 0.5 to yield a neutral pH value. All components were pre-equilibrated at room temperature (set at 20 ºC) before being mixed. An aqueous $CaCO_3$ or $SrCO_3$

suspension previously mixed and vortexed for 1 min was added to the Na-alginate solution (3.5% w/v). A Ca^{2+}/COO^- or Sr^{2+}/COO^- ratio of 0.288 was used, since preliminary results showed that it promotes gelation in an adequate handling period, giving the surgeon enough time to prepare, manipulate, and inject the system. To initiate gel formation, a fresh GDL solution was vortexed for 20 s and subsequently added to each mixture. The curing time of alginate was studied using a rheometer (Kinexus Pro, Malvern Instruments), by monitoring the temporal evolution of storage modulus (G') and loss modulus (G''). The storage modulus is an indicator of the degree of elasticity of the material, and the loss modulus is a measure of the degree of viscous behavior. The crossover of G' and G'', is defined as the gel point, the point at which the material properties change from a more "liquid-like" to a more "solid-like". Parallel-plates measurement system was used, in shear-controlled oscillatory mode. The plate's distance (working gap) was set to 0.5 mm; the shear-strain applied was 5% of the gap (according to the Linear Viscoelastic Region (LVR) of the alginate hydrogels), at a frequency of 1 Hz. The temperature was set to 37 ºC and 20 ºC, and the solvent pool was used to maintain the water-saturated environment and avoid any water evaporation from the alginate solution during the tests.

3. Hybrid system preparation and characterization

3.1 Hybrid system preparation

For the hybrid system, alginate was combined with Ca or Sr microspheres and cross-linked by internal gelation with Ca or Sr, respectively (hereafter designated as Ca- or Sr-hybrid). This formulation and methodology were adapted and optimized from previous works using ceramic microspheres and Ca-cross-linked alginate hydrogels [41, 43, 44, 47, 48]. Alginate was thoroughly mixed with an aqueous suspension of Ca carbonate ($CaCO_3$, Fluka) or Sr carbonate ($SrCO_3$, Sigma) at a $CaCO_3$/COOH or $SrCO_3$/COOH molar ratio of 1.6. A fresh solution of GDL was added to trigger gel formation. The $CaCO_3$/GDL or $SrCO_3$/GDL molar ratio was set at 0.125. The total

polymer concentration ranged from 3 to 4% w/v in deionized water. Microspheres were added to the alginate solution to yield different weight percentages ranging from 10 to 35% w of the total solution and homogeneously suspended in the alginate solution (Fig. 1).

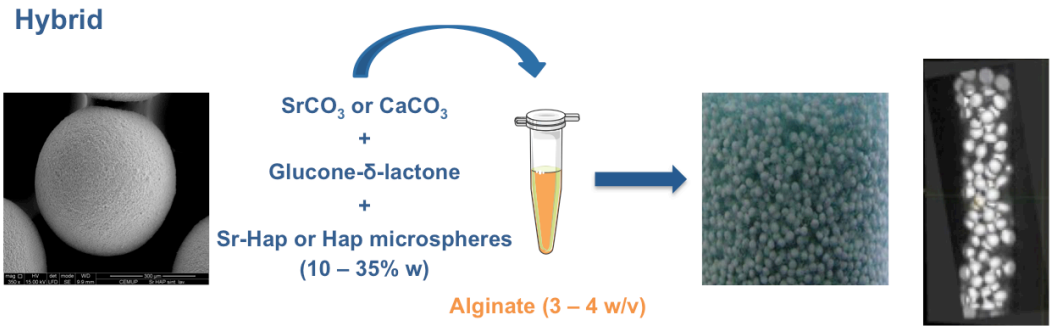

Figure 1. Scheme of hybrid preparation: Alginate was mixed with an aqueous suspension of Ca or Sr carbonate. A fresh solution of GDL was added to trigger gel formation. Microspheres (10 to 35% w of the total solution) were added and homogeneously suspended in the alginate solution.

3.2 Hybrid system characterization

3.2.1 Injectability tests

In the procedure, an injection device commonly used in vertebroplasty surgical procedures was used, which was coupled to a texture analyser [Fig. 2(A and B)]. The device consisted of a plastic syringe (20 mm internal diameter), a cannula (2.7 mm internal diameter, 173 mm length) and a polymeric connection tube. The syringe was filled with extemporaneously prepared microspheres-vehicle mixtures and the whole device was mounted on the texture analyser operating in the compression mode (TA-XT2i, Stable Micro Systems). For extrusion, the load was applied vertically using a load cell of 30 kg and a plunger displacement rate of 1 mm/s for a distance of 35 mm. Results were expressed as the force needed to extrude the mixture out from the syringe at room temperature. All samples were assayed at least in triplicate.

3.2.2 Compression tests

The microspheres-vehicle mixtures were extruded into cylindrical shape molds,

transferred to an oven at 37 ºC under controlled humidity (to prevent dehydration) and incubated for 24 h. At the end, cross-linked systems with a cylindrical shape were obtained.

The compression strength of the systems obtained after 24 h of incubation was evaluated with a texture analyser (TA-XT2i, Stable Micro Systems), with the load applied vertically using a load cell of 30 kg and a disk shaped probe with a 50 mm diameter covering a distance of 5 mm at a displacement rate of 1 mm/s [Fig. 2(C)]. For each hybrid composition, compression tests were performed in a minimum of 3 separate cylinders and the force profile curves were used to estimate the associated compression strength (maximum force).

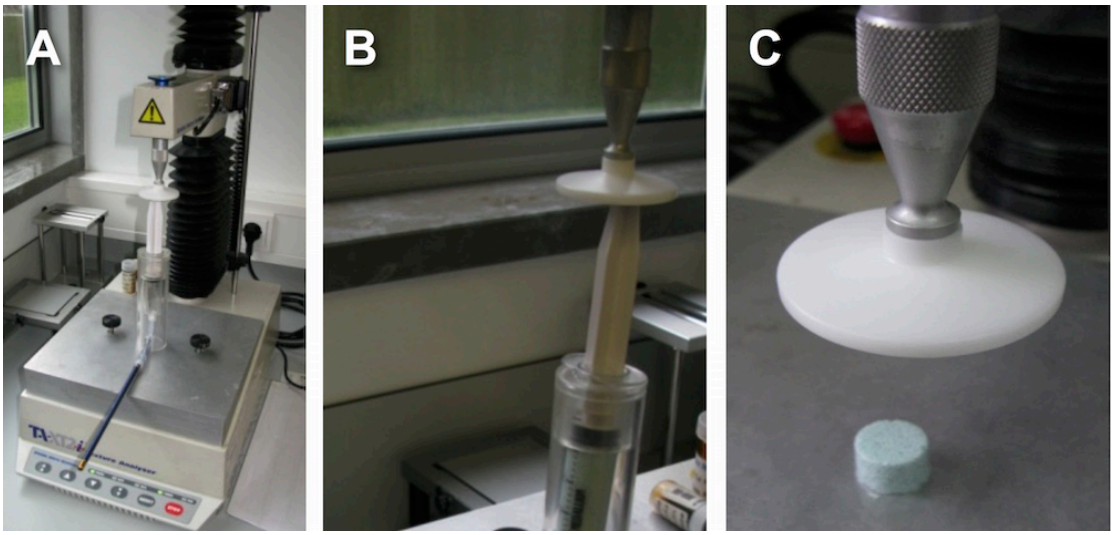

Figure 2. A – Injection device commonly used in vertebroplasty surgical procedures coupled to the texture analyser (A and B); Compression test of cylindrical shape sample (C).

3.2.3 DMA tests

The Dynamic Mechanical Analysis (DMA) supplies an oscillatory force, causing a sinusoidal stress to be applied to the sample, which generates a sinusoidal strain. In DMA, a complex modulus (E* = E´ + iE˝), an elastic modulus (E′) and an imaginary (loss) modulus (E″) are calculated from the material response to the sine wave. The E' and E'' gives information respectively, on the ability of the material to return and lose energy. The ratio of these two effects (Tan δ = E˝/E´) is called damping.

The DMA compression mode (DMA 8000, Perkin Elmer) was used to study the viscoelastic properties of the Ca and Sr vehicle (Alg-Ca and Alg-Sr, respectively) and of the hybrid system cross-linked with Ca and with Sr. Cylinders of 5 mm in diameter and 4 mm height were tested. The system comprises a parallel-plate measuring system to compress the specimen between the upper and lower platen. A frequency of oscillation of 1 Hz, and displacement amplitude of 1% of the thickness were used throughout the experiments. The influence of cross-linking agent of the vehicle, sintering temperature, percentage of microspheres, and time of curing were investigated. All the measurements were carried out at controlled temperature (20 ºC), to prevent the dehydration of the samples. Five specimens were tested for each condition.

3.2.4 Evaluation of the space between particles using micro-CT

The spatial distribution and size of the interstices between the microspheres was evaluated from high-resolution 3D micro-computed tomography (μCT) data sets. Micro-CT analysis was performed on a hybrid system cylinder composed of 3.5%Alg-35%Sr-HAp cross-linked with Sr. Briefly, a cylinder (3x4 mm) prepared in the same conditions described in sections 3.1 and 3.2.2. was incubated for 24h at 37 ºC under controlled humidity, and sequentially analyzed, using a high-resolution μCT Skyscan 1072 scanner (Skyscan, Kontich, Belgium). The sample was scanned in high resolution mode, using a pixel size of 8.79 μm and an integration time of 1.7 ms. The X-ray source was set at 75 keV of energy and 132 μA of current. A 1 mm-thick aluminium filter and a beam hardening correction algorithm were employed to minimize beam-hardening artifacts (Skyscan hardware/software).

Representative datasets of 373 slices were used for morphometric analysis. Binary images were created using two different thresholds, 50-255 and 150-255.

Additionally, 3D virtual models were created, visualized, and registered using image processing software (ANT 3D Creator v2.4, Skyscan). Fully automated computer

algorithms were implemented for segmentation and analysis, using ITK and VTK toolkits.

3.2.5 Statistical analysis

Microspheres diameter, rupture force and molecular weight were reported as mean±standard deviation. Normality tests were performed with Shapiro-Wilk test in order to assure normal distribution of the data obtained. The equality of variances assumption was verified with the Levene's test. The effect of the microspheres composition on rupture force was statistically evaluated by Student´s t-test. The effect of different composition of vehicle and microspheres on the extrusion force and on compression strength was statistically evaluated by one-way ANOVA. Post hoc comparisons of the means of individual groups were performed using Tukey's Honestly Significant Difference test. A value of $p<0.05$ was taken to denote significance. Statistical analysis was performed with IBM SPSS Statistics for Windows, Version 22.0 (Armonk, NY, IBM Corp, USA).

Results

1. Microspheres characterization

Microspheres with mean final diameters of 553±1.97 μm and 556±3.91 μm were obtained for the Sr-HAp and HAp formulations, respectively. Mercury porosimetry results indicated that both microspheres formulations present similar porosity percentage (29%) the median pore diameter for the Sr-HAp microspheres being higher (0.58 μm) than the one observed for the HAp microspheres (0.28 μm). Surface area measurements indicated a specific surface area of 2.860 m^2g^{-1} for Sr-HAp microspheres and 3.647 m^2g^{-1} for the HAp microspheres. Scanning electron microscopy revealed that in both cases microspheres were uniform in size and shape (Fig. 3). At high magnifications, non-sintered microspheres presented a homogeneous distribution of the ceramic phase in the alginate matrix. Upon sintering the polymer phase was substituted by a porous network.

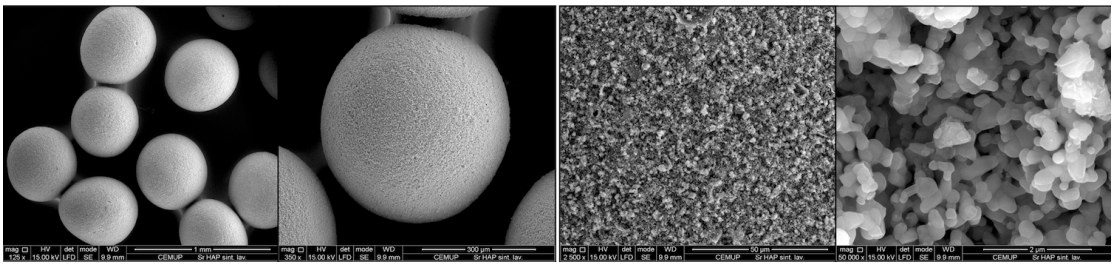

Figure 3. SEM images of Sr-HAp porous microspheres, with increasing magnification revealing the microstructure of the particles.

The isoelectric point of HAp microspheres occurred at approximately pH 4.5 whereas the isoelectric point of Sr-HAp microspheres occurred at approximately pH 4. At physiological pH both microspheres were negatively charged, the potential of Sr-HAp microspheres being more negative than that of HAp microspheres. Subtle spectral changes in the PO_4^{3-} domains were observed in the FTIR spectra of the Sr-HAp microspheres suggesting the incorporation of Sr in the HAp lattice. In what concerns XRD results, after sintering no extraneous phases were observed in HAp and Sr-HAp microspheres. EDS analysis showed that approximately 4.0% w (1.2% At) of Sr was

incorporated in the Sr-HAp microspheres. Significantly different rupture forces of 1.1±0.3 N and 0.5±0.2 N were observed for the Sr-HAp and HAp microspheres, respectively, sintered at 1200 ºC ($p<0.001$). Lower values were obtained for the particles sintered at 1100 ºC. Friability <0.1% was observed for the Sr-HAp and for the HAp microspheres.

2. Vehicle characterization

A molecular weight of 131±13 kDa was obtained for the ultrapure alginate used throughout the experiments.

The gel point occurred at a time of approximately 7 min for the Sr vehicle and 25 min for the Ca vehicle at 37ºC, and 20 min for the Sr vehicle and 45 min for the Ca vehicle at 22 ºC (normal temperature of an operating room) (Fig. 4).

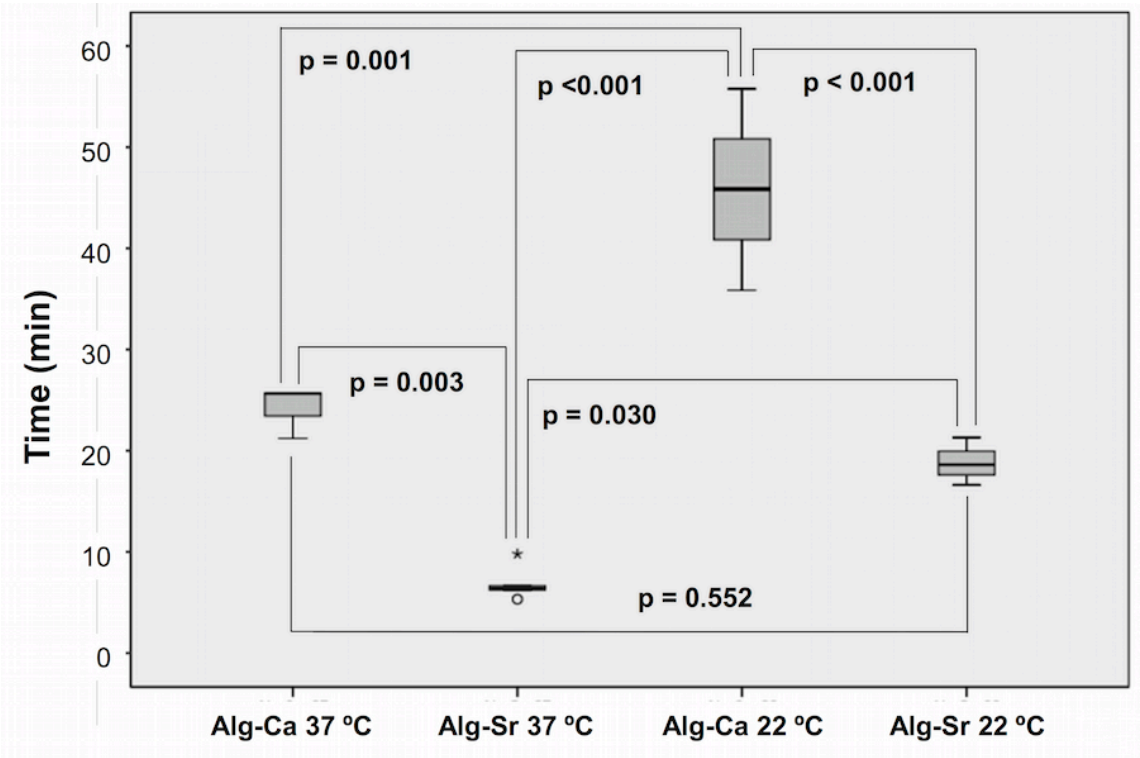

Figure 4. Mean gelation times for 3.5%Alg-Ca and 3.5%Alg-Sr 3.5% gels at 37 ºC and 22 ºC (error bars represent the standard deviation - sd).

3. Hybrid system characterization

3.1 Injectability and compression tests

Using an extrusion rate of 1 mm/s, the maximum force required to extrude the hybrid systems with a composition of 3%Alg-25%HAp and 3%Alg-30%HAp (vehicle cross-linked with Ca) was well below the 100 N, limit commonly referred for manual procedures [49]. Increasing the percentage of microspheres to 35% w, led to an increase of the extrusion force needed, exceeding the 100 N limit.

When Sr was the reticulation agent of the alginate and Sr-HAp microspheres were used, the extrusion force needed was smaller, not exceeding the 100 N limit.

When increasing the alginate concentration of the vehicle from 3 to 3.5% w/v and using Sr as the cross-linking agent, there was an increase in the extrusion force although not exceeding the 100 N limit (Fig. 5 A, 6 A). Keeping the same concentration of alginate but varying the type of microspheres (Sr-HAp instead of HAp microspheres) a higher force was needed to extrude the hybrid system.

Although no statistically significant differences were observed for the compression strength values of the various formulations tested, the maximum mean value (42.6 N) was obtained with 3.5%Alg-35%Sr-HAp-Sr composition (Fig. 5 B, 6 B).

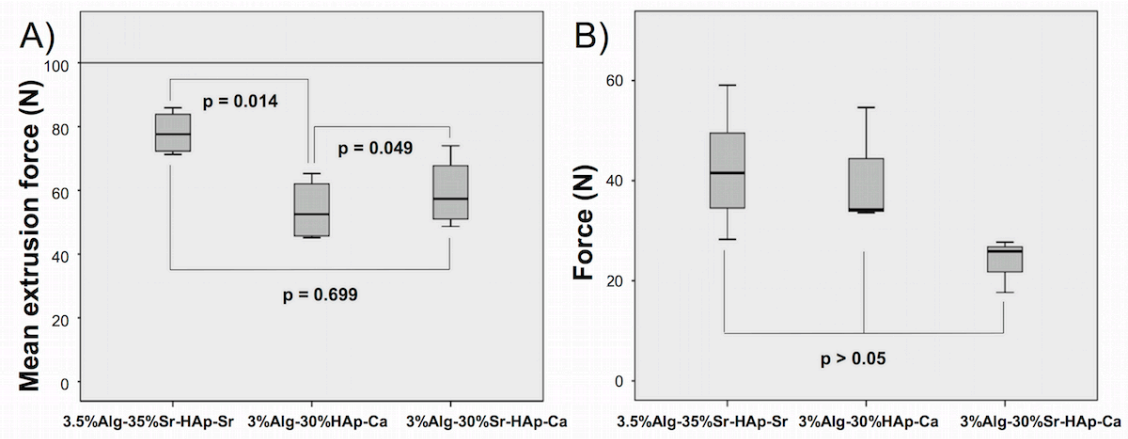

Figure 5. A) Boxplot representing the extrusion force needed for the hybrid compositions of 3.5%Alg-35%Sr-HAp cross-linked with Sr, 3%Alg-30%HAp cross-linked with Ca and 3%Alg-30%Sr-HAp cross-linked with Ca in the extrusion test. B) Boxplot representing the force needed for the hybrid compositions of 3.5%Alg-35%Sr-HAp cross-linked with Sr, 3%Alg-30%HAp cross-linked with Ca and 3%Alg-30%Sr-HAp cross-linked with Ca in the compression test.

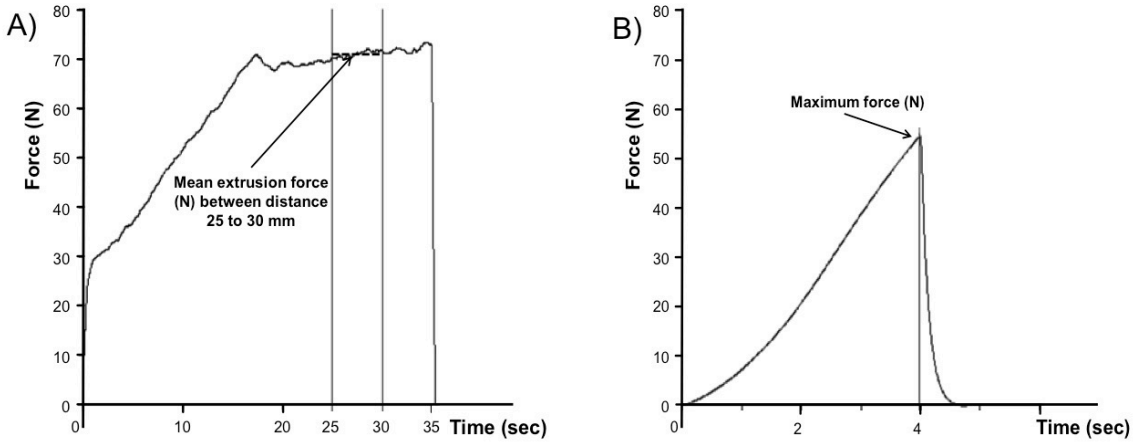

Figure 6. Typical stress-strain curves for injectability (A) and compression tests (B) for the hybrid composition of 3.5%Alg-35%Sr-HAp cross-linked with Sr.

3.2 DMA tests

When comparing the vehicle of alginate cross-linked with Ca with the one cross-linked with Sr, it was observed a higher storage modulus for the former (Fig. 7).

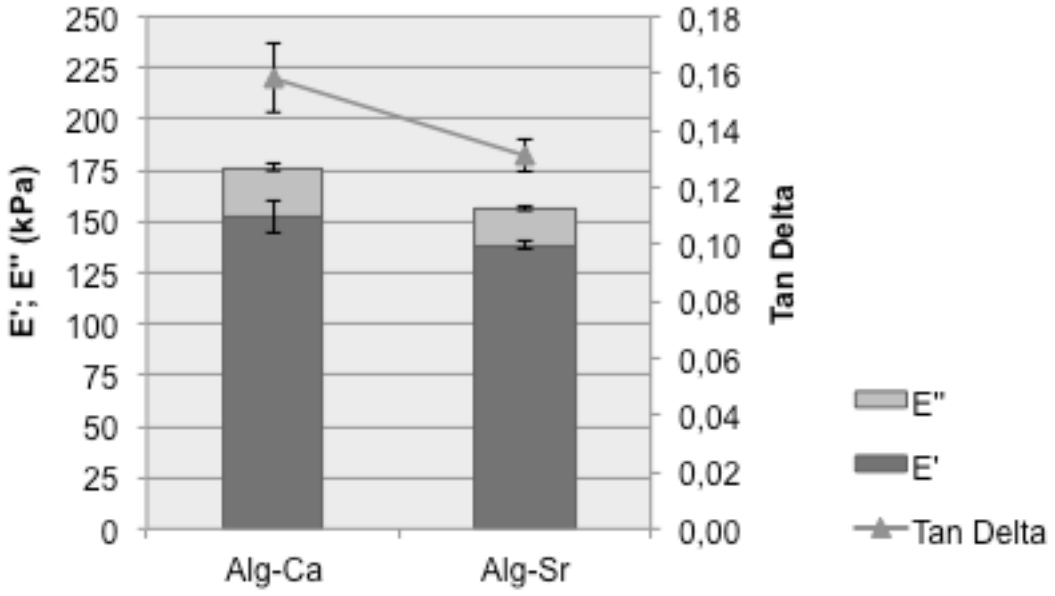

Figure 7. Mean values of storage (E'), loss modulus (E''), and tan δ for alginate cross-linked with Ca (Alg-Ca) and with Sr (Alg-Sr) (error bars represent the standard deviation).

The addition of microspheres to the polymer increased the storage modulus, the increase being proportional to the percentage of microspheres. This is expected because HAp-microspheres are much stiffer than alginate.

The tan δ increased proportionally to the increase of microspheres percentage due to the increase of loss modulus as a consequence of particles friction (Fig. 8).

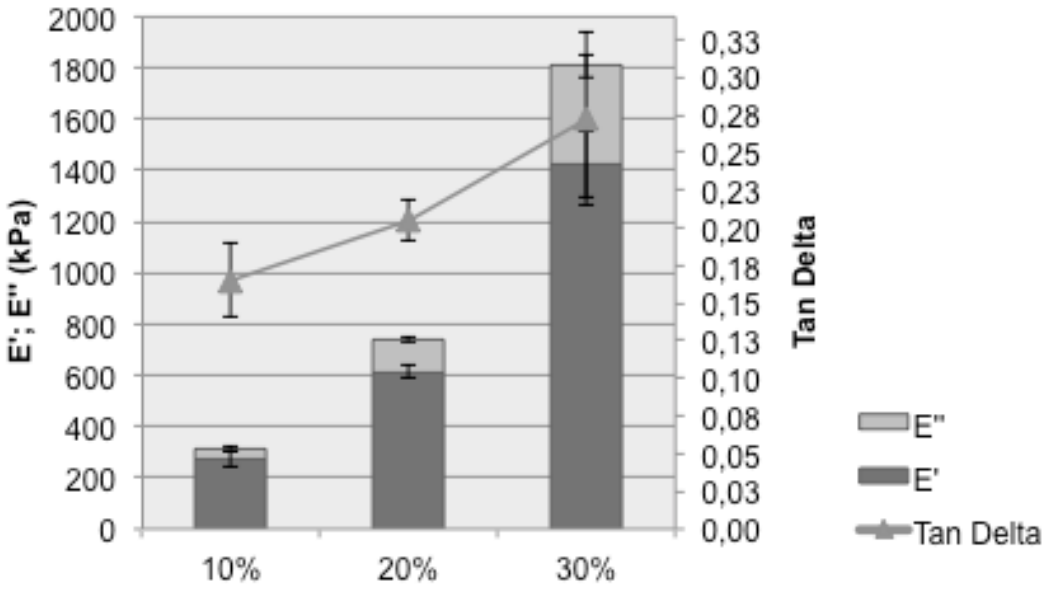

Figure 8. Storage (E'), loss modulus (E''), and tan δ for Sr-hybrid with different microspheres percentages.

It was also observed that the sintering temperature of the microspheres influenced the storage modulus of the hybrid. A sintering temperature of 1200 ºC led to microspheres with higher compression strength, and consequently higher hybrid stiffness.

The influence of time of curing in the mechanical properties of the Sr-HAp hybrid was evaluated. The count up of the time began with the addition of GDL to the alginate solution. The results showed an increase of storage modulus till a time of 24 hours, a consequence of the increasing of cross-linking chains within the alginate, due to the presence of the Sr cation.

In order to increase the compression strength of the hybrid, different vehicle and hybrid preparations were investigated (Fig. 9).

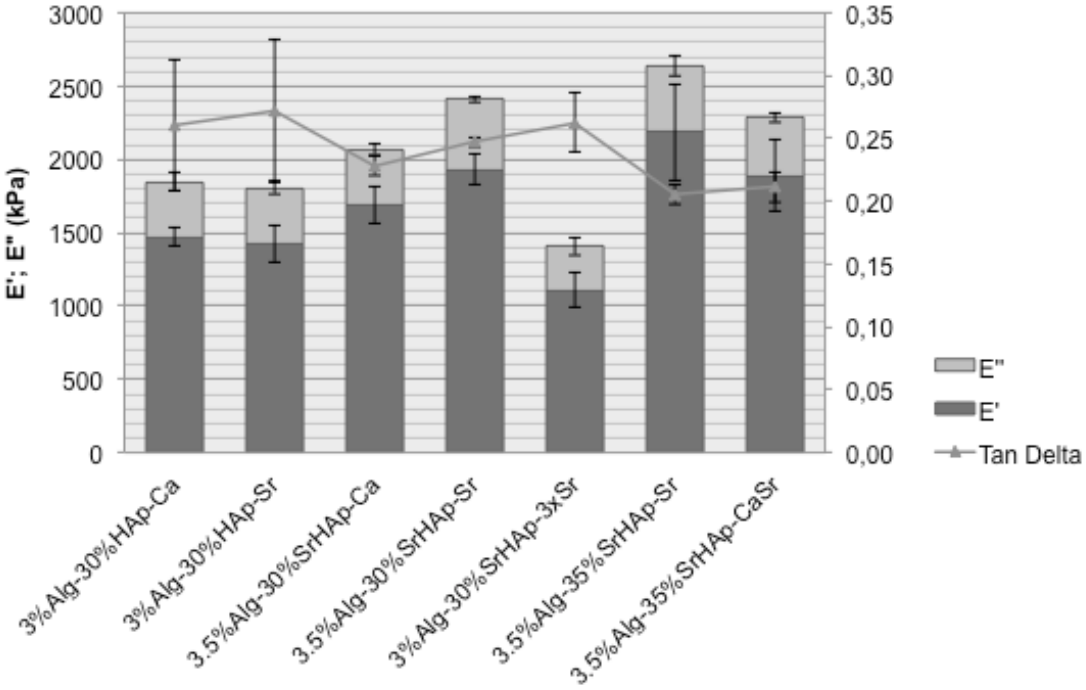

Figure 9. DMA tests of hybrid systems with different formulations (non confined). In the hybrid preparation microspheres sintered at 1200 ºC were used.

The vehicles 3.5%Alg-Ca and 3.5%Alg-Sr were the ones that presented better mechanical properties without limiting the injectability. An increase of alginate and/or microspheres percentage led to better mechanical properties. The possibility of existing a synergistic effect between Ca and Sr, in the cross-linking process of the alginate, was also investigated (1:1 ratio). Results showed that this effect did not seem to occur, being the cross-linking with Sr alone more effective from a mechanical point of view.

When used in bone defects, surrounded by bone which has a higher Young's modulus, mechanical properties of this viscoelastic material may be altered, so dynamic tests were also conducted in confined conditions, in order to better simulate what happened when the hybrid is used as a reinforcement material. The hybrid was kept in a fixed stainless steel cylindrical mold that was positioned in a way that the driveshaft of the instrument did not touch the mold and was only in contact with the hybrid material. In confined conditions the storage modulus increased significantly, over sixteen folds.

3.3 Evaluation of the space between particles using micro-CT

Figure 10 shows a reconstructed μCT image of a hybrid cylinder.

The μCT quantitative analysis of the Sr-hybrid materials showed that 49.4% of the total cylinder volume is occupied by microspheres, with mean interparticle space of 220.7 μm. It was also observed the presence of denser particles distributed between the microspheres in a percentage of 0.3%, possibly corresponding to non-dissolved Sr-carbonate.

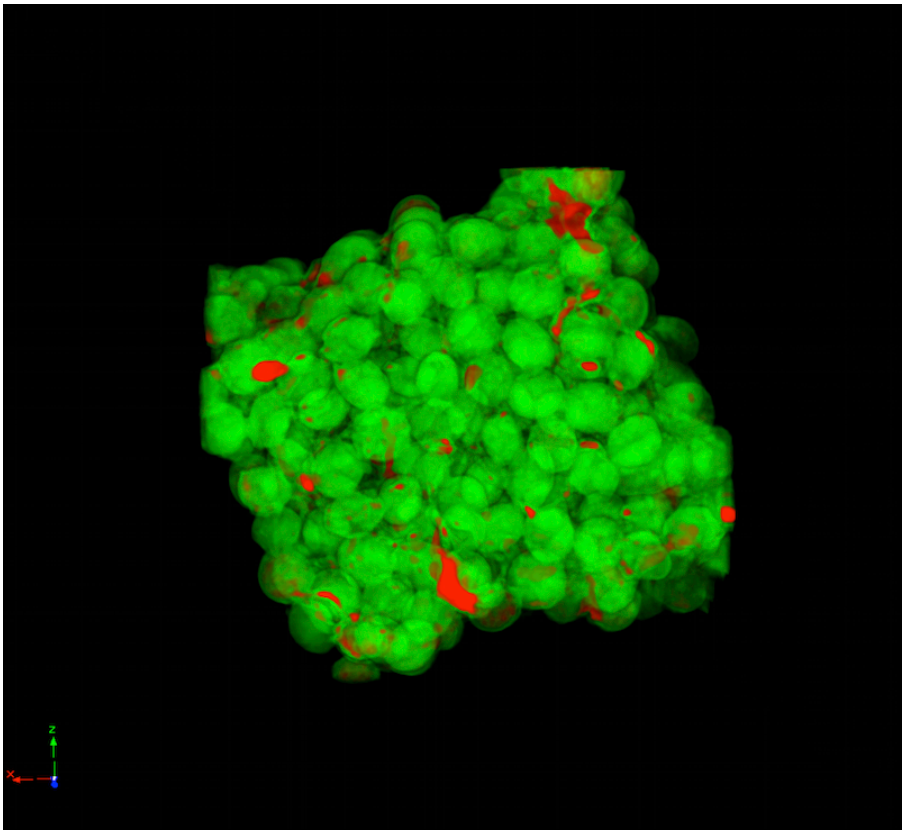

Figure 10. Micro-CT reconstructed image of Sr-hybrid system. Sr-HAp microspheres are represented in green. Denser particles are represented in red, possibly corresponding to non-dissolved Sr-carbonate.

Discussion

A wide variety of particle based fillers for bone regeneration has been described in the literature, including multifaceted granules and smooth spherical particles of various sizes, with or without pores, and with broad or uniform size distributions [3, 5, 6, 16]. The size and shape of the particles dictate their spatial rearrangement within the implant site, playing a critical role in new bone formation. Particles diameter and shape are also relevant parameters when considering injection procedures, since uniform, spherical particles have more predictable flowing properties [12-15]. The microspheres prepared according to the methodology herein described, were uniform, both in terms of size and shape with mean diameters around 555 μm, an appropriate value for effective bone substitution [50]. Adequate mechanical properties of the microspheres are essential so they can resist damage during transportation, packing, handling, and injection. Friability of both microspheres composition (HAp and Sr-HAp) was below detectable levels, and rupture force was adequate to withstand the pressure exerted during extrusion. The addition of Sr also doubles the rupture force of the microspheres. The reason for this can be related to a possible incorporation of Sr into the hydroxyapatite lattice by replacing Ca ions, as supported by FTIR results. It is well known that a wide range of cations and anions, may substitute into the structure of synthetic hydroxyapatite, replacing calcium, phosphate or hydroxyl ions. Ca^{2+} can be substituted to some extent by divalent cations, namely Sr^{2+}. The substitutions alter the crystal lattice, inducing a structural disorder, and consequently changing some of the material properties, including phase stability, solubility, reactivity and mechanical properties. The ionic radius of Ca is about 0.99 Å, while the ionic radius of Sr is higher (1.13 Å). The incorporation of ions larger than Ca into the lattice of hydroxyapatite whereby an elongation of the lattice parameters and, as a result, a deformation of the elementary crystalline cell occurs. Chen *et al.* observed that the incorporation of low doses of Sr (atom ratio of Sr/(Sr+Ca) adjusted to 5%) improved the mechanical properties of hydroxyapatite,

namely compressive strength, Knoop hardness and indirect tensile strength [51].

Alginate is a biomaterial that has found numerous applications in the biomedical field due to its favorable properties such as biocompatibility, ease of gelation and retention of structural similarity to the extracellular matrices in tissues [52]. Alginate is a natural linear polysaccharide that contains 1,4-linked beta-D-mannuronic (M) and alfa-L-guluronic (G) acid residues, arranged in a non-regular and block-wise fashion along the chain. Alginate is well known for its high affinity towards Ca [53]. Ca binds consecutive G-residues (G-blocks) in different alginate chains in a cooperative manner (egg-box model) producing the cross-links of the hydrogel. The cross-linking affects the resulting gel properties, such as stiffness, elasticity, and stability. Hence, the functional properties of alginate gels can be tailored by the selection of alginate composition. In general, alginate having a relatively high content of G (high-G proportion alginates) gives stiff and stable gels with a high porosity, whereas alginate with a low content of G (low-G or high-M proportion alginates) results in more elastic and less stable Ca gels. Having in mind the envisaged application, in the present work alginate with a content of more than 60% of guluronic vs mannuronic acid units was used.

Alginate can also be cross-linked with other divalent ions, including Sr. Strontium ions have very high affinities towards alginate, and have been shown to bind to G- and M- blocks in the alginate [54].

Ca and Sr-alginate gels can be made by internal gelation, meaning that the reticulation agents (Ca or Sr) are leaking at a low rate from an ion provider source within the alginate. In the present work, Ca and Sr were used in the form of carbonate and the release of the metal ions was caused by a reduction in pH due to the addition of GDL. The gelation process is highly dependent upon diffusion of gelation ions into the polymer network. An appropriate gelation time of the hybrid material will be important in clinical practice. It should not be too short so there is enough time to prepare and deliver the system, but not too long, to avoid an

excessively long surgical procedure. The gelation time for the Sr vehicle was significantly shorter than that of the Ca vehicle, but adequate (20 min.), at a normal operating room temperature.

Alginate has been reported to be biocompatible and is, therefore, a good candidate for biomedical applications [47, 52]. Degradation of alginate is slow but can be tuned by manipulating polymer molecular weights and composition [55]. In order to promote bone regeneration, the injectable system that we propose should provide a scaffold capable of supporting cell migration and tissue ingrowth. One well-known strategy to promote cellular infiltration within a cell-free material and to direct *de novo* bone formation at the local implant site is the incorporation of guidance cues such as bio-adhesive motifs derived from extracellular matrices into the biomimetic material [56]. Here, the implanted material provides not only the mechanical support for tissue regeneration but also appropriate guidance signals recognized by protein and proteoglycan receptors on cell surfaces. Grafting of RGD peptides on alginate is pertinent for the application envisaged in this work, since cell attachment is impaired on unmodified alginate. Although in the present work, hybrid system was based on non-functionalized alginate, tests were also performed using RGD functionalized alginate. No significant differences were observed in what concerns to the viscosity of the alginate and the injectability and mechanical properties of the complete system.

The percentage and composition of microspheres, the alginate concentration and the reticulating agent influence the maximum force needed to perform manual injections, which should not exceed 100 N [49]. In a hybrid system of 3% alginate cross-linked with Ca, an increase of the percentage of microspheres to 35% increased the force needed for extrusion above the 100 N limit, and a filtering effect was observed, as the alginate extrudes quicker than the microspheres. Using Sr instead, as the reticulating agent, the extrusion force was smaller, allowing for an increase both in alginate concentration and percentage of microspheres. With the 3.5%Alg-35%Sr-

HAp-Sr composition we obtained the higher compression strength value, still with an extrusion force below the 100 N limit.

Also, the reticulation time when using Sr was smaller than when using Ca, as well as the respective modulus obtained in DMA tests. This is in accordance with the observation of Koo and Ma that alginate hydrogels formed with slower rates of gelation tend to exhibit greater structural homogeneity and therefore larger modulus than those gelled rapidly [46].

The viscoelastic properties of a bone defect filing material determine the capacity of dissipation of energy by bone, and influence the relative response of surrounding damaged and healthy tissue. DMA showed that for all tested materials E' is higher than E" which indicated that the elastic behavior of the hybrid is dominant over the viscous one. Results also showed that the storage modulus was proportional to the HAp microspheres content as indicated in Fig. 7. The obtained results confirmed that the HAp particles acted as reinforcement filler by transferring the sustaining load from the matrix to the rigid particles.

Although important features for bone repair, the mechanical properties of hydrogel/calcium phosphate composites have rarely been reported [57]. Current injectable bone defect fillers, like polymethylmetacrylate (PMMA) or calcium phosphate cements, have maximum compression strength values, which are much higher than that of cancellous bone. Besides, brittleness has limited the use of calcium phosphate cements [58, 59]. The elastic modulus of this hybrid system is below that of cancellous bone (20-5000 MPa) [60, 61], but when tested in a confined setting (as would be the case in bone defects) the elastic mode increases significantly. Low mechanical properties and the non-applicability in load-bearing situations are commonly cited limitations of hydrogels in bone tissue engineering [57]. However they can be used in non load-bearing sites, and, if necessary, supplementary internal fixation devices may be applied [62]. Small size defects (up to 5-10 ml), where mechanical properties are not as critical, may be more adequate for

the use of this hybrid system.

Besides the phase composition, numerous parameters influence bone regeneration. The internal structure of the particles, such as the porosity, the pore size distribution, or the size distribution of the pore interconnections, is of particular relevance. It is expected that the hybrid system that we propose will provide adequate mechanical support in the early phases after surgery and gradual replacement of the artificial scaffold by bone with adequate strength. The system, however, relies on the maintenance of part of its constituents (the microspheres), taking into account that full replacement by healthy, strong bone is not expected due to the age of the patients. Alginate is inherently non-degradable in mammals, as they lack the enzyme (i.e., alginase), which can cleave the polymer chains, but ionically cross-linked alginate gels can be dissolved by release of the divalent ions cross-linking the gel into the surrounding media due to exchange reactions with monovalent cations such as sodium ions. In the model that we propose, it is expected an adequate degradation behavior of alginate leaving a space between particles (220.7 μm) adequate for the invasion of blood vessels and cells.

One advantage of the hybrid system developed in this project was the presence of Sr in its composition. Strontium, in the form of oral strontium ranelate, has been in clinical use as an anti-osteoporotic agent effective in the prevention of both vertebral and non-vertebral osteoporotic fractures [36, 37]. However, cardiovascular safety has been a concern regarding its use. Recently, a small but significant increase in non-fatal myocardial infarctions was observed when analyzing all studies reporting the effect of strontium ranelate in osteoporosis and osteoarthritis [63-65]. Currently, the drug is authorized for the treatment of severe osteoporosis, in postmenopausal women and in adult men, at high risk of fracture for whom treatment with other medicinal products approved for the treatment of osteoporosis is not possible, and the use of strontium ranelate should be restricted to patients with no past or current history of ischemic heart disease, peripheral arterial disease and/or cerebrovascular

disease or uncontrolled hypertension.

The incorporation of Sr in both the microspheres and the vehicle, will allow Sr release since the early stages of implantation, due to the different degradation kinetics of the polymer network (faster) and the ceramic particles (slower). It will be released locally to enhance bone formation, but clinically relevant systemic concentrations are not expected [38, 39, 66]. Baier *et al.* [39] compared the osteointegration of calcium phosphate cement implants containing Sr to calcium phosphate cement implants in ovariectomized rats, and found faster osteointegration and more new bone formation with the addition of Sr, both on the implant surface and within the implant. Systemic release of Sr from the implants did not induce significant effects on bone density in this rat model. Thormann *et al.* [38] studied the effect of Sr modified calcium phosphate cement (SrCPC) in bone formation in critical-size metaphyseal fracture defects in ovariectomized rats. Both higher new bone formation in the SrCPC group compared to CPC group, and high Sr concentration in the interface region of the SrCPC implant were observed. They concluded that Sr release had most probably been responsible for these results, that local delivery of Sr from Sr-loaded biomaterials is possible, and that strontium's biological activity to stimulate new bone formation is preserved within the CPC.

Conclusions

We have developed a strontium rich viscoelastic hybrid system, herein described, that can be manually injected and sets *in situ* at body temperature, providing a scaffold for cell migration and tissue ingrowth. When implanted, the hybrid system will offer structural support while providing a temporary scaffold onto which new bone can grow. The incorporation of two Sr release kinetics (from the alginate and from the microspheres), may further improve effective bone regeneration, which can be especially useful in osteoporotic conditions.

Highlights

- We developed a Sr rich viscoelastic hybrid system (alginate matrix cross-linked *in situ* with Sr, and Sr-rich microspheres)
- It can be manually injected, sets *in situ* and offers structural support, providing a temporary scaffold for bone growth
- The incorporation of Sr relies on the growing evidence of its beneficial effects in bone remodeling and in osteoporosis
- Two Sr release kinetics may further improve effective bone regeneration, which can be especially useful in osteoporosis

Statement of Significance

Current challenges in the development of scaffolds for bone regeneration include the engineering of materials that can withstand physiological mechanical stresses and provide a matrix capable of supporting cell migration and tissue ingrowth. We have developed a strontium (Sr) rich viscoelastic hybrid system (alginate matrix cross-linked in situ in the presence of Sr, and Sr-rich microspheres) that can be manually injected and sets in situ, offering structural support while providing a temporary scaffold onto which new bone can grow. The incorporation of Sr relies on the growing evidence of its beneficial effects in bone remodeling and in the treatment of osteoporosis. The two Sr release kinetics may further improve effective bone regeneration, which can be especially useful in osteoporotic conditions.

Graphical Abstract

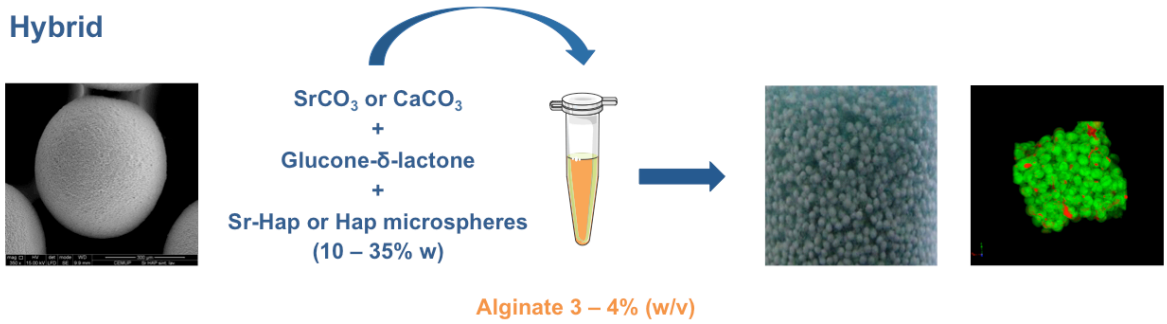

Acknowledgements

This work was financed by FEDER funds, through the Programa Operacional Factores de Competitividade - COMPETE, and by Portuguese funds through FCT - Fundação para a Ciência e a Tecnologia in the framework of the project PTDC/CTM/103181/2008 and of project Pest-C/SAU/LA0002/2011.

The authors thankfully acknowledge the use of Micro-CT in the 3B's Research Group facilities at University of Minho, the use of microscopy services at Centro de Materiais da Universidade do Porto, CEMUP and the technicians responsible for the experimental techniques mentioned, namely Vítor Correlo and Daniela Silva.

References

[1] Zhou H, Lee J. Nanoscale hydroxyapatite particles for bone tissue engineering. Acta Biomater 2011;7:2769-81.

[2] Dorozhkin SV. Amorphous calcium (ortho)phosphates. Acta Biomater 2010;6:4457-75.

[3] Dorozhkin SV. Bioceramics of calcium orthophosphates. Biomaterials 2010;31:1465-85.

[4] Dorozhkin SV. Nanosized and nanocrystalline calcium orthophosphates. Acta Biomater 2010;6:715-34.

[5] Combes C, Rey C. Amorphous calcium phosphates: synthesis, properties and uses in biomaterials. Acta Biomater 2010;6:3362-78.

[6] Low KL, Tan SH, Zein SH, Roether JA, Mourino V, Boccaccini AR. Calcium phosphate-based composites as injectable bone substitute materials. J Biomed Mater Res B Appl Biomater 2010;94:273-86.

[7] Grimandi G, Weiss P, Millot F, Daculsi G. In vitro evaluation of a new injectable calcium phosphate material. J Biomed Mater Res 1998;39:660-6.

[8] Iooss P, Le Ray AM, Grimandi G, Daculsi G, Merle C. A new injectable bone substitute combining poly(epsilon-caprolactone) microparticles with biphasic calcium phosphate granules. Biomaterials 2001;22:2785-94.

[9] Dupraz A, Nguyen TP, Richard M, Daculsi G, Passuti N. Influence of a cellulosic ether carrier on the structure of biphasic calcium phosphate ceramic particles in an injectable composite material. Biomaterials 1999;20:663-73.

[10] Yaszemski MJ, Payne RG, Hayes WC, Langer R, Mikos AG. In vitro degradation of a poly(propylene fumarate)-based composite material. Biomaterials 1996;17:2127-30.

[11] Maruyama M, Ito M. In vitro properties of a chitosan-bonded self-hardening paste with hydroxyapatite granules. J Biomed Mater Res 1996;32:527-32.

[12] Qiu QQ, Ducheyne P, Ayyaswamy PS. New bioactive, degradable composite microspheres as tissue engineering substrates. J Biomed Mater Res 2000;52:66-76.

[13] Hsu FY, Chueh SC, Wang YJ. Microspheres of hydroxyapatite/reconstituted collagen as supports for osteoblast cell growth. Biomaterials 1999;20:1931-6.

[14] Sunny MC, Ramesh P, Varma HK. Microstructured microspheres of hydroxyapatite bioceramic. J Mater Sci Mater Med 2002;13:623-32.

[15] Sivakumar M, Rao KP. Preparation, characterization, and in vitro release of gentamicin from coralline hydroxyapatite-alginate composite microspheres. J Biomed Mater Res A 2003;65:222-8.

[16] Bohner M, Tadier S, van Garderen N, de Gasparo A, Dobelin N, Baroud G. Synthesis of spherical calcium phosphate particles for dental and orthopedic applications. Biomatter 2013;3.

[17] Liu HY, Wu AT, Tsai CY, Chou KR, Zeng R, Wang MF, et al. The balance between adipogenesis and osteogenesis in bone regeneration by platelet-rich plasma for age-related osteoporosis. Biomaterials 2011;32:6773-80.

[18] Cao L, Liu G, Gan Y, Fan Q, Yang F, Zhang X, et al. The use of autologous enriched bone marrow MSCs to enhance osteoporotic bone defect repair in long-term estrogen deficient goats. Biomaterials 2012;33:5076-84.

[19] Cho SW, Sun HJ, Yang JY, Jung JY, Choi HJ, An JH, et al. Human adipose tissue-derived stromal cell therapy prevents bone loss in ovariectomized nude mouse. Tissue Eng Part A 2012;18:1067-78.

[20] Wang Z, Goh J, Das De S, Ge Z, Ouyang H, Chong JS, et al. Efficacy of bone marrow-derived stem cells in strengthening osteoporotic bone in a rabbit model. Tissue Eng 2006;12:1753-61.

[21] Marie PJ, Felsenberg D, Brandi ML. How strontium ranelate, via opposite effects on bone resorption and formation, prevents osteoporosis. Osteoporos Int 2011;22:1659-67.

[22] Grynpas MD, Hamilton E, Cheung R, Tsouderos Y, Deloffre P, Hott M, et al. Strontium increases vertebral bone volume in rats at a low dose that does not induce detectable mineralization defect. Bone 1996;18:253-9.

[23] Bonnelye E, Chabadel A, Saltel F, Jurdic P. Dual effect of strontium ranelate: stimulation of osteoblast differentiation and inhibition of osteoclast formation and resorption in vitro. Bone 2008;42:129-38.

[24] Yang F, Yang D, Tu J, Zheng Q, Cai L, Wang L. Strontium enhances osteogenic differentiation of mesenchymal stem cells and in vivo bone formation by activating Wnt/catenin signaling. Stem Cells 2011;29:981-91.

[25] Baron R, Tsouderos Y. In vitro effects of S12911-2 on osteoclast function and bone marrow macrophage differentiation. Eur J Pharmacol 2002;450:11-7.

[26] Peng S, Liu XS, Huang S, Li Z, Pan H, Zhen W, et al. The cross-talk between osteoclasts and osteoblasts in response to strontium treatment: involvement of osteoprotegerin. Bone 2011;49:1290-8.

[27] Hurtel-Lemaire AS, Mentaverri R, Caudrillier A, Cournarie F, Wattel A, Kamel S, et al. The calcium-sensing receptor is involved in strontium ranelate-induced osteoclast apoptosis. New insights into the associated signaling pathways. J Biol Chem 2009;284:575-84.

[28] Peng S, Zhou G, Luk KD, Cheung KM, Li Z, Lam WM, et al. Strontium promotes osteogenic differentiation of mesenchymal stem cells through the Ras/MAPK signaling pathway. Cell Physiol Biochem 2009;23:165-74.

[29] Caverzasio J. Strontium ranelate promotes osteoblastic cell replication through at least two different mechanisms. Bone 2008;42:1131-6.

[30] Delannoy P, Bazot D, Marie PJ. Long-term treatment with strontium ranelate increases vertebral bone mass without deleterious effect in mice. Metabolism 2002;51:906-11.

[31] Buehler J, Chappuis P, Saffar JL, Tsouderos Y, Vignery A. Strontium ranelate inhibits bone resorption while maintaining bone formation in alveolar bone in monkeys (Macaca fascicularis). Bone 2001;29:176-9.

[32] Ammann P, Shen V, Robin B, Mauras Y, Bonjour JP, Rizzoli R. Strontium ranelate improves bone resistance by increasing bone mass and improving architecture in intact female rats. J Bone Miner Res 2004;19:2012-20.

[33] Ammann P, Badoud I, Barraud S, Dayer R, Rizzoli R. Strontium ranelate treatment improves trabecular and cortical intrinsic bone tissue quality, a determinant of bone strength. J Bone Miner Res 2007;22:1419-25.

[34] Bain SD, Jerome C, Shen V, Dupin-Roger I, Ammann P. Strontium ranelate improves bone strength in ovariectomized rat by positively influencing bone resistance determinants. Osteoporos Int 2009;20:1417-28.

[35] Peng S, Liu XS, Wang T, Li Z, Zhou G, Luk KD, et al. In vivo anabolic effect of strontium on trabecular bone was associated with increased osteoblastogenesis of bone marrow stromal cells. J Orthop Res 2010;28:1208-14.

[36] Meunier PJ, Roux C, Seeman E, Ortolani S, Badurski JE, Spector TD, et al. The effects of strontium ranelate on the risk of vertebral fracture in women with postmenopausal osteoporosis. N Engl J Med 2004;350:459-68.

[37] Reginster JY, Seeman E, De Vernejoul MC, Adami S, Compston J, Phenekos C, et al. Strontium ranelate reduces the risk of nonvertebral fractures in postmenopausal women with osteoporosis: Treatment of Peripheral Osteoporosis (TROPOS) study. J Clin Endocrinol Metab 2005;90:2816-22.

[38] Thormann U, Ray S, Sommer U, Elkhassawna T, Rehling T, Hundgeburth M, et al. Bone formation induced by strontium modified calcium phosphate cement in critical-size metaphyseal fracture defects in ovariectomized rats. Biomaterials 2013;34:8589-98.

[39] Baier M, Staudt P, Klein R, Sommer U, Wenz R, Grafe I, et al. Strontium enhances osseointegration of calcium phosphate cement: a histomorphometric pilot study in ovariectomized rats. J Orthop Surg Res 2013;8:16.

[40] Liu P, Wang N, Hao Y, Zhao Q, Qiao Y, Li H, et al. Entangled titanium fibre balls combined with nano strontium hydroxyapatite in repairing bone defects. Med Princ Pract 2014;23:264-70.

[41] Oliveira SM, Barrias CC, Almeida IF, Costa PC, Ferreira MR, Bahia MF, et al. Injectability of a bone filler system based on hydroxyapatite microspheres and a vehicle with in situ gel-forming ability. J Biomed Mater Res B Appl Biomater 2008;87:49-58.

[42] Barrias CC, Lamghari M, Granja PL, Sa Miranda MC, Barbosa MA. Biological evaluation of calcium alginate microspheres as a vehicle for the localized delivery of a therapeutic enzyme. J Biomed Mater Res A 2005;74:545-52.

[43] Ribeiro CC, Barrias CC, Barbosa MA. Calcium phosphate-alginate microspheres as enzyme delivery matrices. Biomaterials 2004;25:4363-73.

[44] Ribeiro CC, Barrias CC, Barbosa MA. Preparation and characterisation of calcium-phosphate porous microspheres with a uniform size for biomedical applications. J Mater Sci Mater Med 2006;17:455-63.

[45] Barrias CC, Ribeiro CC, Lamghari M, Miranda CS, Barbosa MA. Proliferation, activity, and osteogenic differentiation of bone marrow stromal cells cultured on calcium titanium phosphate microspheres. J Biomed Mater Res A 2005;72:57-66.

[46] Kuo CK, Ma PX. Ionically cross-linked alginate hydrogels as scaffolds for tissue engineering: part 1. Structure, gelation rate and mechanical properties. Biomaterials 2001;22:511-21.

[47] Evangelista MB, Hsiong SX, Fernandes R, Sampaio P, Kong HJ, Barrias CC, et al. Upregulation of bone cell differentiation through immobilization within a synthetic extracellular matrix. Biomaterials 2007;28:3644-55.

[48] Fonseca KB, Bidarra SJ, Oliveira MJ, Granja PL, Barrias CC. Molecularly designed alginate hydrogels susceptible to local proteolysis as three-dimensional cellular microenvironments. Acta Biomaterialia 2011;7:1674-82.

[49] Krebs J, Ferguson SJ, Bohner M, Baroud G, Steffen T, Heini PF. Clinical measurements of cement injection pressure during vertebroplasty. Spine (Phila Pa 1976) 2005;30:E118-22.

[50] Gauthier O, Bouler JM, Weiss P, Bosco J, Aguado E, Daculsi G. Short-term effects of mineral particle sizes on cellular degradation activity after implantation of injectable calcium phosphate biomaterials and the consequences for bone substitution. Bone 1999;25:71S-4S.

[51] Chen DF, YF. Evaluation on the mechanic properties of the solid solution of strontium substituted hydroxyapatite. Chin J Stoma Mater Appar 2001;19:178-83.

[52] Lee KY, Mooney DJ. Alginate: properties and biomedical applications. Prog Polym Sci 2012;37:106-26.

[53] Andersen T, Strand BL, Formo K, Alsberg E, Christensen BE. Chapter 9 Alginates as biomaterials in tissue engineering. Carbohydrate Chemistry: Volume 37: The Royal Society of Chemistry; 2012. p. 227-58.

[54] Morch YA, Donati I, Strand BL, Skjak-Braek G. Effect of Ca2+, Ba2+, and Sr2+ on alginate microbeads. Biomacromolecules 2006;7:1471-80.

[55] Augst AD, Kong HJ, Mooney DJ. Alginate hydrogels as biomaterials. Macromol Biosci 2006;6:623-33.

[56] Sakiyama-Elbert SH, JA Functional biomaterials: Design of novel biomaterials. . Annual Review of Materials Research 2001;31:183-201.

[57] D'Este M, Eglin D. Hydrogels in calcium phosphate moldable and injectable bone substitutes: Sticky excipients or advanced 3-D carriers? Acta Biomater 2013;9:5421-30.

[58] Friedman CD, Costantino PD, Takagi S, Chow LC. BoneSource hydroxyapatite cement: a novel biomaterial for craniofacial skeletal tissue engineering and reconstruction. J Biomed Mater Res 1998;43:428-32.

[59] Xu HH, Quinn JB. Calcium phosphate cement containing resorbable fibers for short-term reinforcement and macroporosity. Biomaterials 2002;23:193-202.

[60] Ouyang J, Yang GT, Wu WZ, Zhu QA, Zhong SZ. Biomechanical characteristics of human trabecular bone. Clin Biomech (Bristol, Avon) 1997;12:522-4.

[61] Keaveny TM, Morgan EF, Niebur GL, Yeh OC. Biomechanics of trabecular bone. Annu Rev Biomed Eng 2001;3:307-33.

[62] Willie BM, Petersen A, Schmidt-Bleek K, Cipitria A, Mehta M, Strube P, et al. Designing biomimetic scaffolds for bone regeneration: why aim for a copy of mature tissue properties if nature uses a different approach? Soft Matter 2010;6:4976-87.

[63] Reginster JY, Neuprez A, Dardenne N, Beaudart C, Emonts P, Bruyere O. Efficacy and safety of currently marketed anti-osteoporosis medications. Best Pract Res Clin Endocrinol Metab 2014;28:809-34.

[64] Cooper C, Fox KM, Borer JS. Ischaemic cardiac events and use of strontium ranelate in postmenopausal osteoporosis: a nested case-control study in the CPRD. Osteoporos Int 2014;25:737-45.

[65] Abrahamsen B, Grove EL, Vestergaard P. Nationwide registry-based analysis of cardiovascular risk factors and adverse outcomes in patients treated with strontium ranelate. Osteoporos Int 2014;25:757-62.

[66] Hulsart-Billstrom G, Xia W, Pankotai E, Weszl M, Carlsson E, Forster-Horvath C, et al. Osteogenic potential of Sr-doped calcium phosphate hollow spheres in vitro and in vivo. J Biomed Mater Res A 2013;101:2322-31.

CHAPTER IV

INJECTABLE HYBRID SYSTEM FOR STRONTIUM LOCAL DELIVERY PROMOTES BONE REGENERATION IN A RAT CRITICAL-SIZED DEFECT MODEL

Article 3

Published in Scientific Reports. 2017 Jul 11;7(1):5098

doi: 10.1038/s41598-017-04866-4

Injectable hybrid system for strontium local delivery promotes bone regeneration in a rat critical-sized defect model

Ana Henriques Lourenço[1,2,3 *], Nuno Neves[1,2,4 *], Cláudia Ribeiro-Machado [1,2], Susana R. Sousa[1,2,5], Meriem Lamghari[1,2], Cristina C. Barrias[1,2], Abel Trigo Cabral[4], Mário A. Barbosa[1,2,6], Cristina C. Ribeiro[1,2,5 #]

[1]i3S - Instituto de Investigação e Inovação em Saúde, Universidade do Porto, Rua Alfredo Allen, 208, 4200 - 135 Porto, Portugal

[2]INEB - Instituto de Engenharia Biomédica, Universidade do Porto, Rua Alfredo Allen, 208, 4200 - 135 Porto, Portugal

[3]Faculdade de Engenharia, Universidade do Porto, Rua Dr. Roberto Frias, s/n, 4200-465 Porto, Portugal

[4]Faculdade de Medicina, Universidade do Porto, Serviço de Ortopedia, Alameda Prof. Hernâni Monteiro, 4200-319 Porto, Portugal

[5]ISEP – Instituto Superior de Engenharia do Porto, Instituto Politécnico do Porto, Rua Dr. António Bernardino de Almeida 431, 4249-015, Porto, Portugal

[6]ICBAS - Instituto de Ciências Biomédicas de Abel Salazar, Universidade do Porto, Rua de Jorge Viterbo Ferreira n. 228, 4050-313 Porto, Portugal

[*] *These authors contributed equally to this work.*

Abstract

Strontium (Sr) has been described as having beneficial influence in bone strength and architecture. However, negative systemic effects have been reported on oral administration of Sr ranelate, leading to strict restrictions in clinical application. We hypothesized that local delivery of Sr improves osteogenesis without eliciting detrimental side effects. Therefore, the in vivo response to an injectable Sr-hybrid system composed of RGD-alginate hydrogel cross-linked in situ with Sr and reinforced with Sr-doped hydroxyapatite microspheres, was investigated. The system was injected in a critical-size bone defect model and compared to a similar Sr-free material. Micro-CT results show a trend towards higher new bone formed in Sr-hybrid group and major histological differences were observed between groups. Higher cell invasion was detected at the center of the defect of Sr-hybrid group after 15 days with earlier bone formation. Higher material degradation with increase of collagen fibers and bone formation in the center of the defect after 60 days was observed as opposed to bone formation restricted to the periphery of the defect in the control. These histological findings support the evidence of an improved response with the Sr enriched material. Importantly, no alterations were observed in the Sr levels in systemic organs or serum.

Keywords: strontium, bone regeneration, injectable bone substitute, alginate, hydroxyapatite, ionic delivery system

Introduction

The management of fractures and bone defects remains a significant challenge, and there is the need for improved therapeutic strategies [1]. Biological (autografts, allografts and xenografts) and synthetic bone grafts are currently used in clinical practice for bone repair. Because of their osteogenic potential and the absence of risks of immune rejection or disease transfer, autografts are clinically preferred. However, they are limited in supply, imply the additional morbidity of a harvest surgery and their properties and shape do not match exactly those of the bone to be replaced [2]. Intensive investigation is being carried out to produce synthetic bone grafts in order to overcome these problems. The use of injectable materials in bone regeneration, especially calcium phosphate based materials, presents several advantages, namely due to their adequate biological responses, osteoconductivity and mechanical properties [3-6]. These materials can be applied by minimally invasive surgical procedures, to efficiently fill-in cavities of non-uniform shapes, with no tissue damage and limited exposure to infectious agents, thus reducing patient discomfort and procedure-associated health costs. The addition of osteoinductive factors or osteoprogenitor/stem cells may improve bone repair, particularly in osteoporotic conditions, characterized by an impaired healing response [7-10].

Oral administration of Strontium (Sr) ranelate has shown effectiveness in the prevention of both vertebral and non-vertebral osteoporotic fractures [11, 12]. Unlike other anti-osteoporotic agents widely used in clinical practice, such as bisphosphonates, estrogen, selective estrogen-receptor modulators (SERMs) and calcitonin, which inhibit bone resorption [9], Sr ranelate also promotes bone formation [13-16]. Several in vitro studies show that Sr ranelate decreases bone resorption, by reducing osteoclast activity [13, 14, 17], decreasing functional osteoclast markers expression [13], disrupting osteoclasts cytoskeleton [14], and increasing osteoclast apoptosis [18]. Simultaneously, it induces positive effects on osteoblastogenesis and osteoblast activity in different in vitro models [19], namely by

enhancing replication of preosteoblastic cells [14, 20-23], increasing osteogenesis [14, 20, 24-26], decreasing osteoblast apoptosis [21, 27], and promoting terminal differentiation of osteoblasts into osteocytes [20]. Some pre-clinical studies performed in both normal and osteopenic/osteoporotic animal models confirmed these in vitro results, showing the beneficial effects of Sr ranelate on bone formation and remodeling [28-32]. Despite these important effects, cardiovascular safety of orally administered Sr ranelate has been questioned due to a small but significant increase in non-fatal myocardial infarctions [12, 33, 34]. Currently, there are strict indications and restrictions to its use [12].

Nevertheless, Sr incorporation into biomaterials for bone regeneration may improve their regeneration potential. In vivo studies showed that doping calcium phosphate cements and other ceramics with Sr promotes bone repair [35-37]. A sustained delivery system for local release of Sr ions can obviate systemic complications with similar rates of bone formation at the site of implantation.

Current injectable bone defect methacrylate-based fillers have compression strengths much higher than that of cancellous bone, and the brittleness of calcium phosphate cements is a limitation [38, 39]. We have previously developed various types of injectable biomaterials for bone regeneration, namely calcium phosphate [40-42] and calcium phosphate/alginate [43] microspheres, as well as different types of bio-functional alginate hydrogels [44-47]. When combined, alginate can act as an appropriate vehicle for ceramic microspheres delivery and immobilization at the injury site. Alginate is a natural linear polysaccharide, biodegradable and biocompatible, extensively studied for biomedical applications [48, 49]. Although generally regarded as a bioinert material, since it does not elicit specific cell-matrix interactions, grafting of alginate with arginine-glycine-aspartic acid (RGD) peptides is an effective strategy to provide appropriate guidance signals to promote cell adhesion and facilitate cell colonization [50]ENREF_49. Alginate forms hydrogels under mild chemical conditions, in the presence of divalent cations, such as Ca and Sr, through a

cytocompatible physical gelation process. These cations bind homoguluronic blocks in adjacent alginate chains in a cooperative manner (egg-box model) producing a cross-linked hydrogel network [51, 52].

Recently, we developed an injectable hybrid system that consists of ~500 μm diameter hydroxyapatite (HAp) microspheres doped with Sr, embedded in a functionalized alginate matrix cross-linked in situ with Sr [53]. As a vehicle for the microspheres delivery, functionalized alginate with RGD peptides was used, providing a scaffold for cell adhesion and migration and allowing for the injectability of the system. However, the use of hydrogels in bone tissue engineering is limited by low mechanical properties and the non-applicability in load-bearing conditions [54]. The packing of the microspheres upon delivery raises the compression strength of the material [53], and alginate creates an interconnected 3D network adequate for the invasion of blood vessels and cells [55]. Moreover, the presence of Sr in both components of the system provides two different release routes upon degradation of the materials. This system presents a clinically relevant compromise between adequate injectability and gelation time and final compression strength [53]. Moreover, in vitro studies showed that this Sr-hybrid scaffold promotes sustained release of Sr^{2+}, supports human mesenchymal stem cells adhesion, survival and osteogenic differentiation, and inhibits osteoclasts differentiation and activity, as compared to a similar Sr-free system [56].

In the current study we aim to evaluate the in vivo response to the designed Sr-rich hybrid system and its influence on new bone formation using a rat metaphyseal femoral critical-sized defect model, compared to a similar Sr-free material. The proposed system is expected to provide an adequate therapeutic approach to fill-in bone defects by minimally invasive surgery, while acting as a scaffold for local Sr^{2+} release to promote bone regeneration.

Results

Radiographical analysis of bone and biomaterial

A cylindrical defect with 3 mm diameter and depth of approximately 4 mm was drilled in the lateral condyle of the right femur (Figure 1A). The defect was filled with the biomaterial, injected using a 1 mL syringe (Figure 1B, C). A picture of the Sr-hybrid material used is shown in Figure 1D, where spherical particles (Sr-HAp microspheres) are embedded within a transparent hydrogel (Sr cross-linked RGD-alginate).

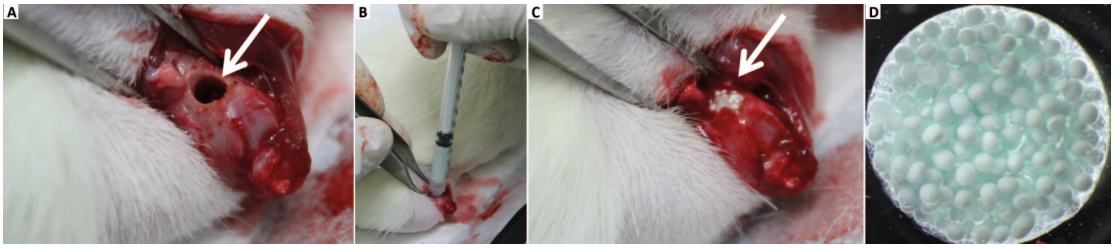

Figure 1. In vivo intraoperative setting. Critical sized defect created in the distal femur (A). Injection of the hybrid material using a 1 mL syringe (B) and filled defect (C). Detail of the hybrid system, composed of HAp microspheres embedded in a RGD-alginate hydrogel (D).

Rat femurs were imaged by X-ray along the experimental period allowing for a follow-up at 15 and 30 days. Representative images of defects filled with materials (Sr-hybrid or Ca-hybrid) or empty defects are shown in Fig. 2. In hybrid-filled defects (Fig. 2A to D), microspheres are located inside the created bone defect (arrows in the images), where the higher radiopacity of the HAp microspheres allowed for the easy monitoring using X-ray. Microspheres were homogeneously distributed within the defects (Fig. 2A to D) and were still detected at day 30, a non-invasive mid-term follow-up (Fig. 2B and D). Empty defects were also imaged (Fig. 2E and F) and the defect could still be observed after 30 days, confirming it to be of a critical size.

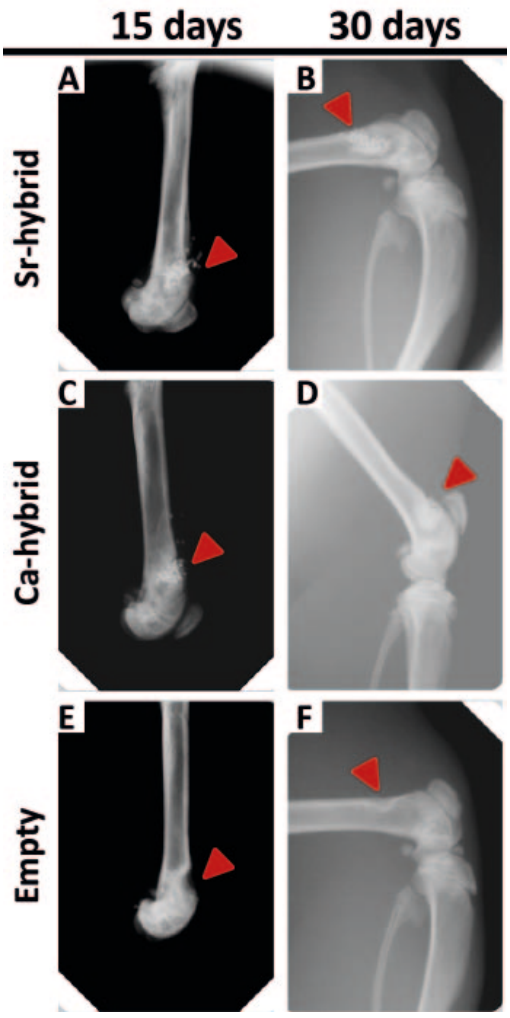

Figure 2. Radiographic imaging follow-up. Representative lateral X-Ray images from right rat femurs of Sr-hybrid (A and B) or Ca-hybrid-filled (C and D) and empty (E and F) defects at 15 days (A, C and E) and 30 days (B ,D and F) post-surgery. Arrows pinpoint site of created defect, filled or empty. Microspheres can be observed as circular objects more radiopaque than bone.

Micro-CT morphometric 3D evaluation

Micro-CT analysis was performed 60 days post-implantation (Fig. 3) to evaluate new bone formation at the defect site and to assess the spatial distribution of ceramic microspheres within the lesion. In Sr-hybrid filled defects (Fig. 3A), microspheres were homogeneously distributed inside the defect with no apparent degradation, with preserved size and without modifications in shape. Similar results were found in Ca-hybrid filled defects. Furthermore, and particularly in Sr-hybrid samples, centripetal bone colonization could be observed by new bone formation surrounding the ceramic microspheres and with the development of new bone trabeculae in the periphery of the defect. 3D morphometric analysis was performed using five femurs per group,

where the ROI was defined in binary images (Fig. 3B) and the percentage of new bone formed (bone volume fraction, BV/TV) was calculated. Values of (31.5±1.7) % and (28.6±1.1) % (BV/TV (%), mean±SE) of new bone was measured in animals that received the Sr-hybrid and Ca-hybrid materials, respectively (Fig. 3C).

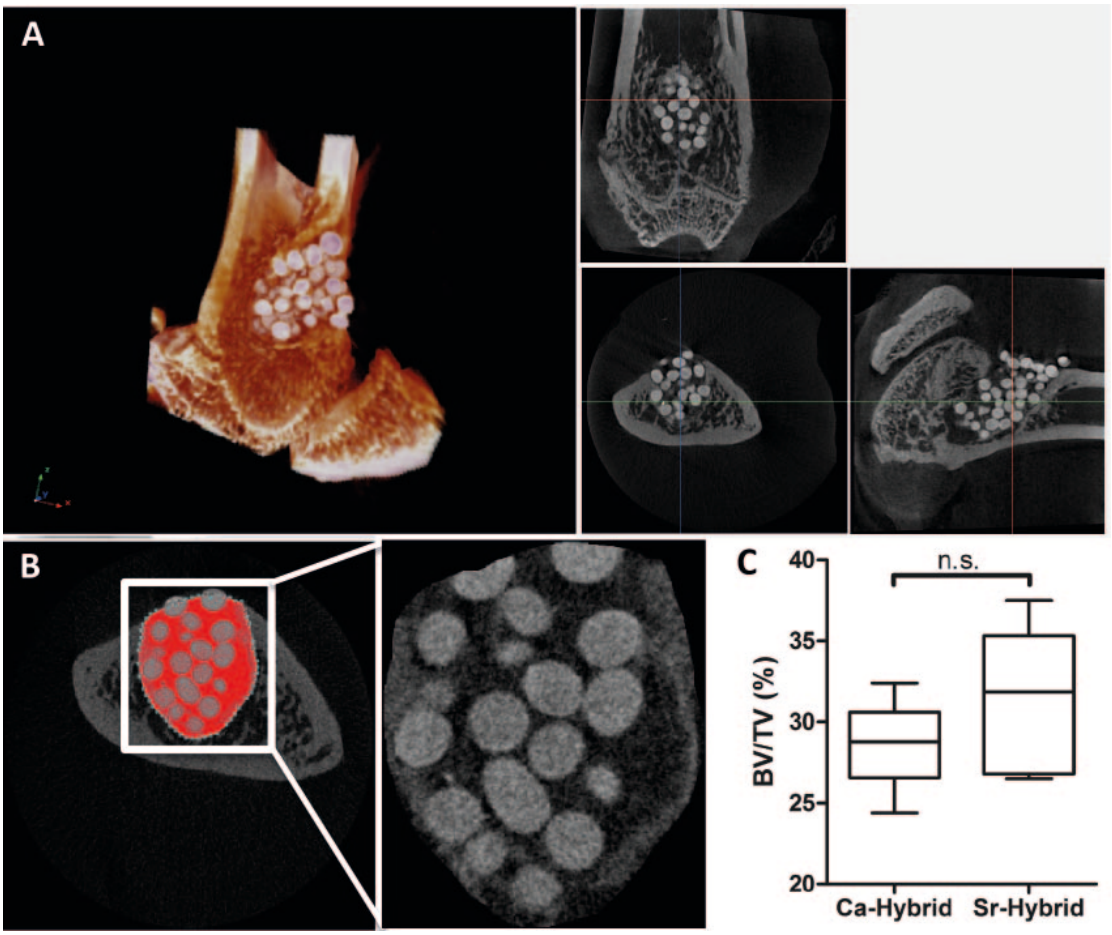

Figure 3. Micro-CT analysis of distal femur after 60 days of implantation. 3D reconstructed image and respective orthogonal slices of micro-CT acquisition of the femur with Sr-hybrid filled defect (A). Morphometric analysis approach used to quantify new bone formation: transversal micro-CT slice of a femur injected with Sr-hybrid after 60 days of implantation highlighting ROI (B). C - New bone formed (BV/TV, %) after 60 days of implantation of Sr-hybrid and Ca-hybrid materials. Data presented as box-plot with median and min to max whiskers of n = 5 samples (n.s. – statistically non-significant).

Histological evaluation of bone/biomaterial interface

In Fig. 4A representative images of femurs with defects filled with Sr-hybrid or Ca-hybrid materials, at days 15 and 60, are portrayed. A global view of the defects and materials (Fig. 4A a to d), as well as a more detailed view of the periphery of the defect (Fig. 4A a' to d' and magnifications a'' to d''), are given. Histological analysis at

day 15 post-implantation showed that the created defects exhibited similar diameter and were filled with approximately 15 to 18 microspheres (Fig. 4A a, b). As early as 15 days post-implantation, all animals showed, to some extent, newly formed bone at the periphery of the defect (Fig 4A a', b'). Sr-hybrid implanted defects also showed new bone formation in close contact with the microspheres, distant from the periphery of native bone (Fig. 4A b'', arrow). SEM images and EDS analysis of this newly formed bone in close vicinity of the microspheres is shown in Fig. 4B. The results confirmed the high content of calcium and phosphate, and a Ca/P ratio in accordance with normal bone composition (Z1 in Fig. 4B), and different from the elemental analysis of the microspheres (Z2 in Fig. 4B), where Sr was also identified.

After 60 days, new bone formation at the periphery was observed in both materials. Sr-hybrid implanted defects exhibited a thicker trabecular bone structure at the periphery of the defect (Fig 4A d', d''), when compared to the Ca-hybrid group (Fig. 4A c', c''). The quantification of new bone formed at the periphery of the defect revealed a statistically significant thicker bone structure in Sr-hybrid group (662.4±48 μm) in contrast to a thinner bone formation (381.1±29 μm) in the Ca-hybrid group (mean±SE, $p<0.001$, Fig. 4C).

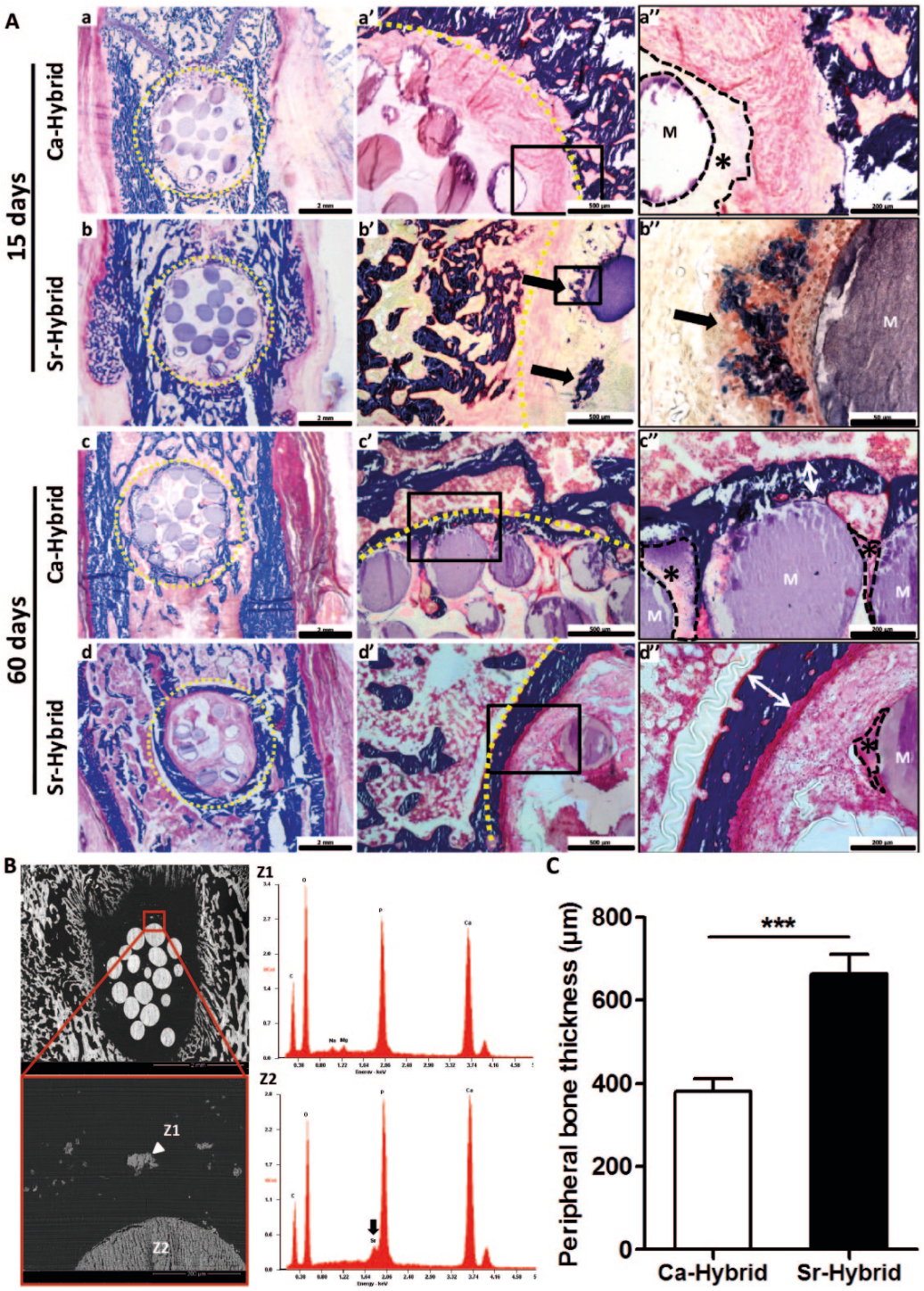

Figure 4. Histological evaluation of bone/biomaterial interface in femurs implanted with Sr-hybrid and Ca-hybrid systems. Coronal histological sections of critical sized defect created in the distal femur, 15 and 60 days post-implantation (A). Global view of the created defects filled with Ca-hybrid (a and c) and Sr-hybrid (b and d) materials, at 15 (a and b) or 60 days (c and d) post-implantation, stained with MT (a to d, dashed yellow line circling the created defect area). Interface bone/biomaterial, 15 days (a' and b') and 60 days (c' and d') post-implantation, with Ca-hybrid (a' and c') and Sr-hybrid (b' and d') systems, and higher magnification of square (a'' to d'', collagen/bone in blue, yellow dashed line – bone/biomaterial interface, * – alginate, M – microspheres, black arrows – new bone). B - SEM image of histological section of Sr-hybrid filled defect 15 days post-implantation with EDS spectra of new bone (Z1) found near the microsphere and microsphere (Z2). C - Thickness of peripheral bone found around the defect (as represented with arrows in A c'' and A d''), 60 days post-implantation of Sr-hybrid and Ca-hybrid systems. Data presented as mean±SEM of 20 different random locations of trabecular bone found around the defect of n=5 animals/group, 3 sections/animal, Asterisks show statistically significant differences (*** $p<0.001$).

Histological evaluation of the center of the defect

Representative images of the center of the defect in both groups are shown in Fig. 5A. Although no evident differences were observed in the diameter of the microspheres with time of implantation, alginate showed different behavior between groups. After 15 days, some alginate was observed surrounding microspheres in both experimental groups (Fig 5A, a and b). In Sr-hybrid group, higher cell invasion at the center was observed, mainly of polymorphonuclear neutrophils (PMN) (Fig 5A, b and b').

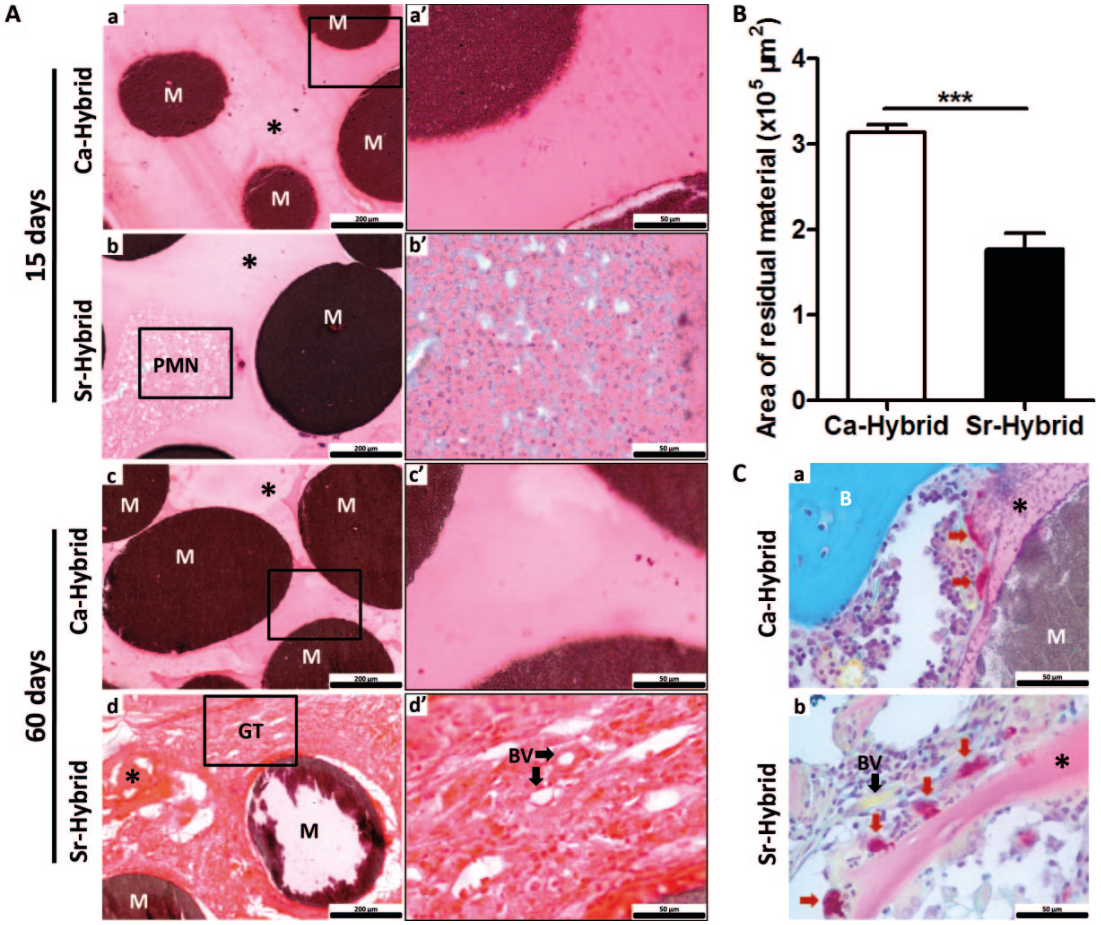

Figure 5. Histological analysis of the center of the defect in femurs implanted with Sr-hybrid and Ca-hybrid systems. Detailed view of the center of the defect implanted with Ca-hybrid (a and c) and Sr-hybrid (b and d) materials, stained with H&E, after 15 (a and b) and 60 days (c and d) of implantation, with higher magnification of square (a' to d', A). B - Area of residual material (microspheres and alginate) found within the defect area, 60 days post-implantation of Sr-hybrid and Ca-hybrid systems. Measurements were performed by delimiting the area of material in MT stained sections using ImageJ software, n=5 animals/group, 3 sections/animal. Data presented as mean±SE and asterisks show statistically significant differences (*** $p<0.001$). C – TRAP-LG staining images of Ca-hybrid (a) and Sr-hybrid (b) systems filled defects, 60 days post-implantation. (M – microspheres, * – alginate, PMN – Polymorphonuclear neutrophils, GT – Granulation Tissue, BV – blood vessels, red arrows – Osteoclasts).

After 60 days, alginate was still present in both groups (Fig. 5A, c and d), although higher degradation was observed in Sr-hybrid filled defects. A statistically significant decrease in the area of residual material (alginate + microspheres) present on the defect site was observed in Sr-hybrid group with an area of 1.77±0.2 x105 μm2 compared to 3.14± 0.1 x105 μm2 in Ca-hybrid group (mean±SE, $p<0.001$, Fig. 5B). In a detailed microscopic analysis of the center of the Sr-hybrid filled defects (Fig. 5A, d and d') granulation tissue could be observed, with the presence of blood vessels (Fig. 5A d') and osteoclasts (Fig. 5C b). In contrast, in Ca-hybrid group osteoclasts were found only at the periphery of the defect (Fig. 5C a). Furthermore, PSR staining images under conventional light (Fig. 6A a and c) showed the presence of collagen (in red) within the area of the defect in Sr-hybrid (Fig. 6A c) at a higher extent than in Ca-hybrid filled defect after 60 days (Fig. 6A a). The use of PSR-polarization method (Fig. 6A b and d) allowed for the quantification of different types of collagen fibrils, i.e. green and red, which are associated with thin/immature/type III and thick/mature/type I collagen, respectively. The quantification was performed within the central area of the defect using a fixed ROI (diameter=2.4 mm, yellow circle in Fig. 6A b and d) and results are shown in Fig. 6B. As expected, an increase in the percentage of red/type I collagen was observed from day 15 to day 60 in both groups. However, 60 days post-implantation, a slightly higher percentage of red/type I collagen was measured in the central defect region in Sr-hybrid group ((3.3±1.3) %, mean±SE) compared to Ca-hybrid group ((1.9±0.3) %, mean±SE).

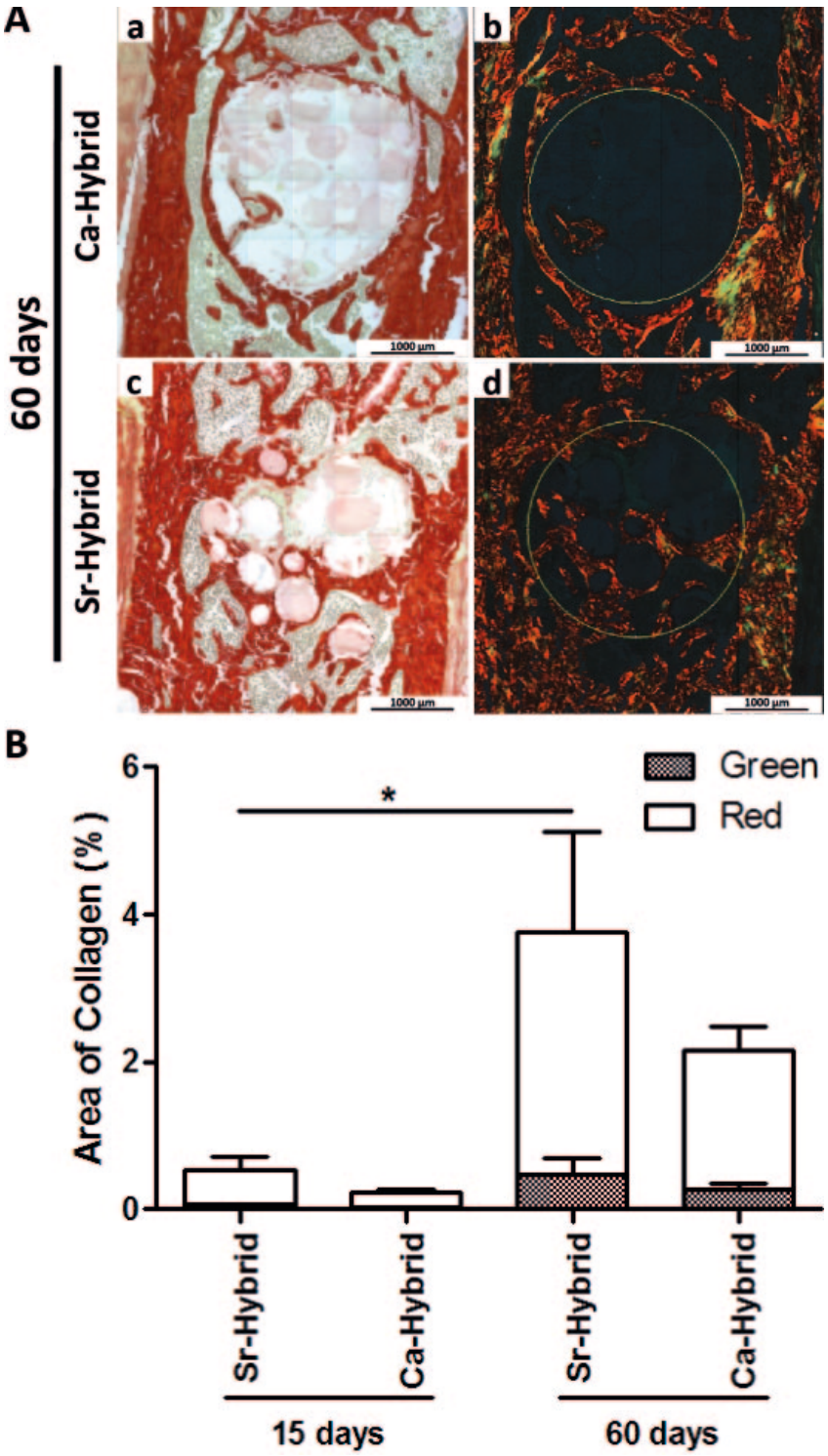

Figure 6. Quantification of birefringent collagen fibers by PSR-polarization method in the center of the defect. PSR staining visualized under conventional light (a and c) and polarized light (b and d) to identify different collagen fiber types, 60 days post-implantation of Ca-hybrid (a and b) and Sr-hybrid (c and d) systems (A). PSR stains collagen in red (conventional light) and collagen fibers are specifically birefringent in polarized light (green - thin fibers/type III; red - thick fibers/type I, MosaicX image, original magnification 20x). Fixed region of interest (ROI) used for quantification is demonstrated in b and d. B - Quantification of area of green or red birefringent collagen fibers in the center of the defect in Sr-hybrid and Ca-hybrid filled defects, 15 and 60 days post-implantation. Data presented as mean±SE of n=5 animals/group, 3 images/animal. Asterisks show statistically significant differences ($p<0.05$) between groups for red collagen data.

Evaluation of Sr systemic effect

Sr levels were quantified in serum (Fig. 7A) and organs (Fig. 7B) associated with excretory/filtration functions, such as liver, spleen and kidneys, by ICP-AES analysis, to evaluate the safety of the designed Sr-hybrid system. The Sr levels in serum of animals that were subjected to Sr-hybrid implantation (27.05±2.7 μg/L after 15 days and 20.61±1.3 μg/L after 60 days) were not statistically different from those in empty defect animals (27.26±3.9 μg/L after 15 days and 23.31±1.9 μg/L after 60 days) or non-operated animals (28.59±0.8 μg/L, mean±SD). Even after 60 days of implantation, no increase in Sr was found in serum (Limit of quantification, LOQ – 5 μg/L).

Sr quantification in organs at 60 days post-implantation supports results from measurements in serum. No statistical significant differences were observed between empty defect animals (0.44±0.1 μg/g kidney, 0.50±0.1 μg/g spleen, 0.48±0.3 μg/g liver, mean±SD) and Sr-hybrid group (0.69±0.3 μg/g kidney, 0.59±0.2 μg/g spleen, 0.36±0.1 μg/g liver, mean±SD). Moreover, histomorphological analyses were also performed in histological sections of organs after 60 days (Fig. 7C). In Sr-hybrid implanted group no morphological alterations at macro or microscopic level were observed, when compared to non-operated animals. Analysis of Ca-hybrid group presented similar results, with no alterations observed.

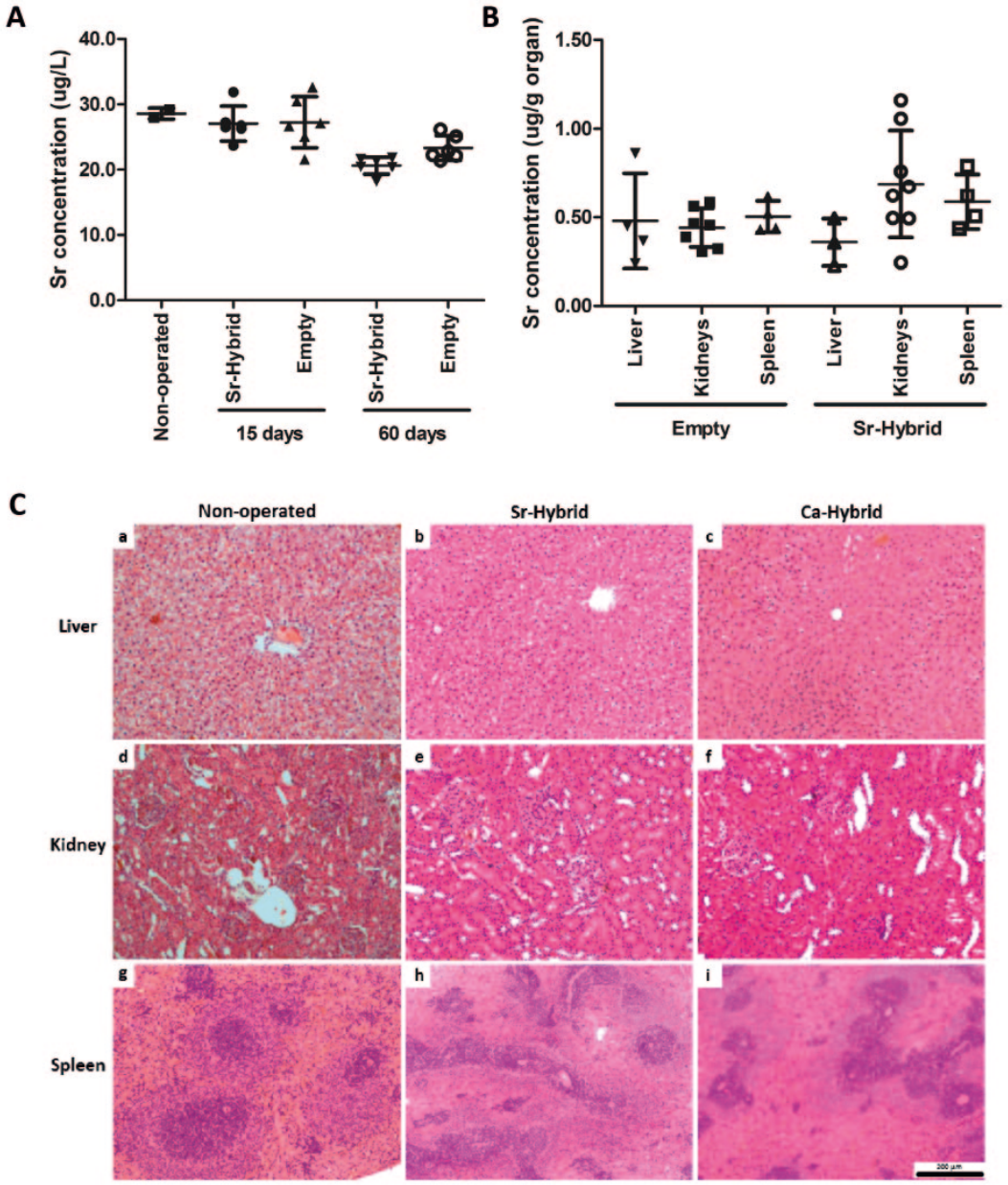

Figure 7. Strontium systemic evaluation. Strontium concentration found in serum in non-operated, empty and Sr-hybrid implanted animals at days 15 and 60 post-surgery (A). Data presented as mean±SD of 6 samples/group/time point and 2 samples non-operated. Strontium concentration found in the liver, kidneys and spleen of animals implanted with Sr-hybrid and empty defect, 60 days post-surgery (B). Data presented as mean±SD of 4 samples/group/time point. Representative histological sections from liver (a to c), kidney (d to f) and spleen (g to i) of non-operated (a, d and g), Sr-hybrid (b, e and h) and Ca-hybrid implanted (c, f, and i) animals, 60 days post-surgery (C).

Discussion

In this study the in vivo response to an injectable Sr-rich hybrid system, composed of Sr-doped HAp microspheres embedded in an Sr-cross-linked RGD-alginate hydrogel, as compared to a similar Sr-free system (Ca-hybrid material), using a rat metaphyseal femoral critical size defect model, is presented.

The designed hybrid system aims at providing adequate mechanical support in the early phases of bone formation and gradual replacement of the artificial scaffold by newly-formed bone with adequate function and mechanical properties. The use of hydrogels is a promising approach in skeletal regenerative medicine [49, 57-59]. Alginate has been used due to its biocompatibility, low toxicity, and mild gelation in the presence of divalent cations. Therefore alginate gels act as a natural extracellular matrix mimic which can be tuned to deliver bioactive agents and cells to the desired site, creating space for new tissue formation and control the structure and function of the engineered tissue [49]. Other works have incorporated alginate in self-setting cements, for improving injectability, cohesion and compression strength [60-62]. In the present study, the ability of alginate to form hydrogels in situ acting as a carrier for HAp microspheres under cytocompatible conditions, was explored. In agreement with our previous results [53], the system showed to be adequate for minimally invasive implantation. A conventional syringe can be used to manually inject the material, perfectly filling complex defects and, once set, creating a 3D matrix with homogeneous distribution of microspheres. Furthermore, alginate was modified with RGD peptides to provide biological cues for promoting cell adhesion and colonization [50, 63]. The main disadvantage regarding load-bearing application is alginate low mechanical properties which can be overcome through the reinforcement with ceramic components, application in non load-bearing areas, and the concomitant use of fixation devices [54]. With an alginate-to-microspheres weight ratio of 0.35, and microspheres with average diameter of 530 μm, the hybrid system allows for a good compromise between mechanical resistance and adequate space between particles

(approximately 220 μm), which is expected to facilitate in situ cell colonization and invasion by blood vessels [53, 55].

Deficient bone healing is expected to occur, especially in osteoporotic conditions. The use of crystalline HAp in the microspheres, with low degradation rate, ensures its permanency at the injury site for longer periods post-implantation, therefore allowing for a mechanical reinforcement of the defect. In this work, the high radiopacity of microspheres allowed for an easy follow-up in vivo of the material using conventional radiological imaging. In clinical practice, this comes as highly advantageous since regular X-rays are required to assess bone healing.

In this system we used alginate cross-linked by internal gelation with Sr2+ as a vehicle for the Sr-doped HAp microspheres. Sr was incorporated both in the hydrogel and the microspheres, which present different release kinetic profiles resulting in sustained Sr2+ release for long periods of time (AH Lourenço et al, unpublished results). In other in vivo studies, Sr has been found to enhance bone formation [35, 37, 64, 65]. For example, Banerjee et al. studied the effect of doping ß-TCP with MgO/SrO on bone formation in Sprague-Dawley rats [64]ENREF_59. Doped ß-TCP promoted more osteogenesis and faster bone formation than pure ß-TCP. In critical calvaria defects of an ovariectomized rat model, macroporous Sr-substituted scaffolds showed superior osteoinductive activity to enhance early bone formation, and could also stimulate angiogenesis compared with calcium silicate scaffolds [65]. The current study showed that Sr-hybrid system presents bioactive properties, promoting cell migration, implant vascularization and supports bone ingrowth. Newly formed bone developed in close contact with the material, without any fibrous interface, growing in a centripetal manner, in continuity with the surrounding host trabecular bone, indicates a good integration with the host tissue. Newly formed bone percentages is in agreement to those observed in other works testing similar materials [66, 67] and a trend towards greater new bone formation was observed in Sr-hybrid filled defects.

Major histological differences were observed between the two groups. Higher cell invasion was seen at the center of the Sr-hybrid filled defects at 15 days post-implantation, with the presence of polymorphonuclear neutrophils (PMN). Bone injury elicits an inflammatory response that is beneficial to healing when acute and highly regulated. Inflammatory cells are recruited to the site of injury for clearance of pathogens and maintenance of bone homeostasis [68]. This higher cell invasion correlates with higher material degradation and bone tissue formation seen after 60 days. We may assume that Sr induces faster bone healing, possibly due to a faster resolution of inflammation, tissue repair and remodeling. This can be appealing since the presence of Sr may be modulating the inflammatory response, a current trend in bone regeneration strategies regarding the development of biomaterials [69-71].

Earlier bone formation was identified in close contact with the microspheres in Sr-hybrid system, highlighting higher osteoinductivity when compared to Ca-hybrid system which was evidenced by the thicker trabecular bone structure at the periphery of the defect observed in Sr-hybrid group 60 days post-implantation. Cardemill et al have also found major differences in the topological distribution of the formed bone in association with Sr-doped calcium phosphate or HAp granules, although both materials showed comparable overall bone formation, when implanted in ovariectomized and non-ovariectomized rats [72]. A larger amount of mineralized bone was observed in the center of the defect in HAp group, mainly in ovariectomized rats, whereas at the periphery of the defect the bone area was higher using Sr-doped granules, irrespective of ovariectomy.

Granulation tissue with blood vessels and increased collagen deposition were observed at 60 days post-implantation in Sr-hybrid filled defects. Several studies have correlated the color of birefringent collagen fibers under polarized light with different collagen types [73, 74]. Our results show an increase in thicker red collagen fibers in Sr-hybrid group. These fibers are associated with type I collagen, the main type found in bone tissue. It has been shown that the incorporation of Sr in

biomaterials may decrease the number of osteoclasts significantly, but these were nevertheless closely associated with newly formed trabeculae, indicating activated bone remodeling [75]. A quantitative analysis of TRAP positive cells was not performed. However, the presence of osteoclasts in the center of the defect supports the higher bone remodeling found in the Sr-hybrid group. Although the microCT calculations did not reveal a statistically different bone volume, these histological findings sustain the evidence of an improved response with the Sr enriched material.

The use of methylmethacrylate embedding histological technique allowed for the study of both bone and material without decalcification. The technique was optimized in our lab [76] using an exothermic process. One of the disadvantages of the procedure is the inability to perform immunohistochemistry studies due to loss of antigenicity, which is worth exploring in future works.

With the use of Sr releasing systems, cardiovascular safety is of concern. Current guidelines indicate that orally administered Sr ranelate should be avoided in patients with past or present history of ischemic heart disease, peripheral arterial disease and/or cerebrovascular disease or uncontrolled hypertension, due to an observed increase of cardiovascular events [12]. Although previous reports have shown that ionic Sr can be added to calcium phosphates and ceramics, potentially stimulating bone formation locally, the risk of systemic adverse effects has been rarely reported. Baier et al studied the addition of Sr to calcium-phosphate cement in a distal methaphyseal femoral defect in ovariectomized rat model. Results have shown faster osteointegration of the implant with the addition of Sr, and Sr serum concentrations of 10.87 ± 4.16 μg/l were found 1 month post-implantation [35]. The systemic Sr levels were very low when compared to those found upon oral Sr ranelate treatment [77]. In the present study, Sr concentration was assessed both in the serum and organs with excretory/filtration functions, as well as the histology of these organs. Serum Sr concentration in operated animals was found to be similar to non-operated and in the same range as previously reported [35]. No statistically significant

difference was observed between Sr-hybrid implanted and empty defects, both in serum and organs. Similarly, Sr concentration levels do not seem to be increased compared to normal levels found in the liver of Wistar rats (~0.2 ug/g of dry weight [78]) . These results, together with the absence of morphological changes in histological sections of the organs suggest that Sr release is restricted to the defect site, corroborating the safety of this osteoinductive hybrid system.

Conclusions

We evaluated the in vivo response of an injectable Sr-rich hybrid system composed of Sr-doped HAp microspheres embedded in Sr-cross-linked RGD-alginate hydrogel intended for bone regeneration. Sr-hybrid system led to an increased bone formation in both center and periphery of a critical size defect compared to a non Sr–doped similar system, where new bone formation was restricted to the periphery. Besides promoting earlier new bone formation, Sr-hybrid system was also found to stimulate higher cell colonization with increased deposition of thick collagen fibers in the center of the defect. Importantly, our results suggest that only local release of Sr from the material was obtained, since no statistically significant differences on Sr concentration were detected in retrieved organs or serum. Together, these data demonstrate that the incorporation of Sr improved the osteoinductive properties of the hybrid system leading to higher bone regeneration without inducing detrimental side effects currently associated with other Sr-based therapeutic strategies. The Sr-hybrid material stands as a promising approach for bone regeneration strategies through minimally invasive procedures.

Materials and Methods

Preparation of the injectable hybrid materials

For the preparation of the hybrid system, RGD-alginate was combined with Sr-doped hydroxyapatite (HAp) or HAp microspheres and cross-linked by internal gelation with Sr or Ca carbonate, respectively (hereafter designated as Sr-hybrid or Ca-hybrid). These formulations and methodologies were adapted and optimized from previous works using Ca-cross-linked alginate hydrogels [47, 48, 63, 79].

Ultra-pure (UP) LVG Alginate (Pronova FMC Biopolymers, G content ≥60%, MW 131±13 kDa) was functionalized with RGD peptides as previously described [63], filtered in 0.22 μm Steriflip units (Millipore), lyophilized and stored at -20 °C until further use. Endotoxin levels were measured in RGD-modified and non-modified UP alginate using the Food and Drug Administration (FDA) approved Endosafe™-PTS system (Charles River). The analysis was performed and certified by an external entity (Analytical Services Unit, IBET/ITQB) revealing endotoxin levels below 0.1 EU/mL (EU - unit of measurement for endotoxin activity), respecting the US Department of Health and Human Services guidelines for implantable devices.

Sterile RGD-Alginate was dissolved in 0.9% (w/v) NaCl solution under sterile conditions to yield a 4% (w/v) solution, which was thoroughly mixed with an aqueous suspension of SrCO3 (Sigma) or CaCO3 (Fluka) at SrCO3/COOH or CaCO3/COOH molar ratio of 1.6. A fresh solution of glucone delta-lactone (GDL, Sigma) was added to trigger gel formation at a final polymer concentration of 3.5% (w/v) and a carbonate/GDL molar ratio of 0.125.

HAp microspheres were prepared as described elsewhere [42]. Briefly, HAp powder (Plasma Biotal) was dispersed in a 3% (w/v) alginate solution (FMC Biopolymers) with a ceramic-to-polymer solution ratio of 0.25. The paste was extruded dropwise into 0.1 M SrCl2 (Merck) or 0.1 M CaCl2 (Merck) cross-linking solution, to produce Sr-HAp or HAp microspheres, respectively. Microspheres were allowed to reticulate for 30 min in the cross-linking solution, and were then washed in deionized water,

dried and sintered at 1200 °C. Upon sintering, the polymer phase is burned out giving rise to a porous network where Sr or Ca ions are incorporate in the ceramic particles. Microspheres with spherical shape and diameter of 500-560 μm were retrieved by sieving and autoclave sterilized for further use. Sterile microspheres were promptly added to the gelling alginate solution to yield 35% in weight of the total mixture, thoroughly homogenized and placed in a 1 mL syringe (Terumo) ready for extrusion of the material.

Animal surgical procedure

All animal experiments were conducted following protocols approved by the Ethics Committee of the Portuguese Official Authority on Animal Welfare and Experimentation (DGAV) – reference no. 0420/000/000/2012. We used a critical size metaphyseal bone defect model adapted from Le Guehennec et al [80], as previously described [81]. Three months old Wistar Han male rats (Charles River Laboratories) with weight ranging from 300 to 400 g were used. Two different experimental groups (n=5 animals/group) were analysed: bone defect filled with Sr-hybrid material and bone defect filled with Ca-hybrid material (control material). Animals with empty defects (n=5) were used as a critical-sized defect model control. Two different time-points were used, 15 days and 60 days, to evaluate the relationship of inflammation and early bone formation, and new bone formation, respectively. Non-operated animals (n=2, 60 days) and animas with empty defects were used as control for serum Sr quantification and organ histological analysis. The analgesic buprenorphine (0.05 mg per kg), was administrated subcutaneously, 30 minutes before surgery. The animals were then subjected to volatile anesthesia with isofluorane, in a chamber, according to standard procedures of the animal facility (inducing anesthesia with 900 cc O2 /min, 5% Isofluorane), confirmed by loss of posture and reflexes. Animals were then moved to a clean surgery area and anesthesia was maintained along all time of surgery with a face mask (300 cc O2 /min, 2.5% Isofluorane). The right knee of each

animal was shaved and skin cleaned and disinfected with 70% ethanol. A lateral incision was performed and both skin and muscles were retracted to expose the articular capsule. After arthrotomy, a cylindrical defect with 3 mm diameter and depth of approximately 4 mm was drilled in the anterolateral wall of the lateral condyle of the femur. The defect was washed with physiological saline solution and either filled with a biomaterial or left empty. All materials were prepared in sterile conditions and injected in the femur's critical defect using a 1 mL syringe. Skin and muscle were sutured and the animal was placed back in its cage. Animals were observed until regaining consciousness. Post-operative care was carried out for 48 hours, where analgesics were given (Buprenorphine) in the same dose as before surgery, every 12 hours, with a subcutaneous injection. Behavior and wound healing were examined along time.

Sample collection

Fifteen and sixty days post-surgery animals were sacrificed. Animals were kept under volatile anesthesia (Isofluorane) and blood collection was performed by cardiac puncture. Pentobarbital (Eutasil) was administered for euthanizing animals, and femurs and organs (liver, left and right kidneys and spleen) were retrieved. Blood was centrifuged and serum collected and stored at -80 1234°C until further use. Femurs were cleaned from surrounding soft tissue and immediately placed in 10% (v/v) formalin neutral solution for 4 days, rinsed in phosphate buffered saline (PBS) solution and dehydrated in serial ethanol solutions (50-70%) for 3 days each. Femurs were maintained in 70% ethanol at 4ºC until further use. Organs were also placed in 10% (v/v) formalin solution for 24h and further processed for paraffin embedding.

Radiographic analysis

Lateral X-ray of femurs retrieved from animals sacrificed at 15 days post-surgery were obtained using a radiographic system (Owandy). For the remaining animals, an

in vivo lateral X-ray was also performed at 30 days post-surgery, to allow for a follow-up of defects and materials.

Micro-computed tomography (micro-CT) analysis

Bone defects and adjacent areas were analyzed using a high-resolution micro-CT (Skyscan 1072 scanner). Specimens (n=5, 60 days post-implantation) were scanned in high resolution mode, using a pixel size of 19.13 μm and an integration time of 1.7 ms. The X-ray source was set at 91 keV of energy and 110 μA of current. A 1-mm-thick aluminum filter and a beam hardening correction algorithm were employed to minimize beam-hardening artefacts (SkyScan hardware/software).

For all scanned specimens, representative datasets of 1023 slices were used for morphometric analysis. To quantify new bone formation, a volume of interest (VOI), corresponding to the femoral defect volume, was delineated using CTAn software (Skyscan Ltd), to enable quantitative analysis to be performed. Binary images were created using two different thresholds, 50-255 (corresponding to particles and new bone) and 90-255 (just particles), and the respective TV (Total volume) determined. The difference between both TV corresponds to the volume of new bone formed (Bone volume, BV). Additionally, 3D virtual models were generated using an image processing software (ANT 3D Creator v 2.4, SkyScan). The micro-CT threshold was first calibrated from a backscattered image with primarily determined quantitative histological measurements, which was then applied equally to all samples.

Histological Analysis

Femurs were dehydrated in 100% ethanol for 3 days, at 4°C, followed by immersion in xylol for 24 h and further embedding in methylmethacrylate and processed for histological analysis as described elsewhere [76, 82].

Serial 7 μm coronal slides were retrieved and the intermediate region of the defect (1200-1500 μm) was stained with Hematoxylin and Eosin (H&E), Masson's

Trichrome (MT), Picrosirius Red (PSR) and Tartarate-resistant acid phosphatase (TRAP)-light green (LG) staining. Briefly, for H&E, undeplastified sections were re-hydrated in deionized water and incubated in Gill's Hematoxylin for 6 min and counterstained with alcoholic Eosin Y for 1 min. For MT staining, an MT kit (Sigma-Aldrich) was used according to manufacturer's instructions in undeplastified sections. TRAP staining was performed according to manufacturer using a TRAP kit (Sigma) and counterstained with LG 0.1% (v/v) in deplastified section with xylol overnight. Sections were visualized under a light microscope (DP25, Olympus) and imaged. For PSR staining, sections were deplastified, hydrated in decreasing ethanol gradient to de-ionized water, stained for 6 min in Celestine blue and another 6 min in Gill's Hematoxylin. After a 10 min washing step in water, sections were stained with Sirius Red for 1 h, washed with acidified water, dehydrated and mounted. Sections were imaged through polarization lens under a light microscope (Axiovert 200M, Zeiss) using MosaiX software.

Regarding the retrieved organs, paraffin sections of 3 μm thickness were sequentially obtained and stained with H&E.

Peripheral bone thickness was determined as the average thickness of twenty different random locations (arrow in Fig.4A c'' and d'') of bone found around the defect area using MT stained sections. AxioVision software was used for the measurements (n=5 animals/group). The area of residual material found within the defect was measured by the same user, manually delimiting the area of the hybrid (microspheres and alginate) in MT stained sections. Alginate and microspheres retain staining and have a different texture, allowing for the easy identification of the material. MosaicJ (ImageJ software, n=5 animals/group, 3 sections/animal) was used for the assembly of microscopic images at 20x magnification and area values were obtained in ImageJ.

Birefrigent green and red fibers were quantified as the percentage of thin/type III and thicker/type I collagen fibers, respectively [73, 74]. The collagen area within the

central region of the defect (diameter=2.4 mm) was quantified in ImageJ software (n=5 animals/group, 3 images/animal). Sections were stained simultaneously and images acquired in the same day with the same parameters.

Serial 7 µm coronal slides were also analysed by Scanning Electron Microscopy/Energy-dispersive X-ray spectroscopy (SEM/EDS) using a High Resolution (Schottky) Environmental Scanning Electron Microscope with X-Ray Microanalysis and Electron Backscattered Diffraction analysis: Quanta 400 FEG ESEM / EDAX Genesis X4M. Samples were coated with an Au/Pd thin film, by sputtering, using the SPI Module Sputter Coater equipment.

Systemic Sr quantification by Inductively Coupled Plasma – Atomic Emission Spectroscopy (ICP-AES)

Sr levels in serum and organs (spleen, liver and kidneys) were quantified by ICP-AES (Horiba Jobin-Yvon, Ultima spectrometer, generator RF of 40,68 MHz). Serum samples (n=6 samples/group/time point and n=2 non-operated) were diluted 5 times in 1% Suprapur nitric acid (Fluka) as described elsewhere [83]. Spleen, liver and kidneys were digested in Suprapure nitric acid (n=4 samples/group/time point). Before use, all glass materials were washed and then immersed in a 20% (v/v) nitric acid solution for at least 1 day in order to eliminate possible contaminations with Sr or other impurities from the vessels walls. Organs (~300 mg) were dried in a microwave (MARS-X 1500 W, CEM) configured with a 14 position carousel. An aliquot of 10 mL of Suprapur nitric acid was added and microwave digestion proceeded during 55 min, according to microwave digestion program (Supplementary - Table 1). The solutions were concentrated until 1 mL and preserved at −20 °C until Sr determination. The limit of detection (LOD – 1 µg/L) and limit of quantification (LOQ – 5 µg/L) for Sr were adequate for the expected concentration range of the samples.

Statistical Analysis

Statistical analysis was performed using non-parametric Mann–Whitney test with GraphPad Prism Program. A value of $p<0.05$ was considered statistically significant: *$p<0.05$; **$p<0.01$; *** $p<0.001$.

Acknowledgements

The authors thankfully acknowledge the use of Micro-CT in the 3B's Research Group facilities at University of Minho, the use of microscopy services at Centro de Materiais da Universidade do Porto (CEMUP) and the technicians responsible for the experimental techniques mentioned, Vítor Correlo and Daniela Silva, respectively; Carla Rodrigues from Requimte at FCT-UNL for the help with ICP-AES analysis. This work was financed by FEDER - Fundo Europeu de Desenvolvimento Regional funds through the COMPETE 2020 - Operational Programme for Competitiveness and Internationalization (POCI), Portugal 2020, and by Portuguese funds through FCT - Fundação para a Ciência e a Tecnologia/ Ministério da Ciência, Tecnologia e Inovação in the framework of the project "Institute for Research and Innovation in Health Sciences" (POCI-01-0145-FEDER-007274) and project PTDC/CTM/103181/2008. AHL acknowledges FCT for PhD grant: SFRH/BD/87192/2012, CCB acknowledges FCT for research position Investigator FCT (IF2013).

Supplementary Material

Stages	1	2	3
Power (W)	600	600	600
Time (min)	5	10	10
Temperature (control, ºC)	50	100	175
Hold (min)	10	10	15

Table 1. Microwave digestion program

References

[1] Goldhahn J, Scheele WH, Mitlak BH, Abadie E, Aspenberg P, Augat P, et al. Clinical evaluation of medicinal products for acceleration of fracture healing in patients with osteoporosis. Bone. 2008;43:343-7.

[2] Campana V, Milano G, Pagano E, Barba M, Cicione C, Salonna G, et al. Bone substitutes in orthopaedic surgery: from basic science to clinical practice. Journal of Materials Science: Materials in Medicine. 2014;25:2445-61.

[3] Dupraz A, Nguyen TP, Richard M, Daculsi G, Passuti N. Influence of a cellulosic ether carrier on the structure of biphasic calcium phosphate ceramic particles in an injectable composite material. Biomaterials. 1999;20:663-73.

[4] Iooss P LRA, Grimandi G, Daculsi G, Merle C. . A new injectable bone substitute combining poly(epsilon-caprolactone) microparticles with biphasic calcium phosphate granules. Biomaterials. 2001:2785-94.

[5] Larsson S. Calcium Phosphates: What Is the Evidence? Journal of Orthopaedic Trauma. 2010;24:S41-S5.

[6] Low KL, Tan SH, Zein SHS, Roether JA, Mouriño V, Boccaccini AR. Calcium phosphate-based composites as injectable bone substitute materials. Journal of Biomedical Materials Research Part B: Applied Biomaterials. 2010;94B:273-86.

[7] Cao L, Liu G, Gan Y, Fan Q, Yang F, Zhang X, et al. The use of autologous enriched bone marrow MSCs to enhance osteoporotic bone defect repair in long-term estrogen deficient goats. Biomaterials. 2012;33:5076-84.

[8] Cho SW, Sun HJ, Yang J-Y, Jung JY, Choi HJ, An JH, et al. Human Adipose Tissue-Derived Stromal Cell Therapy Prevents Bone Loss in Ovariectomized Nude Mouse. Tissue Engineering Part A. 2012;18:1067-78.

[9] Liu H-Y, Wu ATH, Tsai C-Y, Chou K-R, Zeng R, Wang M-F, et al. The balance between adipogenesis and osteogenesis in bone regeneration by platelet-rich plasma for age-related osteoporosis. Biomaterials. 2011;32:6773-80.

[10] Wang Z, Goh J, De SD, Ge Z, Ouyang H, Chong JSW, et al. Efficacy of bone marrow-derived stem cells in strengthening osteoporotic bone in a rabbit model. Tissue engineering 2006:1753-61. .

[11] Meunier PJ, Roux C, Seeman E, Ortolani S, Badurski JE, Spector TD, et al. The Effects of Strontium Ranelate on the Risk of Vertebral Fracture in Women with Postmenopausal Osteoporosis. New England Journal of Medicine. 2004;350:459-68.

[12] Reginster JY, Neuprez A, Dardenne N, Beaudart C, Emonts P, Bruyere O. Efficacy and safety of currently marketed anti-osteoporosis medications. Best Practice & Research Clinical Endocrinology & Metabolism. 2014;28:809-34.

[13] Baron R, Tsouderos Y. In vitro effects of S12911-2 on osteoclast function and bone marrow macrophage differentiation. European Journal of Pharmacology. 2002;450:11-7.

[14] Bonnelye E, Chabadel A, Saltel F, Jurdic P. Dual effect of strontium ranelate: Stimulation of osteoblast differentiation and inhibition of osteoclast formation and resorption in vitro. Bone. 2008;42:129-38.

[15] Grynpas MD, Hamilton E, Cheung R, Tsouderos Y, Deloffre P, Hott M, et al. Strontium increases vertebral bone volume in rats at a low dose that does not induce detectable mineralization defect. Bone. 1996;18:253-9.

[16] Yang F, Yang D, Tu J, Zheng Q, Cai L, Wang L. Strontium Enhances Osteogenic Differentiation of Mesenchymal Stem Cells and In Vivo Bone Formation by Activating Wnt/Catenin Signaling. STEM CELLS. 2011;29:981-91.

[17] Takahashi N, Sasaki T, Tsouderos Y, Suda T. S 12911-2 Inhibits Osteoclastic Bone Resorption In Vitro. Journal of Bone and Mineral Research. 2003;18:1082-7.

[18] Hurtel-Lemaire AS, Mentaverri R, Caudrillier A, Cournarie F, Wattel A, Kamel S, et al. The Calcium-sensing Receptor Is Involved in Strontium Ranelate-induced Osteoclast Apoptosis: NEW INSIGHTS INTO THE ASSOCIATED SIGNALING PATHWAYS. Journal of Biological Chemistry. 2009;284:575-84.

[19] Marie PJ, Felsenberg D, Brandi ML. How strontium ranelate, via opposite effects on bone resorption and formation, prevents osteoporosis. Osteoporosis International. 2011;22:1659-67.

[20] Atkins GJ, Welldon KJ, Halbout P, Findlay DM. Strontium ranelate treatment of human primary osteoblasts promotes an osteocyte-like phenotype while eliciting an osteoprotegerin response. Osteoporosis International. 2009;20:653-64.

[21] Brennan TC, Rybchyn MS, Green W, Atwa S, Conigrave AD, Mason RS. Osteoblasts play key roles in the mechanisms of action of strontium ranelate. British Journal of Pharmacology. 2009;157:1291-300.

[22] Caverzasio J. Strontium ranelate promotes osteoblastic cell replication through at least two different mechanisms. Bone. 2008;42:1131-6.

[23] Chattopadhyay N, Quinn SJ, Kifor O, Ye C, Brown EM. The calcium-sensing receptor (CaR) is involved in strontium ranelate-induced osteoblast proliferation. Biochemical Pharmacology. 2007;74:438-47.

[24] Barbara A, Delannoy P, Denis BG, Marie PJ. Normal matrix mineralization induced by strontium ranelate in MC3T3-E1 osteogenic cells. Metabolism. 2004;53:532-7.

[25] Choudhary S, Halbout P, Alander C, Raisz L, Pilbeam C. Strontium Ranelate Promotes Osteoblastic Differentiation and Mineralization of Murine Bone Marrow Stromal Cells: Involvement of Prostaglandins. Journal of Bone and Mineral Research. 2007;22:1002-10.

[26] Zhu L-L, Zaidi S, Peng Y, Zhou H, Moonga BS, Blesius A, et al. Induction of a program gene expression during osteoblast differentiation with strontium ranelate. Biochemical and Biophysical Research Communications. 2007;355:307-11.

[27] Fromigué O, Haÿ E, Barbara A, Marie PJ. Essential Role of Nuclear Factor of Activated T Cells (NFAT)-mediated Wnt Signaling in Osteoblast Differentiation Induced by Strontium Ranelate. Journal of Biological Chemistry. 2010;285:25251-8.

[28] Ammann P, Badoud I, Barraud S, Dayer R, Rizzoli R. Strontium Ranelate Treatment Improves Trabecular and Cortical Intrinsic Bone Tissue Quality, a Determinant of Bone Strength. Journal of Bone and Mineral Research. 2007;22:1419-25.

[29] Ammann P, Shen V, Robin B, Mauras Y, Bonjour J-P, Rizzoli R. Strontium Ranelate Improves Bone Resistance by Increasing Bone Mass and Improving Architecture in Intact Female Rats. Journal of Bone and Mineral Research. 2004;19:2012-20.

[30] Bain SD, Jerome C, Shen V, Dupin-Roger I, Ammann P. Strontium ranelate improves bone strength in ovariectomized rat by positively influencing bone resistance determinants. Osteoporosis International. 2009;20:1417-28.

[31] Buehler J, Chappuis P, Saffar JL, Tsouderos Y, Vignery A. Strontium ranelate inhibits bone resorption while maintaining bone formation in alveolar bone in monkeys (Macaca fascicularis). Bone. 2001;29:176-9.

[32] Delannoy P, Bazot D, Marie PJ. Long-term treatment with strontium ranelate increases vertebral bone mass without deleterious effect in mice. Metabolism. 2002;51:906-11.

[33] Abrahamsen B, Grove EL, Vestergaard P. Nationwide registry-based analysis of cardiovascular risk factors and adverse outcomes in patients treated with strontium ranelate. Osteoporosis International. 2014;25:757-62.

[34] Cooper C, Fox KM, Borer JS. Ischaemic cardiac events and use of strontium ranelate in postmenopausal osteoporosis: a nested case–control study in the CPRD. Osteoporosis International. 2014;25:737-45.

[35] Baier M, Staudt P, Klein R, Sommer U, Wenz R, Grafe I, et al. Strontium enhances osseointegration of calcium phosphate cement: a histomorphometric pilot study in ovariectomized rats. Journal of Orthopaedic Surgery and Research. 2013;8:1-8.

[36] Hulsart-Billström G, Xia W, Pankotai E, Weszl M, Carlsson E, Forster-Horváth C, et al. Osteogenic potential of Sr-doped calcium phosphate hollow spheres in vitro and in vivo. Journal of Biomedical Materials Research Part A. 2013;101A:2322-31.

[37] Thormann U, Ray S, Sommer U, ElKhassawna T, Rehling T, Hundgeburth M, et al. Bone formation induced by strontium modified calcium phosphate cement in critical-size metaphyseal fracture defects in ovariectomized rats. Biomaterials. 2013;34:8589-98.

[38] Friedman CD CP, Takagi S, Chow LC. BoneSource hydroxyapatite cement: a novel biomaterial for craniofacial skeletal tissue engineering and reconstruction. J Biomed Mater Res. 1998.

[39] Xu HH QJ. Calcium phosphate cement containing resorbable fibers for short-term reinforcement and macroporosity. Biomaterials. 2002.

[40] Barrias CC, Ribeiro CC, Lamghari M, Miranda CS, Barbosa MA. Proliferation, activity, and osteogenic differentiation of bone marrow stromal cells cultured on calcium titanium phosphate microspheres. Journal of Biomedical Materials Research Part A. 2005;72A:57-66.

[41] Oliveira SM, Barrias CC, Almeida IF, Costa PC, Ferreira MRP, Bahia MF, et al. Injectability of a bone filler system based on hydroxyapatite microspheres and a vehicle with in situ gel-forming ability. Journal of Biomedical Materials Research Part B: Applied Biomaterials. 2008;87B:49-58.

[42] Ribeiro CC, Barrias CC, Barbosa MA. Preparation and characterisation of calcium-phosphate porous microspheres with a uniform size for biomedical applications. Journal of Materials Science: Materials in Medicine. 2006;17:455-63.

[43] Ribeiro CC, Barrias CC, Barbosa MA. Calcium phosphate-alginate microspheres as enzyme delivery matrices. Biomaterials. 2004;25:4363-73.

[44] Barrias CC, Lamghari M, Granja PL, Sá Miranda MC, Barbosa MA. Biological evaluation of calcium alginate microspheres as a vehicle for the localized delivery of

a therapeutic enzyme. Journal of Biomedical Materials Research Part A. 2005;74A:545-52.

[45] Fonseca KB, Gomes DB, Lee K, Santos SG, Sousa A, Silva EA, et al. Injectable MMP-Sensitive Alginate Hydrogels as hMSC Delivery Systems. Biomacromolecules. 2014;15:380-90.

[46] Maia FR, Barbosa M, Gomes DB, Vale N, Gomes P, Granja PL, et al. Hydrogel depots for local co-delivery of osteoinductive peptides and mesenchymal stem cells. Journal of Controlled Release. 2014;189:158-68.

[47] Maia FR, Lourenço AH, Granja PL, Gonçalves RM, Barrias CC. Effect of Cell Density on Mesenchymal Stem Cells Aggregation in RGD-Alginate 3D Matrices under Osteoinductive Conditions. Macromolecular Bioscience. 2014;14:759-71.

[48] Evangelista MB, Hsiong SX, Fernandes R, Sampaio P, Kong H-J, Barrias CC, et al. Upregulation of bone cell differentiation through immobilization within a synthetic extracellular matrix. Biomaterials. 2007;28:3644-55.

[49] Lee KY, Mooney DJ. Alginate: properties and biomedical applications. Progress in polymer science. 2012;37:106-26.

[50] Sakiyama-Elbert S, Hubbell J. Functional Biomaterials: Design of Novel Biomaterials. Annual Review of Materials Research. 2001;31:183-201.

[51] Andersen T, Strand BL, Formo K, Alsberg E, Christensen BE. Alginates as biomaterials in tissue engineering. Carbohydrate Chemistry: Volume 37: The Royal Society of Chemistry; 2012. p. 227-58.

[52] Mørch ÝA, Donati I, Strand BL. Effect of Ca2+, Ba2+, and Sr2+ on Alginate Microbeads. Biomacromolecules. 2006;7:1471-80.

[53] Neves N, Campos BB, Almeida IF, Costa PC, Cabral AT, Barbosa MA, et al. Strontium-rich injectable hybrid system for bone regeneration. Materials Science and Engineering: C. 2016;59:818-27.

[54] D'Este M ED. Hydrogels in calcium phosphate moldable and injectable bone substitutes: Sticky excipients or advanced 3-D carriers? Acta Biomater. 2013.

[55] Bohner M, Tadier S, van Garderen N, de Gasparo A, Dobelin N, Baroud G. Synthesis of spherical calcium phosphate particles for dental and orthopedic applications. Biomatter. 2013;3.

[56] Lourenço A, Torres A, Santos S, Barbosa M, Barrias C, Ribeiro C. Sr-Hybrid system for bone regeneration: an in vitro study. 4th Interrogations at the Biointerface Advanced Summer School. Barcelona2014.

[57] Fedorovich NE, Alblas J, de Wijn JR, Hennink WE, Verbout AJ, Dhert WJ. Hydrogels as extracellular matrices for skeletal tissue engineering: state-of-the-art and novel application in organ printing. Tissue Eng. 2007;13:1905-25.

[58] Khademhosseini A, Langer R. Microengineered hydrogels for tissue engineering. Biomaterials. 2007;28:5087-92.

[59] Patenaude M, Smeets NMB, Hoare T. Designing Injectable, Covalently Cross-linked Hydrogels for Biomedical Applications. Macromolecular Rapid Communications. 2014;35:598-617.

[60] Lee G-S, Park J-H, Won J-E, Shin US, Kim H-W. Alginate combined calcium phosphate cements: mechanical properties and in vitro rat bone marrow stromal cell responses. Journal of Materials Science: Materials in Medicine. 2011;22:1257-68.

[61] Xu C, Wang X, Zhou J, Huan Z, Chang J. Bioactive tricalcium silicate/alginate composite bone cements with enhanced physicochemical properties. Journal of Biomedical Materials Research Part B: Applied Biomaterials. 2017:n/a-n/a.

[62] Sprio S, Dapporto M, Montesi M, Panseri S, Lattanzi W, Pola E, et al. Novel Osteointegrative Sr-Substituted Apatitic Cements Enriched with Alginate. Materials. 2016;9:763.

[63] Bidarra SJ, Barrias CC, Fonseca KB, Barbosa MA, Soares RA, Granja PL. Injectable in situ crosslinkable RGD-modified alginate matrix for endothelial cells delivery. Biomaterials. 2011;32:7897-904.

[64] Banerjee SS, Tarafder S, Davies NM, Bandyopadhyay A, Bose S. Understanding the influence of MgO and SrO binary doping on the mechanical and biological properties of β-TCP ceramics. Acta Biomaterialia. 2010;6:4167-74.

[65] Lin K, Xia L, Li H, Jiang X, Pan H, Xu Y, et al. Enhanced osteoporotic bone regeneration by strontium-substituted calcium silicate bioactive ceramics. Biomaterials. 2013;34:10028-42.

[66] Daculsi G, Uzel AP, Weiss P, Goyenvalle E, Aguado E. Developments in injectable multiphasic biomaterials. The performance of microporous biphasic calcium phosphate granules and hydrogels. Journal of Materials Science: Materials in Medicine. 2010;21:855-61.

[67] Gauthier O, Müller R, von Stechow D, Lamy B, Weiss P, Bouler J-M, et al. In vivo bone regeneration with injectable calcium phosphate biomaterial: A three-dimensional micro-computed tomographic, biomechanical and SEM study. Biomaterials. 2005;26:5444-53.

[68] Loi F, Córdova LA, Pajarinen J, Lin T-h, Yao Z, Goodman SB. Inflammation, fracture and bone repair. Bone. 2016;86:119-30.

[69] Vasconcelos DP, Costa M, Amaral IF, Barbosa MA, Águas AP, Barbosa JN. Modulation of the inflammatory response to chitosan through M2 macrophage polarization using pro-resolution mediators. Biomaterials. 2015;37:116-23.

[70] Vasconcelos DP, Costa M, Amaral IF, Barbosa MA, Águas AP, Barbosa JN. Development of an immunomodulatory biomaterial: Using resolvin D1 to modulate inflammation. Biomaterials. 2015;53:566-73.

[71] Vasconcelos DM, Gonçalves RM, Almeida CR, Pereira IO, Oliveira MI, Neves N, et al. Fibrinogen scaffolds with immunomodulatory properties promote in vivo bone regeneration. Biomaterials. 2016;111:163-78.

[72] Cardemil C, Elgali I, Xia W, Emanuelsson L, Norlindh B, Omar O, et al. Strontium-Doped Calcium Phosphate and Hydroxyapatite Granules Promote

Different Inflammatory and Bone Remodelling Responses in Normal and Ovariectomised Rats. PLoS ONE. 2013;8:e84932.

[73] Montes GS, Junqueira LCU. The use of the Picrosirius-polarization method for the study of the biopathology of collagen. Memórias do Instituto Oswaldo Cruz. 1991;86:1-11.

[74] Vieira AE, Repeke CE, Ferreira Junior SdB, Colavite PM, Biguetti CC, Oliveira RC, et al. Intramembranous Bone Healing Process Subsequent to Tooth Extraction in Mice: Micro-Computed Tomography, Histomorphometric and Molecular Characterization. PLoS ONE. 2015;10:e0128021.

[75] Wei L, Ke J, Prasadam I, Miron RJ, Lin S, Xiao Y, et al. A comparative study of Sr-incorporated mesoporous bioactive glass scaffolds for regeneration of osteopenic bone defects. Osteoporosis International. 2014;25:2089-96.

[76] Carvalho C, Magalhães J, Pereira L, Simões-Silva L, Castro-Ferreira I, Frazão JM. Evolution of bone disease after kidney transplantation: A prospective histomorphometric analysis of trabecular and cortical bone. Nephrology. 2016;21:55-61.

[77] Marie PJ, Hott M, Modrowski D, De Pollak C, Guillemain J, Deloffre P, et al. An uncoupling agent containing strontium prevents bone loss by depressing bone resorption and maintaining bone formation in estrogen-deficient rats. Journal of Bone and Mineral Research. 1993;8:607-15.

[78] Takahashi S, Takahashi I, Sato H, Kubota Y, Yoshida S, Muramatsu Y. Determination of major and trace elements in the liver of Wistar rats by inductively coupled plasma-atomic emission spectrometry and mass spectrometry. Laboratory Animals. 2000;34:97-105.

[79] Fonseca KB, Bidarra SJ, Oliveira MJ, Granja PL, Barrias CC. Molecularly designed alginate hydrogels susceptible to local proteolysis as three-dimensional cellular microenvironments. Acta Biomaterialia. 2011;7:1674-82.

[80] Le Guehennec L, Goyenvalle E, Aguado E, Houchmand-Cuny M, Enkel B, Pilet P, et al. Small-animal models for testing macroporous ceramic bone substitutes. Journal of Biomedical Materials Research Part B: Applied Biomaterials. 2005;72B:69-78.

[81] Santos SG, Lamghari M, Almeida CR, Oliveira MI, Neves N, Ribeiro AC, et al. Adsorbed fibrinogen leads to improved bone regeneration and correlates with differences in the systemic immune response. Acta Biomaterialia. 2013;9:7209-17.

[82] Sousa DM, Baldock PA, Enriquez RF, Zhang L, Sainsbury A, Lamghari M, et al. Neuropeptide Y Y1 receptor antagonism increases bone mass in mice. Bone. 2012;51:8-16.

[83] Fuchs RK, Allen MR, Condon KW, Reinwald S, Miller LM, McClenathan D, et al. Strontium ranelate does not stimulate bone formation in ovariectomized rats. Osteoporosis International. 2008;19:1331-41.

CHAPTER V
CONCLUDING REMARKS AND FUTURE PERSPECTIVES

This PhD thesis aims to contribute to the development of alternative injectable biomaterials, which may be particularly suitable for minimally invasive implantation in bone defects of osteoporotic patients. Synthetic biomaterials have been used as bone substitutes for decades, and advances in tissue engineering have enabled the design of bioactive scaffolds capable of inducing bone formation and vascularization [1, 2]. Following previous works of our group, we sought to develop an alternative biomaterial suitable for this application. Our specific objectives were: 1) assess the current evidence of the benefits and safety of incorporating Sr in bone substitutes, 2) develop and characterize a new Sr-enriched injectable hybrid system, and 3) evaluate the effect of Sr enrichment *in vivo*.

Recently, the focus turned onto the possibility of incorporating different growth factors, drugs, genes or stem cells in biomaterials to accelerate and improve bone healing [2]. Biomolecules such as growth hormone (GH), transforming growth factor-β (TGF-β), bone morphogenetic proteins (BMP), insulin-like growth factor (IGF), fibroblast growth factor (FGF), and vascular endothelial growth factor (VEGF), trace elements (zinc (Zn), magnesium (Mg), silicate (Si), and Sr), drugs like zolendronate and alendronate, and mesenchymal stem cells, have all shown a positive effect in bone healing when added to CaP biomaterials [2-4]. This *in situ* administration allows the scaffold to support new bone formation while the released doping agent induces a local tissue specific response, potentially obviating systemic side effects [4, 5].

Sr is an obvious candidate for effective scaffold doping due to its dual osteoanabolic and anti-osteoclastic activity. An increasing number of publications reported on the beneficial effects of incorporating Sr in biomaterials [6-8]. However, most are *in vitro* studies, and the few *in vivo* reports available generally do not present an adequate control group. As such, current literature does not provide sufficient evidence on the effectiveness and safety of adding Sr to biomaterials, and its use is still a matter of debate. In the context of this thesis we have performed the first systematic review that summarizes the *in vivo* effect of Sr-enriched biomaterials

in bone formation and remodeling. In order to accurately define this specific role of Sr, we restricted our selection to *in vivo* original studies comparing at least two groups that solely differed in Sr addition to the experimental group biomaterial. Only 27 papers matched these inclusion criteria. None used a large animal model and a single one was performed in humans. Moreover, follow up was variable, but usually short, and less than half reported on osteoporosis. Nevertheless, all articles showed similar or increased effect of Sr incorporation in bone formation and/or regeneration, impacted by time and concentration, supporting the beneficial role of Sr as a doping agent. Although there are current restrictions to the use of oral strontium ranelate in the management of osteoporosis due to cardiovascular events, surprisingly only 4 of the included studies have addressed the systemic side effects of local Sr release [7, 9-11]. In spite of the apparent absence of significant side effects, additional studies are needed to provide an adequate clarification on this matter.

This review also points to the lack of specific guidelines for evaluation of substitute biomaterials. Therefore, studies with different methodologies and strategies to assess Sr effect compromised a reliable quantitative synthesis and analysis of data. Different size, location and type of defect, animal species, and measurement protocols can all impact results and preclude direct comparisons [12]. Relevant and consistent healthy as well as diseased bone defect models, and clearly defined evaluation methodologies are needed for both translational preclinical and clinical future studies [12, 13].

The hybrid injectable viscoelastic system presented in this thesis is based on previous works from our group on the development of different types of microspheres and hydrogels [14-22]. Unlike traditional block scaffolds, small particles can be combined with appropriate vehicles to be administered through minimally invasive surgery. These injectable hybrid biomaterials can easily conform to irregular defects, while assuring space between particles for tissue and vascular ingrowth, as required for effective healing. In previous works ceramic microspheres and biocompatible

polymeric solutions were studied and optimized to produce an adequate injectable bone filler [21, 23]. The injectability of this system, consisting of hydroxyapatite microspheres and an alginate vehicle with *in situ* gel-forming ability, was also evaluated [24].

Based on these results, we intended to develop an alternative biomaterial, not only to be injected and fill defects of any size and shape, but also to elicit an improved healing response. Sr was incorporated in both the microspheres and the vehicle, allowing different release rates, due to both faster degradation kinetics of the polymer network and a slower one of the ceramic particles. Accordingly, besides offering structural support for cell migration and tissue ingrowth, the hybrid system enables a continuous Sr release, that begins at the early stages of implantation. An improvement in the effectiveness of bone regeneration is therefore expected, especially useful in osteoporotic conditions.

In Chapter III we have described the process of development and characterization of the biomaterial. Besides mechanical properties, we sought to develop a system that could be easily handled in any operating room, with adequate working time and manual injectability. We observed that the incorporation of Sr in the microspheres almost doubles their rupture force. Also, when Sr is used as the reticulating agent, the extrusion force is smaller, allowing for an increase in alginate concentration and percentage of microspheres, leading ultimately to an improvement in mechanical properties. The best compromise between injectability and compression strength was obtained with a hybrid system of 3.5% alginate cross-linked with Sr, and 35% of Sr enriched microspheres. However, the elastic modulus is still below that of cancellous bone [25, 26]. Thus, the system appears more adequate for use in non load-bearing regions, or combined with internal fixation devices. Nevertheless, reports on the mechanical properties of hydrogel/calcium phosphate composites are scarce, and our results are an important addition to the existing literature [27]. Other adjustments, as the number of cross-links, type of

monomer and local environment, are available strategies in order to fine-tune the alginate hydrogel biochemical and viscoelastic properties. Additionally, biomechanical tests were performed with unsterilized ultra pure alginate, and the impact of sterilization in the biomaterial needs further assessment.

The use of alginate, combined with ceramic microspheres not only works as a carrier but also allows improved cohesion and resistance to wash out as the polymer forms a gel *in situ* [27, 28]. In our *in vivo* study, a conventional syringe was used to manually inject the material, perfectly filling the defect. Radiographic analysis showed a homogeneous distribution of microspheres, which remained in place for the full duration of the experiment.

Microspheres have a uniform shape and diameter, adequate for effective bone substitution [29], and are homogeneously distributed within the hybrid system. Although alginate is a non cell-interactive polymer, RGD-grafting promotes osteogenic cell adhesion, focal adhesion formation, proliferation, and differentiation, and progressive degradation [30], leaving an appropriate space between particles for blood vessels invasion and cell colonization [31].

In Chapter IV we investigated the *in vivo* response to this novel hybrid system in a critical size defect model. Both Sr-hybrid and Sr-free hybrid systems induced newly formed bone percentages comparable to those reported in other works testing similar materials [32, 33]. However, there were significant histological differences between these groups. Sr incorporation promoted earlier new bone formation and greater cell colonization, with increased deposition of thick collagen fibers in the center of the defect, leading to increased bone formation in both center and periphery of a critical size defect. These results emphasize the impact of Sr-doping in improving bone remodeling. One can speculate that this may be due to a role of Sr in the modulation of the inflammatory response.

Another important finding was the absence of significant differences in Sr levels both in serum and excretory/filtration organs between animals with Sr-hybrid

implanted and empty defects. Although the evidence on the effectiveness of Sr-doping is mounting, safety is still a concern, as previously stated. This work provides additional evidence on this topic, but future studies should focus on this important problem.

Testing our system in a clinical setting would be important. Due to logistic and cost constrains an osteoporotic model was not tested in the present thesis. As evidenced by our systematic review, osteoporosis may influence the impact of Sr doping, and such study should be undertaken. Besides, no appropriate study has yet been carried out in large animal models, and only one has been reported on humans [34]. Further studies on these settings are of upmost importance in the translation of this system to the daily clinical practice.

Conclusions

In conclusion, this thesis presents an alternative viscoelastic hybrid system for the management of bone defects, composed of an alginate matrix cross-linked *in situ* with Sr, and Sr-rich HA microspheres. The reasoning for this strategy lies in the growing evidence of the beneficial effect of Sr enrichment of biomaterials, which was confirmed in the systematic review conducted. This system can be manually injected, sets *in situ* and offers structural support, providing a temporary scaffold for bone growth. In a critical-size rat femoral bone defect model, we observed that Sr incorporation promoted earlier new bone formation and greater cell colonization, with increased material degradation and deposition of thick collagen fibers in the center of the defect, leading to increased bone formation in both center and periphery of the defect. Moreover, no changes were observed in Sr levels both in systemic organs and serum. This Sr-hybrid injectable biomaterial stands as a promising approach for bone regeneration.

References

[1] Marmor M, Alt V, Latta L, Lane J, Rebolledo B, Egol KA, et al. Osteoporotic Fracture Care: Are We Closer to Gold Standards? J Orthop Trauma. 2015;29 Suppl 12:S53-6.

[2] Bose S, Roy M, Bandyopadhyay A. Recent advances in bone tissue engineering scaffolds. Trends Biotechnol. 2012;30:546-54.

[3] Bose S, Tarafder S. Calcium phosphate ceramic systems in growth factor and drug delivery for bone tissue engineering: A review. Acta biomaterialia. 2012;8:1401-21.

[4] Verron E, Khairoun I, Guicheux J, Bouler JM. Calcium phosphate biomaterials as bone drug delivery systems: a review. Drug Discov Today. 2010;15:547-52.

[5] Lee SH, Shin H. Matrices and scaffolds for delivery of bioactive molecules in bone and cartilage tissue engineering. Adv Drug Deliv Rev. 2007;59:339-59.

[6] Hulsart-Billstrom G, Xia W, Pankotai E, Weszl M, Carlsson E, Forster-Horvath C, et al. Osteogenic potential of Sr-doped calcium phosphate hollow spheres in vitro and in vivo. J Biomed Mater Res A. 2013;101:2322-31.

[7] Baier M, Staudt P, Klein R, Sommer U, Wenz R, Grafe I, et al. Strontium enhances osseointegration of calcium phosphate cement: a histomorphometric pilot study in ovariectomized rats. J Orthop Surg Res. 2013;8:16.

[8] Thormann U, Ray S, Sommer U, Elkhassawna T, Rehling T, Hundgeburth M, et al. Bone formation induced by strontium modified calcium phosphate cement in critical-size metaphyseal fracture defects in ovariectomized rats. Biomaterials. 2013;34:8589-98.

[9] Zhang Y, Wei L, Chang J, Miron RJ, Shi B, Yi S, et al. Strontium-incorporated mesoporous bioactive glass scaffolds stimulating in vitro proliferation and differentiation of bone marrow stromal cells and in vivo regeneration of osteoporotic bone defects. Journal of Materials Chemistry B. 2013;1:5711-22.

[10] Jebahi S, Oudadesse H, Feki He, Rebai T, Keskes H, Pellen P, et al. Antioxidative/oxidative effects of strontium-doped bioactive glass as bone graft. In vivo assays in ovariectomised rats. Journal of Applied Biomedicine. 2012;10:195-209.

[11] Tarafder S, Davies NM, Bandyopadhyay A, Bose S. 3D printed tricalcium phosphate scaffolds: Effect of SrO and MgO doping on in vivo osteogenesis in a rat distal femoral defect model. Biomater Sci. 2013;1:1250-9.

[12] Li Y, Chen S-K, Li L, Qin L, Wang X-L, Lai Y-X. Bone defect animal models for testing efficacy of bone substitute biomaterials. Journal of Orthopaedic Translation. 2015;3:95-104.

[13] Goldhahn J, Scheele WH, Mitlak BH, Abadie E, Aspenberg P, Augat P, et al. Clinical evaluation of medicinal products for acceleration of fracture healing in patients with osteoporosis. Bone. 2008;43:343-7.

[14] Barrias CC, Lamghari M, Granja PL, Sa Miranda MC, Barbosa MA. Biological evaluation of calcium alginate microspheres as a vehicle for the localized delivery of a therapeutic enzyme. J Biomed Mater Res A. 2005;74:545-52.

[15] Ribeiro CC, Barrias CC, Barbosa MA. Calcium phosphate-alginate microspheres as enzyme delivery matrices. Biomaterials. 2004;25:4363-73.

[16] Barrias CC, Ribeiro CC, Lamghari M, Miranda CS, Barbosa MA. Proliferation, activity, and osteogenic differentiation of bone marrow stromal cells cultured on calcium titanium phosphate microspheres. J Biomed Mater Res A. 2005;72:57-66.

[17] Ribeiro CC, Barrias CC, Barbosa MA. Preparation and characterisation of calcium-phosphate porous microspheres with a uniform size for biomedical applications. J Mater Sci Mater Med. 2006;17:455-63.

[18] Maia FR, Lourenco AH, Granja PL, Goncalves RM, Barrias CC. Effect of cell density on mesenchymal stem cells aggregation in RGD-alginate 3D matrices under osteoinductive conditions. Macromol Biosci. 2014;14:759-71.

[19] Fonseca KB, Gomes DB, Lee K, Santos SG, Sousa A, Silva EA, et al. Injectable MMP-sensitive alginate hydrogels as hMSC delivery systems. Biomacromolecules. 2014;15:380-90.

[20] Maia FR, Barbosa M, Gomes DB, Vale N, Gomes P, Granja PL, et al. Hydrogel depots for local co-delivery of osteoinductive peptides and mesenchymal stem cells. J Control Release. 2014;189:158-68.

[21] Oliveira SM, Barrias CC, Ribeiro CC, Almeida IF, Bahia MF, Barbosa MA. Morphology and mechanical properties of injectable ceramic microspheres2009.

[22] Bidarra SJ, Barrias CC, Fonseca KB, Barbosa MA, Soares RA, Granja PL. Injectable in situ crosslinkable RGD-modified alginate matrix for endothelial cells delivery. Biomaterials. 2011;32:7897-904.

[23] Oliveira SM, Almeida IF, Costa PC, Barrias CC, Ferreira MR, Bahia MF, et al. Characterization of polymeric solutions as injectable vehicles for hydroxyapatite microspheres. AAPS PharmSciTech. 2010;11:852-8.

[24] Oliveira SM, Barrias CC, Almeida IF, Costa PC, Ferreira MR, Bahia MF, et al. Injectability of a bone filler system based on hydroxyapatite microspheres and a vehicle with in situ gel-forming ability. J Biomed Mater Res B Appl Biomater. 2008;87:49-58.

[25] Ouyang J, Yang GT, Wu WZ, Zhu QA, Zhong SZ. Biomechanical characteristics of human trabecular bone. Clin Biomech (Bristol, Avon). 1997;12:522-4.

[26] Keaveny TM, Morgan EF, Niebur GL, Yeh OC. Biomechanics of trabecular bone. Annu Rev Biomed Eng. 2001;3:307-33.

[27] D'Este M, Eglin D. Hydrogels in calcium phosphate moldable and injectable bone substitutes: Sticky excipients or advanced 3-D carriers? Acta Biomater. 2013;9:5421-30.

[28] Bohner M. Design of ceramic-based cements and putties for bone graft substitution. Eur Cell Mater. 2010;20:1-12.

[29] Gauthier O, Bouler JM, Weiss P, Bosco J, Aguado E, Daculsi G. Short-term effects of mineral particle sizes on cellular degradation activity after implantation of injectable calcium phosphate biomaterials and the consequences for bone substitution. Bone. 1999;25:71S-4S.

[30] Rowley JA, Madlambayan G, Mooney DJ. Alginate hydrogels as synthetic extracellular matrix materials. Biomaterials. 1999;20:45-53.

[31] Bohner M, Tadier S, van Garderen N, de Gasparo A, Dobelin N, Baroud G. Synthesis of spherical calcium phosphate particles for dental and orthopedic applications. Biomatter. 2013;3.

[32] Daculsi G, Uzel AP, Weiss P, Goyenvalle E, Aguado E. Developments in injectable multiphasic biomaterials. The performance of microporous biphasic calcium phosphate granules and hydrogels. J Mater Sci Mater Med. 2010;21:855-61.

[33] Gauthier O, Muller R, von Stechow D, Lamy B, Weiss P, Bouler JM, et al. In vivo bone regeneration with injectable calcium phosphate biomaterial: a three-dimensional micro-computed tomographic, biomechanical and SEM study. Biomaterials. 2005;26:5444-53.

[34] Izci Y, Secer HI, Ilica AT, Karacalioglu O, Onguru O, Timucin M, et al. The efficacy of bioceramics for the closure of burr-holes in craniotomy: case studies on 14 patients. J Appl Biomater Funct Mater. 2013;11:e187-96.